الجمهورية الجزائرية الديمقراطية الشعبية
RÉPUBLIQUE ALGÉRIENNE DÉMOCRATIQUE
ET POPULAIRE
وزارة التعليم العالي والبحث العلمي
MINISTÈRE DE L'ENSEIGNEMENT
SUPÉRIEUR ET DE LA RECHERCHE
SCIENTIFIQUE
UNIVERSITE BADJI MOKHTAR– ANNABA

FACULTÉ DES SCIENCES

DÉPARTEMENT DE BIOLOGIE

LABORATOIRE DE BIOSURVEILLANCE
ENVIRONNEMENTALE

Thèse En vue de l'obtention d'un Diplôme de Doctorat

Domaine : SCIENCE DE LA NATURE ET DE LVIE

Filière : Sciences biologiques

Option : physiopathologie

Intitulé

Effet du stress oxydatif sur certains organes cibles et leur protection par le composé de la plante originale

Présentée par : Mme KAOUDOUNE Chahrazed

Directrice de thèse :	**Dr. BENCHIKH Fatima**	**Dr. Université de Sétif**
Co- Directrice :	**Pr. ABDENNOUR Cherif**	**Pr. Université de Annaba**

Membres de Jury :

Pr. KHELILI Kamel	**President**	**Université de Annaba**
Pr. BAAZIZ Nasser	**Examinateur**	**Université de Constantine**
Pr. NECIB Youcef	**Examinateur**	**Université de Constantine**

Année universitaire: 2024/2025

الجمهورية الجزائرية الديمقراطية الشعبية
DEMOCRATIC PEOPLE'S REPUBLIC OF ALGERIA
وزارة التعليم العالي والبحث العلمي
MINISTRY OF HIGHER EDUCATION AND RESEARCH
SCIENTIFIC
BADJI MOKHTAR UNIVERSITY–ANNABA

FACULTY OF SCIENCES DEPARTMENT OF BIOLOGY
LABORATORY OF BIOSURVEILLANCE ENVIRONNEMENTAL

Thesis in view of obtaining a Doctorate Degree

Domain: SCIENCE OF NATURE AND LIFE

Field: BIOLOGIC SCIENCES

Option : PHYSIOPATHOLOGY

TOPIC

Effect of oxidative stress on some target organs and their protection by compound of plant original

Presented by: Chahrazed KAOUDOUNE

Supervisor: Dr. Fatima BENCHIKH — **Dr. University of Setif**

Co- Supervisor: Pr. Cherif ABDENNOUR — **Pr. University of Annaba**

In front of a jury composed of:

Pr. Kamel KHELILI	**President**	**University of Annaba**
Pr. Nasser BAAZIZ	**Examiner**	**University of Constantine**
Pr. Youcef NECIB	**Examiner**	**University of Constantine**

University year: 2024/2025

Acknowledgment

First and foremost, we express our gratitude to the Almighty for bestowing upon us health, strength, courage, patience, and persistence, as well as for enabling us to utilize the available resources to accomplish this modest work. Thank you for helping us to succeed.

I would like to express my deepest gratitude and many thanks to my academic supervisor, Dr. **Fatima Benchikh** and my assistant supervisor, **Pr. Cherif Abdennour**, who guided, instructed, and motivated me throughout my research journey. Their feedback enabled me to deepen and refine my research, and without their supervision, the results presented in my thesis would not have been possible.

I also express my sincere and deep thanks to Pr. **Kamel KHELILI** and Dr. **Farida LOUDJANI** from Badji Mokhtar Annaba University. Pr. **Nasser BAAZIZ** and Pr. **Youcef NECIB** from Mentouri Brothers Constantine University for having agreed to judge this work, thank you for your availability.

I express my profound gratitude and thanks to my husband, **Dr. Aydi Abdelkarim** from Mohamed Lamine Debaghine University (Setif 2), who has continuously supported me, sacrificed his time, and always believed in me.

My sincere gratitude and big thanks go to **Pr. Djamel Abdellouche**, Head of Pathological Anatomy Laboratory at the University Hospital Center, Setif for his great and valuable assistance in reading and photographing histological sections.

I would also like to express my sincere gratitude to my laboratory collaborators: **Pr. Smain Amira**, team leader in the Laboratory of Applied Phytotherapy for Chronic Diseases (LPAMC), and the following members: **Dr. Lakhdar Gasmi**, **Pr. Hassiba Benabdallah**, **Dr. Ismahan Derafa, Dr. Walid Mamache, Dr. Karima Loucif, Dr. Soulaf Mehlous, Dr. Roumaisa Ounis, and Dr. Hind Amira** for their help and support.

I extend my sincere thanks to **Pr. Mounira Amran**, Head of Analysis Laboratory at the Cancer Centre (CAC), Setif, for helping me to conduct blood analyses. I would like to thank **Dr. K. Hammoudi**, Head of Pathological Anatomy Laboratory at the Cancer Centre (CAC), for providing all the facilities to conduct histological sections.

I also thank **Dr. BENSOUICI Chawki**, Research Supervisor at the Biotechnology Research Center (CRBT), (Algeria), for his help, which has allowed me to carry out several tests.

My sincere thanks and appreciation **to Pr. Ouali Kheireddine**, Director of the «Environmental Biomonitoring» Laboratory, at Badji Mokhtar University.

I also extend my sincere gratitude and thanks to **Prof. Dr. Mustafa Abdullah YILMAZ**, Director of Chromatography and Mass Spectrometry Unit at Dicle University Science and Technology Research and Application Centre (DUBTAM). Diyarbakir, Turkey. as well **as Oguz Cakir** and **Abbas Tarhan**, who are members of (DUBTAM), Turkey. for their gracious hospitality in their laboratory and their assistance in carrying out the LC-MS/MS analysis. I am also grateful to **Associate Professor Gokhan Zengin** from the physiology and biochemistry laboratory, Department of Biology, Science Faculty, Selcuk University, Konya, Turkey, for conducting some tests that support my research.

I am deeply grateful to my life partners, my **mother** and my sisters, **Dr. Hannan** and **Dr. Assia**, for their unwavering support and encouragement throughout my doctoral journey.

DEDICATION

I am dedicating this thesis
To beloved person who have meant and continue to mean so much to me.
Although it is not present in this life, but his memories continue
in my life. my beloved father “Abderrahmane” whose love for me knew no bounds. Thank you so much “Dad”, I will never forget you

To my dear mother, ‘**ZERARGA Drifa**,’ who devoted her life for her daughters.

To my husband; who has been a source of strength, patience, and motivation for me throughout this experience. I am truly blessed to have you as a partner in this life

To **my faithful sisters**; those who always helped me

My parents-in-law; who have always considered me as a daughter

To the entire **KAOUDOUNE** family and all my **in-laws.**

List of publications

Kaoudoune, C., Benchikh, F., Abdennour, C., Benabdallah, H., Souici, C. B., Derafa, I., ... & Amira, S. (2024). Phenolic content and antioxidant activity of hydroethanolic and aqueous extracts of the inflorescences of Allium sphaerocephalon L. Research Journal of Pharmacy and Technology, 17(2), 903-909. http://dx.doi.org/10.52711/0974-360X.2024.00140

Kaoudone, C., Benchikh, F., Abdennour, C., Benabdallah, H., Mamache, W., & Amira, S. (2022). Free Radical Scavenging and Antinociceptive Activities of the Aqueous Extract from Matricaria chamomilla L. Flowers. Turkish Journal of Agriculture-Food Science and Technology, 10(10), 2076-2080. https://doi.org/10.24925/turjaf.v10i10.2076-2080.5330

Kaoudoune, C., Benchikh, F., Benabdallah, H., Loucif, K., Mehlous, S., & Amira, S. (2020). Gastroprotective effect and in vitro Antioxidant Activities of the Aqueous Extract from Artemisia absinthium L Aerial Parts. Journal of drug delivery and therapeutics, 10(4), 153-156. https://doi.org/10.22270/jddt.v10i4.4253

Loucif, K., Benabdallah, H., Benchikh, F., Mehlous, S., **Kaoudoune, C.**, Souici, C. B., & Amira, S. (2020). Metal chelating and cupric ion reducing antioxidant capacities of Ammoides atlantica aqueous extract. Journal of Drug Delivery and Therapeutics, 10(4-s), 108-111. https://doi.org/10.22270/jddt.v10i4-s.4245

Mehlous, S., Benchikh, F., Benabdallah, H., Loucif, K., **Kaoudoune, C**., Laouer, H., & Amira, S. (2020). Evaluation of antioxidant activity and polyphenols content of the hydro-methanolic extract from Saccocalyx satureioides Coss and Dur. Journal of Drug Delivery and Therapeutics, 10(4), 188-190. https://doi.org/10.22270/jddt.v10i4.4166

Mehlous, S., Benchikh, F., Benabdallah, H., Loucif, K., **Kaoudoune, C**., Laouer, H., & Amira, S. (2020). Total phenolic contents, DPPH radical scavenging and β-carotene bleaching activities of ethyl acetate extract from saccocalyx satureioides Coss and Dur.

Derafa, I., Amira, S., Benchikh, F., Mamache, W., & **Kaoudoune, C.** (2022). Phenolic content and antioxidant activity of hydromethanolic and aqueous extracts of aerial parts of Phlomis crinita. Turkish Journal of Agriculture-Food Science and Technology, 10(10), 2061-2066. https://doi.org/10.24925/turjaf.v10i10.2061-2066.5173

List of communications

KAOUDOUNE C., BENCHIKH F., Benabdallah H. AMIRA S. Analgesic activity and in vitro antioxidant activities of the aqueous extract from *Olea europaea* L. leaves parts, First International Webinar on: Promotion and Exploitation of Plants of Ecological and Economic Interest, University of Khenchela, Algeria, 15-16 Mars, 2023.

KAOUDOUNE C., BENCHIKH F., ABDENNOUR C., BENABDALLAH H., AMIRA S. Free radical scavenging and lipid peroxidation inhibition activities of the hydroethanolic extract from *Allium sphaerocephalon* L inflorescences, National seminar on phytotherapy and pharmacognosy, University of Setif, Algeria, 14-15 Mars, 2023.

KAOUDOUNE C., BENCHIKH F., BENABDALLAH H., AMIRA S. DPPH radical scavenging and lipid peroxidation inhibition activities of the aqueous extract from *Allium sphaerocephalon* L inflorescences. 1er Webinar National Natural Products and Bioactive Compounds, an issue of sustainable development, University of Telemcen, Algeria, 11 Mars, 2023.

KAOUDOUNE C., BENCHIKH F., BENABDALLAH H., NADJI L., SELMANE H., MAMACHE W. and AMIRA S., Antioxidant and gastroprotective activities of *Matricaria Chamomilla* L. hydroethanolic extract», 1st National Seminar on Agriculture and Sustainable Development in Semi-Arid Zones, University of Souk-Ahras, Algeria, 15 et 16 Novembre, 2022.

KAOUDOUNE C., BENCHIKH F., ABDENNOUR C., AMIRA S., Reducing power and ferrous ions chelation activities of *Allium sphaerocephalon* L. inflorescences. First International seminar on green biotechnology and food security University of Khenchela, Algeria, 16 et 17 Novembre, 2022.

KAOUDOUNE C., BENCHIKH F., BENABDALLAH H., AMIRA S. Free radical scavenging and analgesic activities of the aqueous extract from *Matricaria chamomilla* L. flowers parts, 1st International Webinar on Plant and Microbial Biodiversity and Valuation, University of Oran, Algeria, 13-15 Décembre, 2022.

KAOUDOUNE C., BENCHIKH F., BENABDALLAH H., AMIRA S. Analgesic activity and in vitro antioxidant activities of the Aqueous extract from *Matricaria chamomilla* L flowers Parts, International Seminar on Biodiversity, Valorization and Conservation of Urban and Forest Ecosystems, University of M'sila, Algeria, 28-29 Avril, 2021.

KAOUDOUNE C., BENCHIKH F., BENABDALLAH H., AMIRA S. Analgesic and antioxidant activities of ethanol extract from Artemisia absinthium areal parts, 1stNational Seminar on the Contribution of Biotechnologies to Environment Protection, University of M'sila, Algeria, 15-16 December, 2019.

Contents

List of figures

List of tables

Abstract

Allium sphaerocephalon L. (AS) is a wild-growing plant frequently utilized as an alternative to onion. The present study focuses on estimation of chemical analysis and antioxidant properties of plant *(*AS), Furthermore, the study of the preventive action against stomach ulcers induced by 70% ethanol in *vivo*, as well as the hepatoprotective and nephroprotective from toxicity induced by the administration of doxorubicin (2mg/ kg) for 3 times weekly. The antioxidant properties were assessed using five various assays: DPPH radical scavenging assay, reducing power, cupric reducing antioxidant capacity, ferrous ion chelating, and β-carotene bleaching test. These assays demonstrated acceptable antioxidant activities in the hydroethanolic (ASHE) and aqueous (ASAQ) extracts. LC-MS/MS analysis disclosed the existence of 16 phytochemical constituents in the hydroethanolic extract (ASHE), of which 75% are flavonoids, with quinoic acid and acetin (13.808 and 12.616 mg/g of dry extract, respectively) being the major compounds. In other hand, the pretreatment of (ASHE) at dosages of 25, 50, and 100 mg/kg yielded a dose-dependent response enhancement of gastric protection, where the highest dose gave a better protection (99.76%) than ranitidine as a drug reference (90.77%). The ASHE adopted the NO and COX pathways as its protective mechanism in stomach. ASHE (50 and 100 mg/kg) decreased the toxicity of doxorubicin in the liver and kidney by increasing serum levels (AST, ALT, ALP) and (urea, creatinine). Furthermore, ASHE extract improved oxidative stress parameters (GSH, catalase, and MDA) as well as histopathological damage in all organs studied (stomach, liver, and kidney).

Keywords: *Allium sphaerocephalon* L., antioxidant properties, LC-MS/MS analysis, gastroprotective effect, doxorubicin, hepatoprotective effect, nephroprotective effect.

Résumé

Allium sphaerocephalon (AS) est une plante sauvage couramment utilisée comme substitut à l'oignon. Cette étude concerne l'évaluation de l'analyse chimique et les propriétés antioxydantes de la plante (AS), ainsi que sur son effet protecteur sur l'ulcère gastrique induit par 70% d'éthanol *in vivo*. De plus, l'étude examine les effets hépato protecteurs et néphroprotecteurs face à la toxicité induite par l'administration de doxorubicine (2mg/kg) administrée trois fois par semaine. Les propriétés antioxydantes ont été déterminées à l'aide de cinq essais différents : Le test de piégeage du radical DPPH, le dosage du pouvoir réducteur, la capacité antioxydante par réduction de cuivre, le test de chélation des ions ferreux et le test de blanchissement de β-carotène. Ces essais ont démontré des activités antioxydantes acceptables dans les extraits hydroéthanoliques (ASHE) et aqueux (ASAQ). L'analyse LC-MS/MS a révélé la présence de 16 composés phytochimiques dans l'extrait hydroéthanolique (ASHE), dont 75 % sont des flavonoïdes, avec de l'acide quinoïque et l'acétine (13.808 et 12.616 mg/g d'extrait sec), respectivement étant les principaux composés. D'autre part, le prétraitement de l'ASHE à des doses de 25, 50 et 100 mg/kg a entraîné une amélioration a dose-dépendante de la protection gastrique, où la dose la plus élevée donne une meilleure protection (99.76 %) que la ranitidine comme médicament de référence (90,77 %). L'ASHE a agi via les voies NO et COX comme mécanisme de protection dans l'estomac. De plus, l'ASHE (50 et 100 mg/kg) a diminué la toxicité de la doxorubicine dans le foie et les reins, en augmentant les taux sériques (AST, ALT, ALP) et (urée, créatinine). De plus, l'extrait d'ASHE a amélioré les paramètres du stress oxydatif (GSH, catalase et MDA) ainsi que les dommages histopathologiques dans tous les organes étudiés (estomac, foie et rein).

Mots-clés : *Allium sphaerocephalon* L., propriétés antioxydantes, analyse LC-MS/MS, effect gastro protecteur, doxorubicine, effet hépato protecteur, effet néphro protecteur.

الملخص

يُستعمل نبات الثوم البري *Allium sphaerocephalon* L. (AS) تقليديًا كبديل للبصل. تهدف هذه الدراسة إلى تحليل التركيب الكيميائي للنبات وتقييم خصائصه المضادة للأكسدة، إضافةً إلى استقصاء تأثيره الوقائي ضد القرحة المعدية المستحثة بالإيثانول (70٪)، وكذلك قدرته على الحد من السمية الكبدية والكلوية الناجمة عن إعطاء عقار الدوكسوروبيسين (DOX) بجرعة (2 ملغ/كغ) مرة أسبوعيًا لمدة ثلاثة أسابيع. تم تحديد النشاط المضاد للأكسدة لمستخلصي النبات (المستخلص الكحولي ASHE والمستخلص المائي ASAQ)باستخدام عدة اختبارات بيوكيميائية، شملت: اختبار DPPH لإزالة الجذر ، قياس القدرة الإرجاعية، النشاط المخلبي للمعادن، واختبار تبييض بيتا-كاروتين. وقد أظهرت النتائج أن المستخلصين يمتلكان نشاطًا مقبولًا لمضادات الأكسدة، مع تفوق(ASHE) .أظهر تحليل LC-MS/MS لمستخلص (ASHE)وجود 16 مركبًا نباتيًا ، كان 75٪ منها من الفلافونويدات، وتبيّن أن حمض الكينويك والأسيتين هما المركبان الرئيسيان بتركيزين يبلغان (13.80 و12.61 ملغ/غ من المستخلص الجاف، على التوالي).من الناحية الدوائية، أظهرت المعالجة المسبقة بمستخلص ASHE بجرعات 25، 50، و100 ملغ/كغ تأثيرًا وقائيًا ضد القرحة المعدية بشكل يعتمد على الجرعة، حيث سجلت أعلى جرعة (100 ملغ/كغ) نسبة حماية بلغت 99.76٪، متفوقة على الرانيتيدين المستخدم كدواء مرجعي (90.77٪). وتشير النتائج إلى أن الآلية الوقائية للمستخلص ترتبط بتفعيل مساري أكسيد النيتريك (NO) وإنزيم.(COX) . كما ساعد المستخلص الكحولي (ASHE) بجرعتي 50 و100 ملغ/كغ في التخفيف من السمية الكبدية والكلوية الناجمة عنDOX ، من خلال تحسين المؤشرات الحيوية لوظائف الكبد(AST ، ALT، ALP)والكلية (اليوريا، الكرياتينين)، بالإضافة إلى تعزيز مضادات الأكسدة الذاتية (GSH، catalase) وخفض مستويات بيروكسيد الدهون .(MDA) علاوة على ذلك، أظهر المستخلص تأثيرًا إيجابيًا في الحد من التغيرات المرضية النسيجية في المعدة والكبد والكلى.

الكلمات المفتاحية: *Allium sphaerocephalon* L.، الأنشطة المضادة للأكسدة، تحليل LC-MS/MS، دوكسوروبيسين، التأثير الوقائي المعدي، التأثير الوقائي الكبدي، التأثير الوقائي الكلوي.

List of abbreviations

ALP: Alkaline phosphatase

ALT: Alanine aminotransferase

AQE: Aqueous extract

ASHE: *Allium sphareocephalon* L. hydroethanolic extract

AST: Aspartate aminotransferase

BHA: Butylated hydroxyanisole

BHT: Butylated hydroxytoluene

CAC: Anti-cancer center

cGMP: Cyclic guanosine monophosphate

CMC: Carboxymethyl cellulose

cNOS: Nitric oxide synthase

COX: Cyclooxygenase

CUPRAC: Cupric Reducing Antioxidant Capacity

DAS: Diallyl disulphide

DATS: Diallyl trisulphide

DDC: Diethyldithiocarbamate

DOX: Doxorubicin.

DPPH: 2,2-diphenyl-1-picrylhydrazyl

DTNB: 5,5'-dithiobis (2-nitrobenzoic acid)

ECL: Enterochromaffin-like cells

EDTA: Ethylenediaminetetraacetic acid

EOH: Hydroethanolic extract

FCR: Folin–Ciocalteu reagent

GC: Guanylate cyclase

GGT: Gamma-glutamyl transferase

GI: Gastrointestinal

GMBF: Blood flow of the gastric mucosa

GOT: Glutamate oxaloacetate transaminase

GPT: Glutamate pyruvate transaminase

H&E: Hematoxylin and eosin

HAT: Transfers H-atom

HCl: Hydrochloric acid

IκB kinase (IKK): Ikappa B kinase

LC-MS/MS: liquid chromatography-mass spectrometry/mass spectrometry

LD: Lactate dehydrogenase

L-NNA: L-N^G-Nitroarginine N^G-nitro-L-Arginine

LPO: Lipid peroxidation

MDA: Malondialdehyde

MDH: malate dehydrogenase

NF-kB: Facteur nucléaire kappa B

NF-κB: Nuclear factor kappa B

NSAIDs: Non-steroidal, anti-inflammatory drugs

PGE_2: Prostaglandin E_2

p-NPP: p-nitrophenyl phosphate

PPI: Proton Pump Inhibitors

PUD: Peptic ulcer disease

RNS: Reactive Nitrogen Species.

ROS: Reactive oxygen species.

SAC: Sallycysteine

SET-PT: Single-electron transfer via proton transfer

SH: Sulfyhydryl groups

SOD: Superoxide dismutase

TBA: Thiobarbituric acid

TCA: Trichloroacetic acid

TFC: Total flavonoid content

TMC: Transition metal chelation

TNB: 2-nitro-5-mercapto-benzoic acid

TNF-α: necrosis factor-α

UHPLC: Ultrahigh performance liquid chromatograph

VIP: Vasoactive intestinal peptide

WHO: World Health Organization

Introduction

Introduction

There has been a growing emphasis on disease prevention recently, particularly regarding free radicals's role. The study of free radicals in biology and medicine is advancing swiftly due to its significant implications for health, illness, and overall quality of life. After the discovery of free radicals almost a century ago, it seemed that they mediated all oxidation events pertaining to organic compounds (Martemucci *et al*., 2022).

The term peptic originates from the Greek word peptikos, signifying digestion. Acid peptic digestion causes a mucosal breach in the upper gastrointestinal (GI) tract, which leads to ulceration that goes beyond the muscularis mucosae and into the submucosa. This is what peptic ulcer disease (PUD) is all about. It most frequently manifests in the stomach and the proximal duodenum, but it can also arise in the distal esophagus and distal duodenum, and jejunum, as well as in the Meckel's diverticulum containing heterotopic stomach mucosa (Ahmed, 2019; Beiranvand, 2022).

Doxorubicin (Dox), a typical anthracycline, was first isolated from *Streptomyces peucetius*. It is commonly used as anticancer agent for breast cancer, acute lymphoblastic leukemia, and prostate cancer. The therapeutic application of Dox is constrained by the avoidance of adverse consequences including cardiotoxicity, hepatotoxicity, and nephrotoxicity. Dox is known to stimulate the production of reactive oxygen species (ROS), diminish antioxidative defense, and stabilize mitochondrial damage (Zhao *et al*., 2017; Zhao *et al*., 2019).

As per the World Health Organization (WHO), Over 80% of the global population depends on traditional medicinal systems for their health issues (WHO, 2003). Herbal products have historically served as primary sources for the identification of many bioactive chemicals. They are extensively utilized in traditional medicinal systems for the treatment of numerous ailments and other health advantages, and are regarded as significantly safer than synthetic compounds (Gupta *et al*., 2021).

Species of Allium, classified within the Alliaceae family, are among the most ancient cultivated vegetables used as food. Their applications are many, encompassing ornamentals, spices, vegetables, and medicinal uses for treating various ailments (Bastaki, 2021).

Numerous species of the Allium genus have been the subject of extensive research regarding their chemical composition, antioxidant activity, and other biological characteristics., especially those cultivated as garlic and onion, nevertheless, limited research have been performed

on spontaneous species such as *A. sphaerocephalon* L. especially. so, we have advanced in this study by focusing on this type of allium.

Therefore, the objectives of this study were as follows:

- Quantification of polyphenols and phytochemical analysis of the plant extracts.
- Assessment of the *in vitro* antioxidant efficacy of plant extracts.
- Assessment of the acute oral toxicity of the plant extracts.
- To investigate the impact of *Allium sphareocephalon* L. hydroethanolic extract on:
    - Gastric ulcers produced by ethanol in rats
    - Hepathotoxicity and nephrotoxicity induced by doxorubicin
- Assessment of *in vivo* antioxidant efficacy of plant extracts.

Chapter 01:
Literature review

1. The anatomical and physiological structure of the stomach

1.1. Anatomy

The stomach is the initial entirely intra-abdominal intestinal organ. It is adapted for mechanical rippling, storage and digestion of food, and contributes to the coordination of neuroendocrine for intestinal function. The stomach is largely located in the left hypochondrial area, under the cover of the lower part of the rib cage. The inferior and distal sections of the stomach are situated in the epigastric and upper umbilical areas of the abdomen. The stomach is a J-shaped pouch situated between the oesophagus and the small intestine, characterized by lesser and greater curvatures orientated to the right. The spleen is positioned on the left, while the pancreas is located inferiorly and posteriorly. The liver is positioned on the right side. Anatomical, histological, and functional characteristics categorize it into the following segments (Figure1). (Keshav, 2009; Sherwood, 2015).

Cardia: The region where the oesophagus opens, featuring a physiological sphincter mechanism to inhibit reflux. **Fundus:** The dome-shaped, superolateral region of the stomach, situated superiorly and to the left of the cardia. **Body**: It extends from the cardia to the angular notch (incisura angularis), a minor anatomical notch on the stomach's lesser curvature that delineates the boundary between the body and the antrum. **Pyloric Antrum**: Extends from the incisura angularis to the pyloric orifice. **Pylorus**: The pylorus is a tubular section of the stomach, approximately 2.5 cm in length, characterised by a thick muscular wall that constitutes the pyloric sphincter, regulating the egress of gastric contents (Keshav, 2009; Sherwood, 2015).

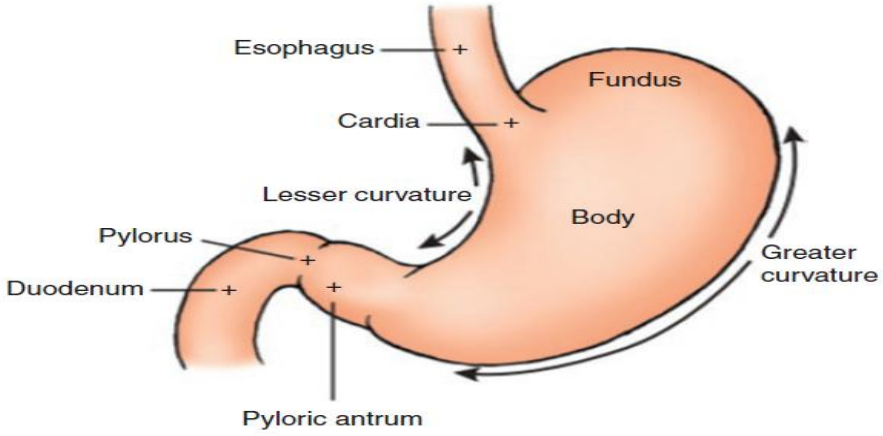

Figure 1: Anatomy of the stomach (Borys and Kurtz, 2023).

1.2. Histology

The stomach wall comprises four layers: mucosa, submucosa, smooth muscle layer, subserosa and serosa (Figure 2) (Chandan, 2019).

a. **Mucosa:** The lamina propria is a type of loose connective tissue, supporting the epithelium that makes up the gastric mucosa. The epithelial component comprises of two compartments: the deep glandular compartment and the gastric pits (foveolae), which represent the invagination of the surface epithelial lining. The different types of glands (cardiac, fundic, and pyloric) define the different zones of the stomach (cardia, fundus, body, and antrum). The glandular compartment disperses endocrine cells throughout the stomach. Normally, a thick mucin gel layer covers the mucosal surface (Ban, 2013).
b. **The submucosa:** comprises of ganglion cells and vascular structures, including blood and lymphatic vessels, all situated inside a loose connective tissue interspersed with adipose cells (Miranda-Bautista *et al*., 2017).
c. **The smooth muscle layer:** Consists of three muscular layers. the middles circular muscle layer (encircles the entire stomach), the outer longitudinal muscle layer and the inner oblique muscle layer (situated internal to the circular layer) (Miranda-Bautista *et al*., 2017).
d. **The subserosa and serosa**: The subserosa is a slim layer of loose areolar tissue that encompasses blood arteries, lymphatics, and nerve fibers. It is encased by the serosa, consisting of a layer of flattened mesothelial cells that is continuous with the serosal lining of the peritoneal cavity (Ban, 2013).

1.3. Arterial vascular supply

The stomach is rich in blood vessels, receiving blood supply from five primary sources. **The left gastric artery:** It is a branch of the axis of celiac, which supplies the cephalad part of the lesser curvature. **The right gastric artery:** a branch of the common hepatic artery, which supplies the caudal portion of the lesser curvature, **The right gastroepiploic artery:** a branch of the gastroduodenal artery, which supplies the antrum and lower corpus. **The left gastroepiploic artery**: a branch of the splenic artery, which supplies the upper corpus. **The short gastric arteries:** pass to the fundus and cephalad portion of the corpus from the splenic hilum, and thus ultimately from the splenic artery (David and Soybel, 2005).

1.4. Innervation

The vagus nerve supplies the stomach's parasympathetic innervation via the anterior and posterior vagal fibers. Stomach rotation during development positions the left vagus nerve anteriorly and the right vagus nerve posteriorly. The anterior and posterior vagal fibers travel toward the lesser curvature and give rise to anterior and posterior gastric branches, respectively. The stomach's sympathetic innervation arises from the T5 to T9 spinal cord segments via the greater splanchnic nerve, which transits toward the celiac plexus to be distributed along with the region's arterial supply.

The Auerbach or myenteric plexus is a network of neurons located between the longitudinal and circular layers of the gastrointestinal tract's muscularis externa. This plexus regulates gut motility. The Meissner or submucosal plexus is situated within the submucosal layer. The Meissner plexus primarily regulates local blood flow and gastric secretion. The Auerbach and Meissner plexuses are part of the enteric nervous system, an autonomous and extensive network of neurons comprising what is known as the "brain of the gut. (Chaudhry *et al*., 2024).

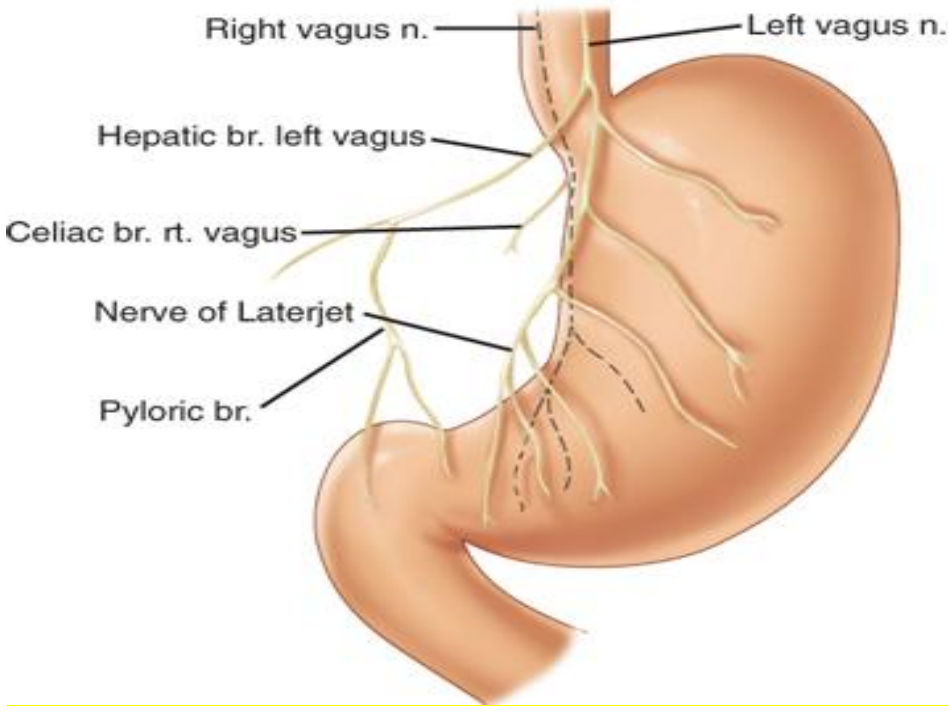

Figure 2: Diagram of the vagal innervation of the human stomach. (Wilson and Stevenson, 2019)

1.5. Physiology and secretion of the stomach

The stomach mucosa is composed of columnar glandular epithelium. The structure of the glandular epithelium differs across the various areas of the stomach. The epithelium of the cardia predominantly secretes mucus through **mucus-producing cells**. The stomach's body houses the majority of **parietal** and **chief cells**. **Parietal cells** primarily secrete acid, ghrelin, and leptin. **Chief cells** secrete pepsin and leptin**. Enterochromaffin-like cells (ECL cells)** that secrete histamine are predominantly located in the body of the stomach while **G cells** that secrete gastrin are located in the antrum**. D cells** that secrete somatostatin are located in both the body and the antrum of the stomach (Figure 3 and table 1) (Monnet, 2020).

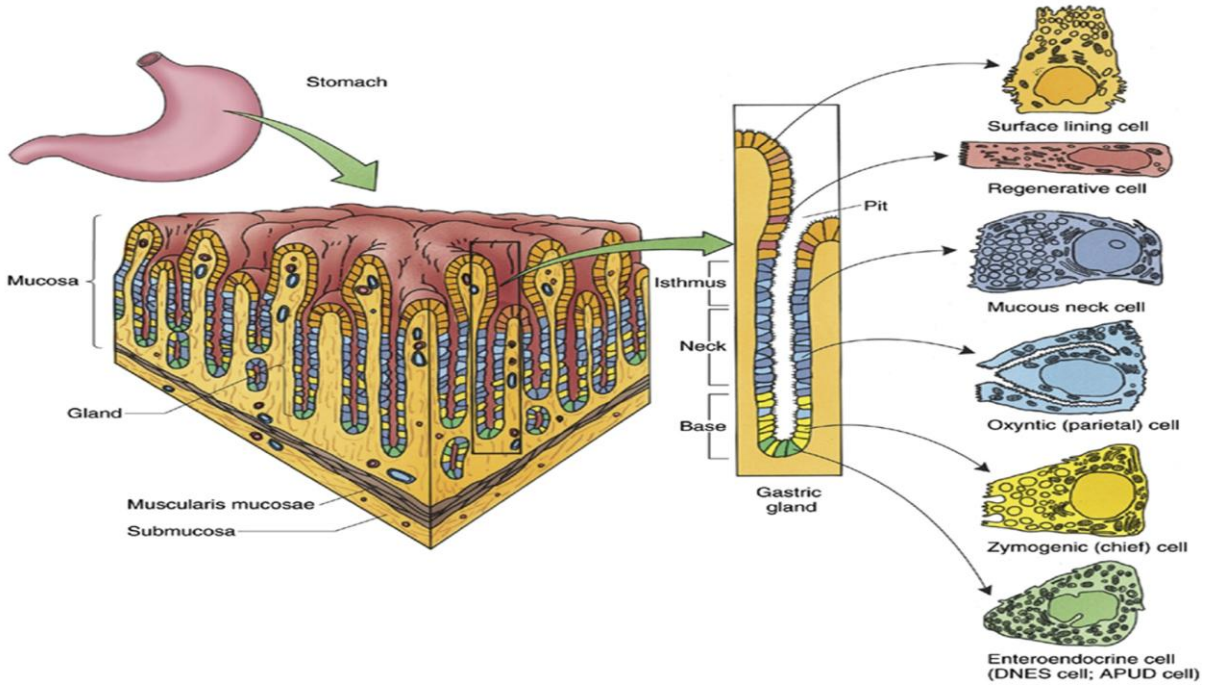

Figure 3: The structure of the stomach mucosa illustrating the cells of gastric glands (McQuilken, 2021).

Table 01: Important Gastric Secretory Products (Sherwood, 2015; Wilson and Stevenson, 2019).

Type of cell secret	Security product	Stimulus of the secretion	Roles of secretion products
surface mucous cells	Mucus, Bicarbonate, Trefoil factors	Stimulation Mechanical content	Gastroprotection against mechanical attack, pepsin, and acid
Parietal cell	hydrochloric acid (HCl), Intrinsic factor	Acetylcholine, histamine, or gastrin	Activated pepsinogen, Hydrolysis; sterilization of meal, Vitamin B_{12} absorption
Chief cell	Pepsinogen	Acetylcholine, gastrin	Protein digestion
ECL cells	histamine	Acetylcholine, gastrin	Partial cell stimulation
G cells	gastrin	Protein products, Acetylcholine	Partial and ECL cell stimulation
D cells	Somatostatin	hydrochloric acid (HCl)	inhibiting partial cells, G cells, and ECL cells

2. Liver anatomy and physiology

The liver is regarded as the largest and heaviest glandular organ in the human body, exhibiting a greater weight in males than in females, it weighs 1.5 kg in adult (approximately 2% of body weight.). In its normal state, the liver exhibits a deep burgundy hue, indicative of its abundant vascularity, a smooth surface, and a soft-to-firm and floppy consistency (Mahadevan, 2020).

The liver is a wedge-shaped organ located in the right upper quadrant of the abdominal cavity, beneath the diaphragm. It is wholly enclosed by the rib cage. The liver is the largest gland and visceral organ in the body, extending from the right fifth intercostal space to the right costal border and laterally to the left midclavicular line. It is encased in a delicate layer of connective tissue known as Glisson's capsule. The Glisson capsule penetrates the liver parenchyma to provide support for the biliary and vascular systems (Zhang *et al*., 2020).

Couinaud partitioned the liver into two functional lobes with comparable dimensions, divided on the liver surface by an imaginary line traversing the inferior vena cava sulcus and the center of the gallbladder fossa.

The liver comprises a total of eight parts, which are represented in the posterior and anterior sectors of the right lobe, the medial and lateral parts of the left lobe, and the inferior and superior parts of each of the two segments. Consequently, each of these eight distinct segments, have nearly a blood supply, are established as follows: (1) caudate lobe, (2) superior subsegment of the left lateral segment, (3) inferior subsegment of the left lateral segment, (4) left medial segment, (5) inferior subsegment of the right anterior segment, (6) inferior subsegment of the right posterior segment, (7) superior subsegment of the right posterior segment, (8) superior subsegment of the right anterior segment (Figure 4) (Cotoi and Quaglia, 2016).

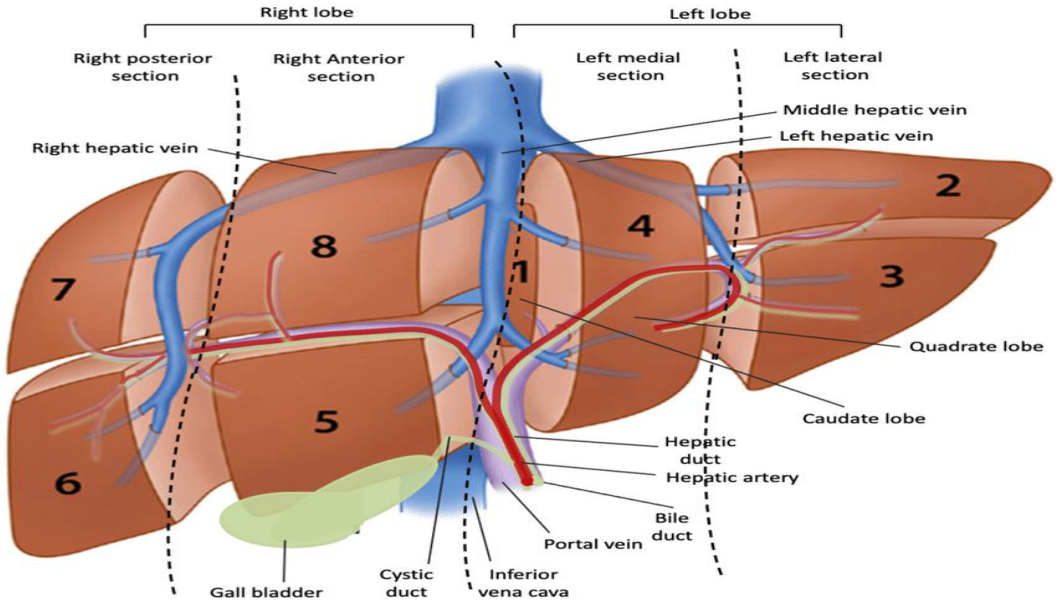

Figure 4: Anatomy of the liver (Survarachakan *et al*., 2022).

In general, the liver consists of five distinct types of specialized cells that can be categorized as either parenchymal or nonparenchymal (Table 2). The liver parenchyma is organized in hexagonal lobules at the cellular level. A portal triad is formed by the arrangement of branches of the hepatic artery, portal vein, and bile duct at the periphery of each lobule. The lobes contain thin-walled sinusoidal capillaries draining the portal triad toward a central vein (Figure 4). Each sinusoidal capillary is lined with specialized fenestrated endothelial cells that facilitate communication between the portal blood and the neighboring hepatocytes. Hepatocytes constitute the predominant mass of the liver, organized in cords encircling individual sinusoidal capillaries. They are accountable for many hepatic functions, encompassing synthesis, storage, and filtration of portal venous blood (Figure 5) (Juza and Pauli, 2014).

Table 02: Types of Hepatic Cell and Their Distinct Functions (Juza and Pauli, 2014).

Type of cells	Function
Parenchymal Hepatocytes	Primary cellular type of the liver. Synthesis, storage, degradation of portal substances, metabolic, endocrine, and exocrine functions
Nonparnchymal Sinusoidal endothelial cells Kupffer cells	Fenestrated plexus allows communication between portal blood and hepatocytes. Liver phagocytes, release of cytokines
Stellate cells	Role in regeneration post-injury, precursor to myofibroblasts, storage of vitamin A
Cholangiocyte	Transport bile, secrete bicarbonate, and Water

The liver possesses both endocrine and exocrine functions. it synthesizes bile, which the right and left hepatic ducts deliver to the gallbladder for storage, concentration, and release. Moreover, hepatocytes possess the capability to detoxify harmful chemicals and eliminate them via bile. The liver facilitates lipid metabolism, carbohydrates, and proteins; hormone degradation; and drug detoxification. It serves as a crucial supply for glycolysis, gluconeogenesis, and coagulation factors. Furthermore, it retains the body's biggest reserves of vitamin A and substantial quantities of vitamins D and B12 (Zhang *et al*., 2020).

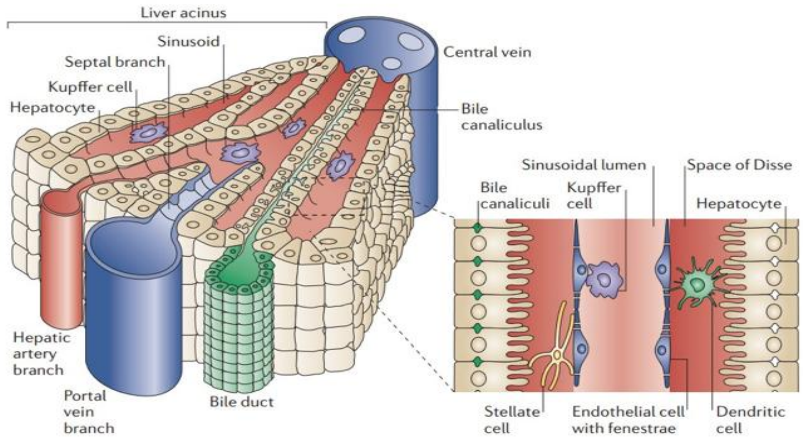

Figure 5: Architecture of a hepatic lobule (Adams and Eksteen, 2006).

2.1. Blood supply of liver

The primary blood vessels supplying the liver are the portal vein and hepatic artery, the former supplying roughly two-thirds of the total blood flow. The portal vein sequentially develops interlobar, segmental, interlobular veins and preterminal branches, with the terminal portal venules measuring about 20–30 μm in diameter and seen in the smaller triangular portal tracts. The vascular inflow from the portal veins is controlled by various sphincters. The hepatic artery branches accompany the portal vein and divide within the smaller portal tracts into two segments: the periportal plexus, which branches around the portal vein and drains into the sinusoids; and the peribiliary plexus, which provides blood supply to the accompanying interlobular bile ducts by way of small capillaries that are layered around the ducts. Various connections are seen between the small arterioles and the sinusoids that are most prominent in the periportal zone. The arterial flow depends on both sphincters and contractile mechanisms that define the degree of arterial versus portal venous blood flow, with the arterial flow varying inversely with the portal venous circulation (Sibulesky, 2013).

3. Anatomy and physiology of the kidney

The typical human kidneys are encapsulated organs weighing approximately 120–170 grammes and measuring 10–12 centimeters in length. The kidneys are situated in the retroperitoneum and are encased in significant perinephric fat and Gerota's fascia, which provide cushioning and protection for the organs. The kidney capsule (Glisson’s capsule) encases the kidney parenchyma but is discontinuous across the papillae within the renal sinus. This discontinuity serves as a significant pathway for the extension of renal tumors beyond the kidney. The kidney parenchyma can be divided into the cortex and the medulla in cut sections (Figure 5) (Akilesh, 2014).

a. **The cortex**: the renal cortex is filled distal convoluted tubules of nephrons. Here, clusters of them converge to create collecting ducts that extend into the renal medulla. The collecting ducts converge into bigger structures known as the papillary ducts. The renal cortex extends into the neighboring renal pyramids, creating the renal columns of Bertin (Moinuddin and Dhanda, 2015).
b. **The medulla:** The renal medulla consists of triangular tissue masses known as renal pyramids. Their bases are directed toward the convex surface of the kidney and apices of several of these pyramids open together into a renal papilla that bears the openings of

collecting ducts. The renal papilla extends into a secondary calyx (Moinuddin and Dhanda, 2015).

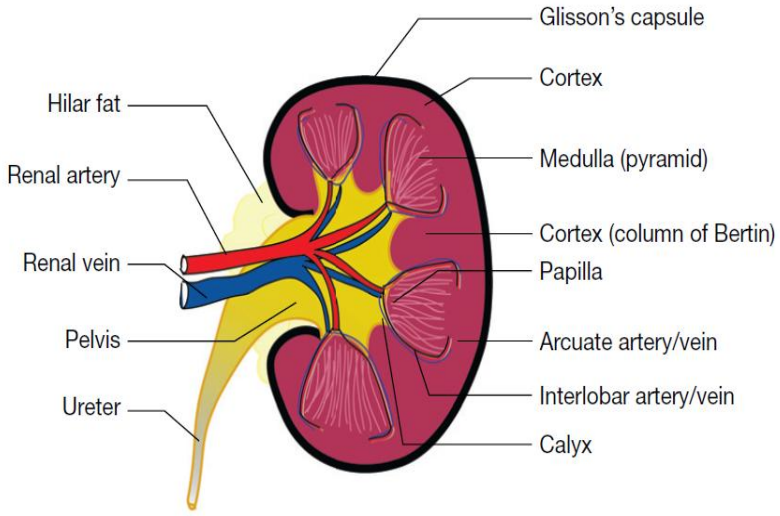

Figure 6: Internal anatomy of the kidneys (Akilesh, 2014).

3.1. The Nephron

The kidney's functional unit is the nephron, comprising a glomerulus and a tubule. Glomeruli are aggregates of specialized capillaries situated within the Bowman's capsule in the renal cortex. Blood enters the glomeruli via the afferent arteries and exits through the efferent arteries. Urine starts as a glomerular ultrafiltrate (blood excluding plasma proteins) that flows from the glomerulus to the tubule. The kidney tubule has several segments: the proximal tubule, the hairpin-shaped loop of Henle, and the distal tubule, which connect the glomerulus to the collecting duct that drains into the renal pelvis. As the glomerular ultrafiltrate moves through the tubules, its volume diminishes, and its composition alters due to tubular reabsorption and secretion. The urine flows into the renal pelvis, then through the ureter into the urinary bladder, where it is retained before to excretion (Figure 7) (Moorthy and Blichfeldt, 2009).

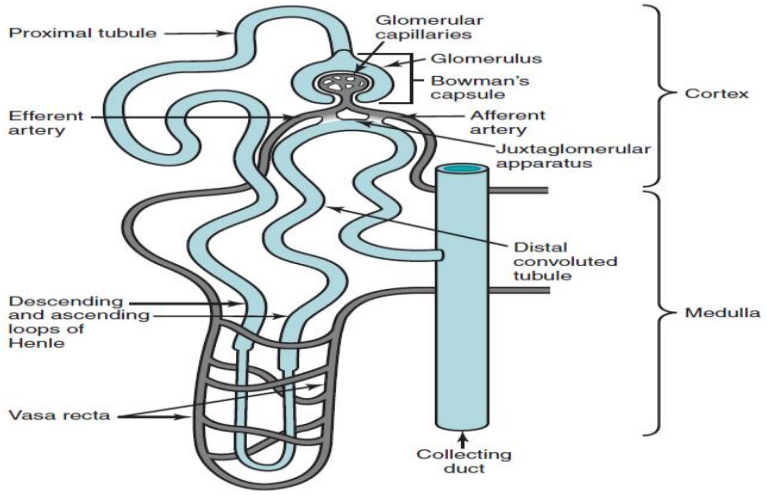

Figure 7: The anatomical configuration of the kidney, illustrating the nephron and its vascular supply (Moorthy and Blichfeldt, 2009).

3.2. Glomerular

Each kidney comprises around 1 million glomeruli, which collectively filter about 20% of cardiac output. The glomerular capillaries receive nearly all renal blood flow, and they filter 20% of this plasma. Bowman's capsule, which consists of an inner visceral epithelium encasing the capillaries and an outer parietal epithelium, surrounds the glomerular capillaries. Between these two membranes is a space, which is named Bowman's space and is where plasma filtrate begins its path down the nephron. Blood flows into the glomerular capillaries through the afferent arteriole and exits through the efferent arteriole (Figure 8) (Dean and Molitoris, 2019).

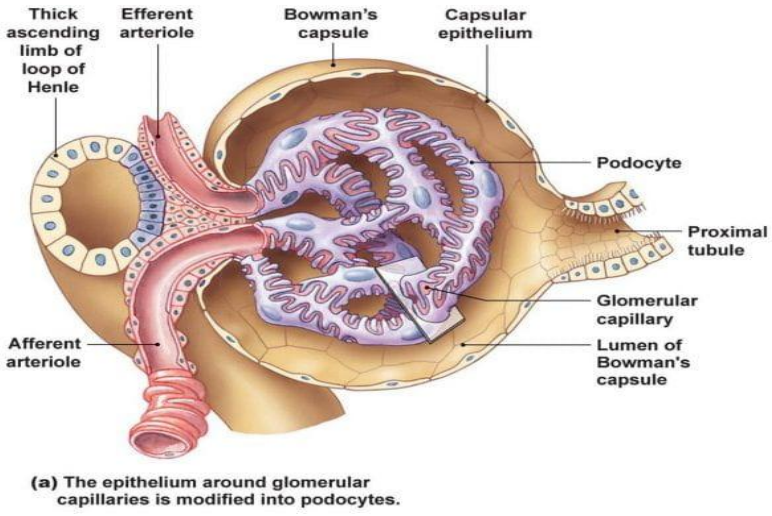

Figure 8: Glomerular structure **(**Fredric Coe, 2017).

3.2. The Functions of the Kidney

There are three primary classifications for renal function:

- The excretory function involves the elimination of metabolic waste products through urine.
- The endocrine function regulates the synthesis of erythrocytes in the bone marrow and triggers the activation of vitamin D.
- The homeostatic function involves regulating blood pressure, tissue osmolality, electrolyte and water equilibrium, and plasma pH levels.

Excretory and homeostatic functions are executed via a complex process involving filtration, reabsorption, secretion, and excretion (Patel, 2012).

4. Peptic ulcers

Peptic ulcers are lesions in the gastroduodenal mucosa. These ulcers cause significant distress by inducing abdominal pain and frequently result in gastrointestinal (GI) hemorrhage. PUD denotes ulcerative conditions affecting the lower esophagus, upper duodenum, and lower segment of the stomach (Dunlap and Patterson, 2019). PUD is a common illness that impacts 5–10% of the worldwide population, with notable racial and regional disparities.

4.1. Epidemiology

PUD continues to cause significant morbidity and mortality worldwide, with more than half of the world population infected (Shell, 2021). The incidence of PUD increases with age, with most ulcers occurring between 25 and 64 years of age (Dunlap and Patterson,2019). According to statistics on 735 patients in Algeria, the prevalence of *H. pylori* infection was 66.12%. The infection was more important in the age group 60–69 years (71.43%). The prevalence of H. pylori infection was statistically higher in women than men (69.3% *vs*. 60.7%, $p < 0.01$). *H. pylori* most commonly colonized the antral region (71.73%). In addition, the infection was associated mainly with atrophic gastritis (69.65%) (Kasmi *et al*., 2020).

4.2. Etiology

Even though it is strong and complex, the epithelial barrier can be changed by many things that are directly linked to impaired mucosal defense. These include acid secretion, bacteria and their byproducts, nonsteroidal anti-inflammatory medications, alcohol, ROS, and many chemical

substances. Their impact on the gastric barrier constitutes important mechanisms of the pathogenesis of gastric ulcers, chronic gastritis, and other gastric disorders, often arising from an imbalance between mucosal aggressive and protective forces (Silva and de Sousa, 2011). on the other hand, Anecdotal evidence indicates that a tendency for ulcer formation may be hereditary (Gelberg, 2014).

4.3. Pathophysiology

The pathophysiology of PUD can be understood as a complicated interplay between protective factors (such as the mucus-bicarbonate layer, prostaglandins, cellular regeneration, and blood flow) and harmful agents (including hydrochloric acid, pepsin, ethanol, bile salts, and certain drugs, ect) (Bertleff and Lange, 2010). Peptic ulcers are characterized as lesions in the stomach or duodenal mucosa and submucosa that penetrate through the muscularis mucosa. The epithelial cells of the stomach and duodenum release mucus in response to cholinergic stimulation or irritation of the epithelial surface. Foveolar cells synthesize mucus and bicarbonate, creating a gel barrier that is resistant to harmful agents like acid and pepsin. This layer is of paramount significance, as it deters the stomach from autodigestion. In cases of damage, supplementary mechanisms assist in preventing acid and pepsin from infiltrating the epithelial cells. For example, Augmented blood flow, eliminates acid that permeates the injured mucosa and ensures sufficient HCO3- concentration in the superficial gel layer next to epithelial cells. Epithelial cells also regulate intracellular pH by expelling excess hydrogen ions via ion pumps in the basolateral cell membrane (Figure 9) (Zatorski, 2017).

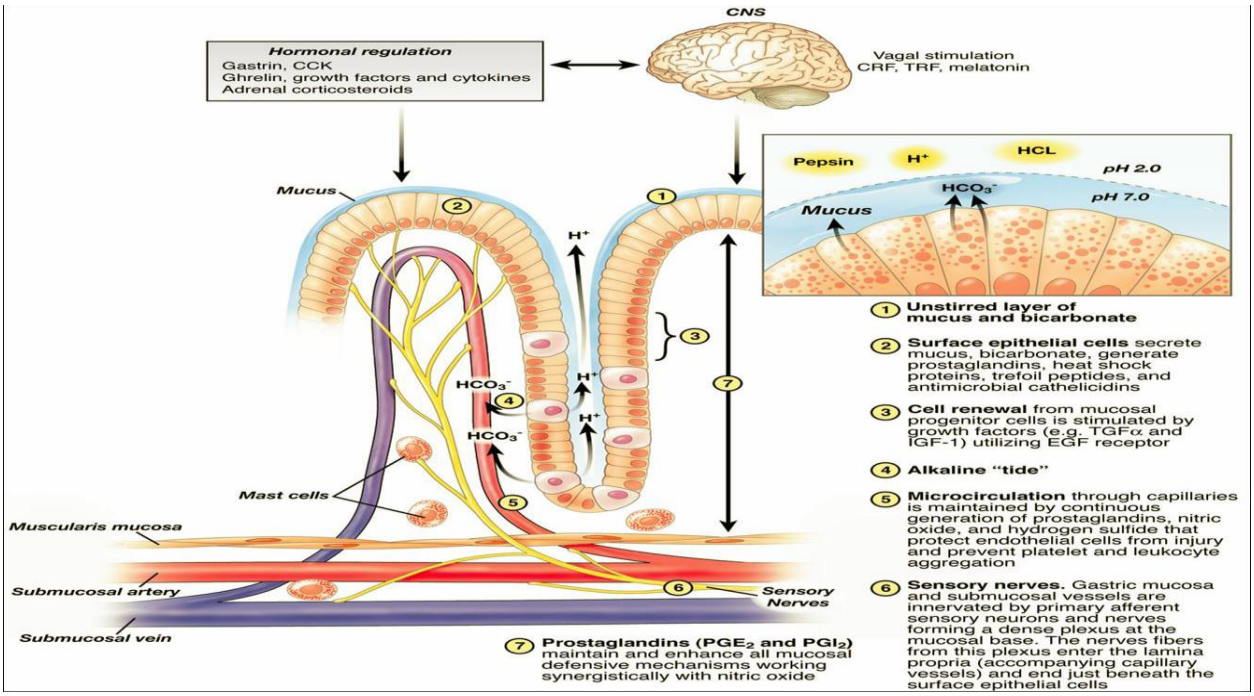

Figure 9: Gastric mucosal defense mechanism (Prajapati *et al.*, 2014).

4.4. The models of in *vivo* gastric ulcer

To assess the anti-ulcer (prevention of ulcer) effects of plants and drugs, valid experimental models are required. Models serve as valuable instruments for elucidating the pathophysiological mechanisms of wounds and the antioxidant capabilities of key pharmaceuticals or medicines with antiulcer characteristics. Consequently, the existence of multiple models for assessing antiulcer medications complicates the selection of a suitable model. The selection of a specific model is frequently determined by local resources, research aims, test hypotheses, or the enquiries posed by the researcher, given that each model possesses distinct advantages and disadvantages (Beiranvand, 2022).

Peptic ulcers may be generated by physiological, pharmacological, or surgical interventions in several animal species. Nonetheless, the majority of investigations in peptic ulcer research are conducted on rodents. Various models are employed experimentally to assess the antipeptic ulcer action of medicines or agents (Table 3).

Table 03: The different method-induced gastric ulcers (Adinortey *et al*., 2013; Fulga *et al*., 2019).

Surgical methods	**Chemically methods**	**Author methods**
pylorus-ligated-induced peptic ulcers	NSAIDs- (indomethacin, aspirin, and ibuprofen	water-immersion stress or cold-water-restraint or cold-restraint stress
gastric ulcers induced by ischemia reperfusion-	gastric ulcers produced by ethanol	Acetic acid-H. pylori-induced ulcers
	gastric ulcers produced by histamine	
	gastric ulcers produced by reserpine	
	gastric ulcers produced by serotonin	
	diethyldithiocarbamate- (DDC)-induced peptic ulcers	
	methylene blue-induced ulcers	
	ferrous iron-ascorbic acid-induced gastric ulcers	

4.5. Model of stomach ulcers caused by ethanol

Alcohol intake is frequently associated with stomach mucosal diseases, including gastritis, gastric ulcers, and gastric cancer (Arab *et al*., 2015).

The mechanism underlying ethanol-induced stomach ulcers is intricate and multifarious. Ethanol impairs mucosal cells by reducing mucus levels, decreasing the flow of blood to the mucosa, and excreting acid (utilizing a mechanism akin to histamine) (Beiranvand, 2022). Ethanol induces disruptions in cellular antioxidant mechanisms. For instance, it promotes the formation of superoxide anion and hydroperoxyl free radicals, hence elevating oxidative stress in the tissues, demonstrated by elevated concentrations of malondialdehyde, an indicator of elevated lipid peroxidation (Adinortey *et al*., 2013). Moreover, ethanol facilitates the formation of necrotic

lesions in the stomach mucosa by diminishing HCO_3^- output and decreasing mucus production (Beiranvand, 2022).

In addition, ethanol exacerbates gastric insult, by Activation of neutrophils which is associated with an upregulated inflammatory response with increased gastric expression of nuclear factor kappa B (NF-κB) which controls the generation of proinflammatory cytokines including tumor necrosis factor-α (TNF-α). These events amplify the inflammatory cascade by triggering other proinflammatory mediators' release and enhancing further recruitment of macrophages and neutrophils (Arab *et al*., 2015).

4.6. The treatment

Although the pathophysiology of conditions of gastric ulcer is varied, the control of gastric acid is important in their treatment (MacAllister, 1999). Since Karl Schwarz's dictum of no acid, no ulcer, the development of medical therapies has targeted gastric acid secretion and mucosal defense mechanisms. Many drugs have been used to treat ulcers, but few early treatments have stood the test of time. The most successful classes of drugs were those inhibiting gastric acid secretion. A second group of drugs targets the reinforcement of the mucosal barrier, primarily serving as protection against NSAIDs and aspirin. The current treatment for ulcers includes getting rid of H. pylori in peptic ulcers that are positive for it and using PPI to heal and stop peptic ulcers caused by drugs that are bad for the stomach. A small role exists for drugs that enhance mucosal resistance (Malfertheiner *et al*., 2009), antiulcer treatment options are summarized in table 4.

Table 04: Mechanisms of action and side effects of the most frequently utilized antiulcer therapies (Kuna, *et al*., 2019).

Medicine	Mode of Action	Negative Consequences	References
Proton Pump Inhibitors (Omeprazol, Rabeprazole, Esomeprazole, Lansoprazole, Pantoprazole)	Inhibition of H+/K+-ATPase (proton pump), the gastric, Enzyme system	Headache, Abdominal pain, Diarrhea, Nausea, Vomiting, Constipation, Flatulence, Vitamin B12 deficiency, Osteoporosis	(Mössner, 2016; Maes *et al*.,2017)
H2 Receptor Blockers Cimetidine Famotidine Nizatidine Ranitidine	Inhibiting the activity of histamine at the histamine H2 receptors of parietal cells	Headache, Anxiety, Depression Dizziness, Cardiovascular events Thrombocytopenia	(Pension, and Wormsley,1986)
Antacids Aluminum hydroxide Magnesium hydroxide	Elevates gastric pH above four and suppresses the proteolytic function of pepsin.	Frequency not defined: Nausea, Vomiting, Hypophosphatemia Chalky taste, Constipation, Abdominal cramping Diarrhea, Electrolyte imbalance	(Tsuchiya *et al*., 2017; Mizokami *et al*., 2018)
Potassium-competitive acid Blocker Vonoprazan **Cytoprotective Agents** Misoprostol Sucralfate	Inhibits H+, K+-ATPase in gastric parietal cells at the terminal phase of the acid secretion route. Induce mucus secretion and improve blood circulation within the gastrointestinal tract lining.	Nasopharyngitis, Fall, Contusion Diarrhea, Upper respiratory tract inflammation, Eczema, Constipation Back pain, Diarrhea, Abdominal pain Headache, Constipation	(Marks,1991; Chen *et al*., 2016)

5. Doxorubicin

Doxorubicin (DOX, Adriamycin) is a compound soluble in water characterized by an orange to red hue at neutral pH, photosensitive chemotherapeutic drug, extracted from *Streptomyces peucetius* var. caesius. Following its FDA clearance in 1974, DOX used singularly or in conjunction with other chemotherapeutic drugs, is extensively utilized as the primary treatment for numerous solid and metastatic tumors (Sritharan and Sivalingam, 2021).

5.1 Chemical structure

DOX is a non-selective class I anthracycline drug, consisting of two different moieties.

a. The aglyconic moiety consists of tetracyclic (anthraquinone) rings having a quinine-hydroquinone adjacent group and a methoxy substituted short chain followed by a hydroxy group.

b. a daunosamine and consisting of a 3-amino-2,3,4-trideoxy-L-fucosyl moiety, which is attached via a glycosidic bond to one of the tetracyclic rings.

Several active sites comprising three functional groups: Ketone, amine and hydroxyl are present in the structure. Besides hydrophobic interactions possible through the rings, the functional groups allow electrostatic interactions such as hydrogen bonds to occur between DOX and other molecules (Micallef, and Baron, 2020). (Figure 10)

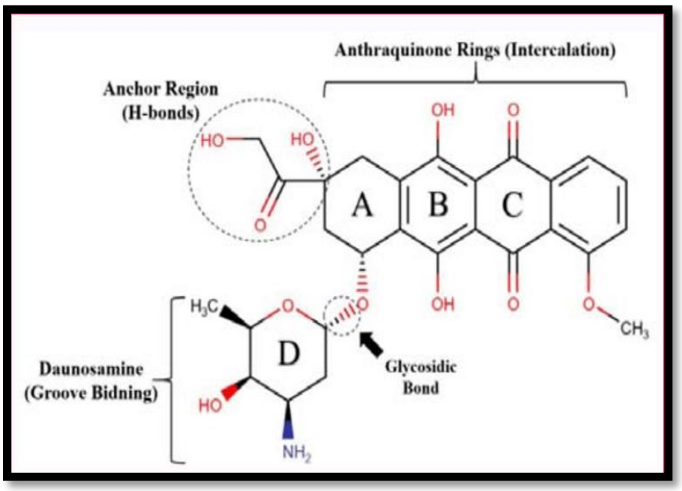

Figure 10: Doxorubicin's neutral chemical structure**.** Ring A is bound via a glycosidic bond to Ring D known as daunosamine, ring B is the hydroquinone, and ring C is the quinone (Micallef and Baron, 2020).

The utilization of doxorubicin is restricted because of its dangerous impacts on different organs, for example, heart causing cardiotoxicity and diabetic cardiomyopathy, liver causing hepatotoxicity, kidney causing nephrotoxicity, diabetes mellitus like condition, dysfunction of fat metabolism in adipose tissue, neurotoxicity, and fertility issues (Renu *et al*., 2022).

5.2. Mechanism of action and toxicity

Two suggested mechanisms exist by which doxorubicin exerts its effects in cancer cells: DOX like other anthracyclines, is an intercalating agent which (i) penetrates the interstitial region between the DNA base pairs. Furthermore, these molecules are inhibitors of type II DNA

topoisomerases, enzymes involved in the maintenance of the three-dimensional structure of the DNA during transcription and of the phenomena of replication. Complex DNA /topoisomerase strands are stabilized thereby preventing DNA replication (Bengaied *et al*., 2017). (ii) production of free radicals and their detrimental effects on cellular membranes, DNA and proteins. (*Thorn et al*., 2011). (Figure 11)

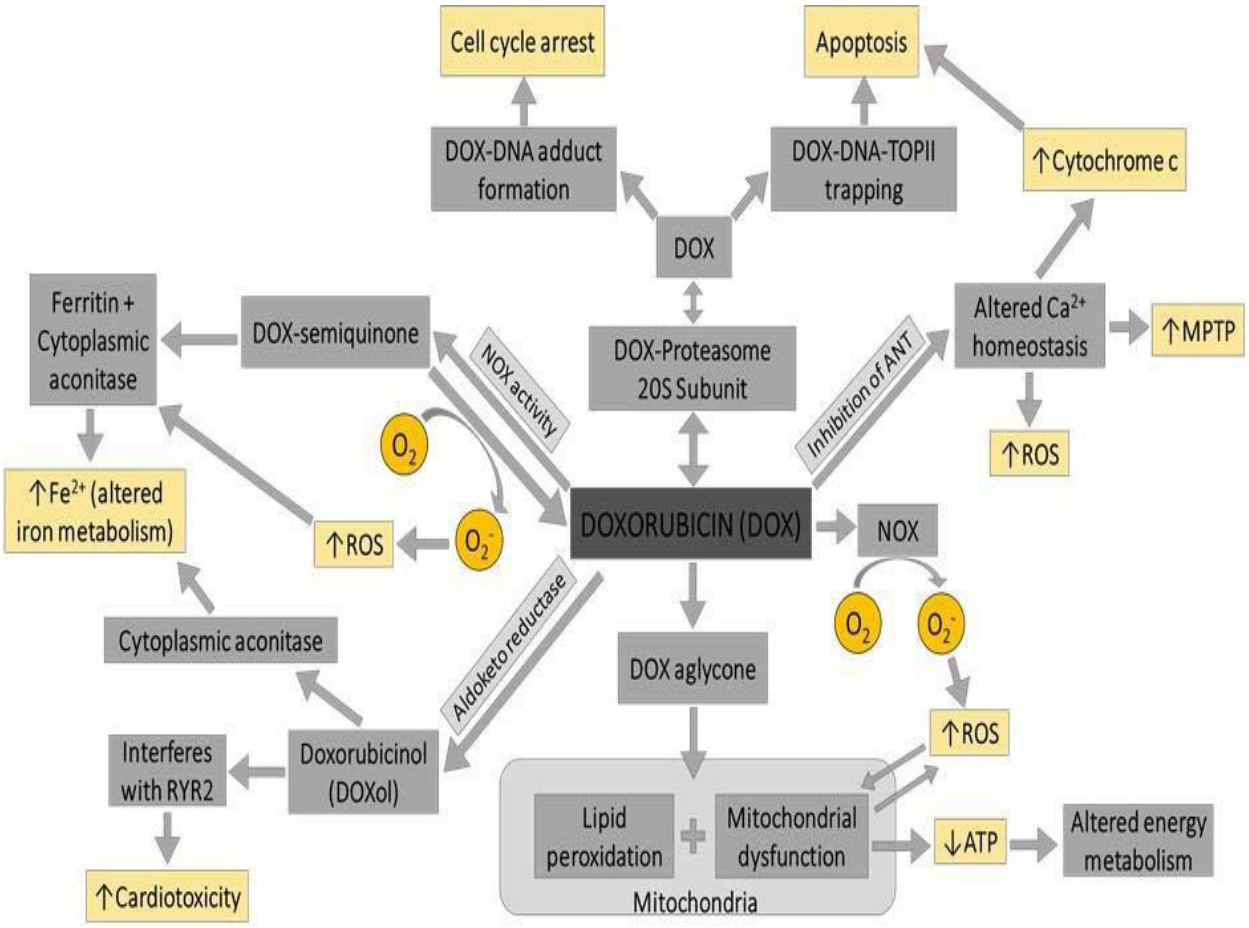

Figure 11: Molecular mechanisms initiated by DOX (Micallef and Baron, 2020).
Abbreviations: ATP: Adenosine Triphosphate; Ca2+: Calcium; Fe2+: Iron; NOX: NAD(P)H Oxidase; O_2: Oxygen; O2-: Superoxide Anion; MPTP: Mitochondrial Permeability Transition Pore; ROS: Reactive Oxygen Species; RYR2: Cardiac Calcium Release Channel.

5.3. Molecular processes behind doxorubicin-induced hepatotoxicity

Elevated serum levels of ALT, AST, and GGT are primary indicators of liver injury. Examining the molecular mechanisms by which doxorubicin induces liver damage involves, the activation of genes associated with oxidative stress response, DNA damage, DNA repair, drug transport, cell cycle progression, mitochondrial malfunction, and apoptosis (Prasanna *et al*., 2020).

The DOX-induced formation of ROS, may activate IκB kinase (IKK), which phosphorylates IκB inhibitors, so activating IκB. This activation subsequently triggers NF-kB, resulting in the release of proinflammatory cytokines and ultimately leading to cell death. On the other hand, increased ROS generation results in heightened lipid peroxidation and elevated activity of SOD, CAT, and glutathione peroxidase (GPx), DNA damage, and a decrease in GSH and vitamin E levels, which confirm DOX hepatotoxicity (Figure 12) (Carvalho *et al*., 2009).

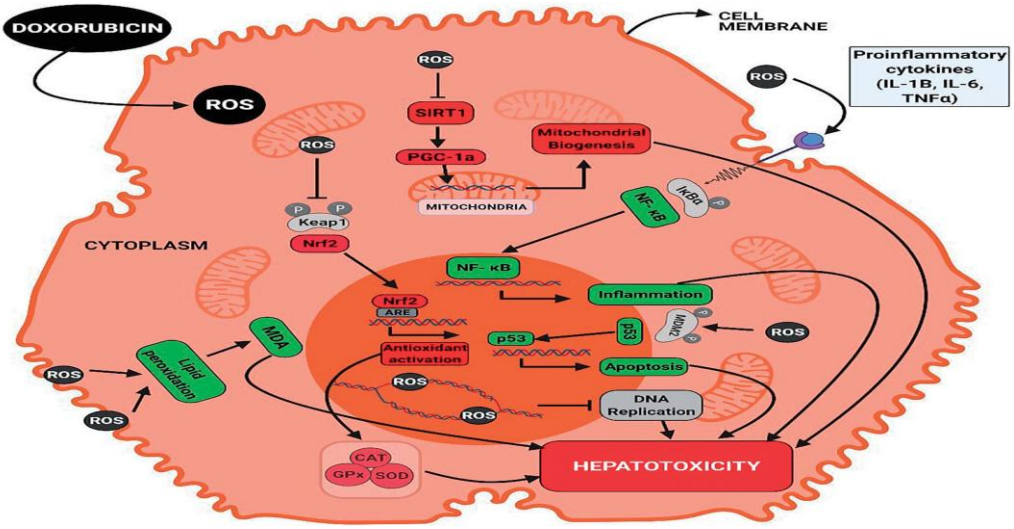

Figure 12: The molecular processes underlying doxorubicin-induced hepatotoxicity (Rivankar, 2014; Renu *et al*., 2022).

5.4. Doxorubicin-induced nephrotoxicity

The kidney is one of the principal homeostatic organs of the body. DOX disrupts glomerular podocytes, resulting in their damage, and subsequent nephropathy. The most common events promoted by DOX treatment is the presence of severe proteinuria. The predominant occurrences associated with DOX medication include severe proteinuria, elevated plasma creatinine levels, hypoalbuminemia, dyslipidaemia, hypercoagulability, increased kidney size, and enhanced glomerular capillary permeability. DOX disrupts mitochondrial function, resulting in diminished activities of mitochondrial complexes I and IV, elevated citrate synthase activity, and increased levels of triglycerides and superoxide (O2•-). DOX can induce lipid peroxidation and diminish the amounts of antioxidant molecules, specifically vitamin E and reduced glutathione (GSH), which may contribute to DOX-induced nephropathy (Carvalho *et al*., 2009). The DOX activates the MAPK signaling system, which then stimulates the pro-inflammatory NF-jB

signaling pathway and facilitates the production of inflammation-promoting cytokines, including IL-1b, TNF-ά, and adiponectin, ultimately leading to renal tissue inflammation. Conversely, the downregulated FXR concurrently increases the NF-kB signaling pathway. Ultimately, all activities culminate in the activation of the apoptotic pathway by enhancing the expression of pro-apoptotic factors such as Bax (Figure 13) (Renu *et al*., 2022).

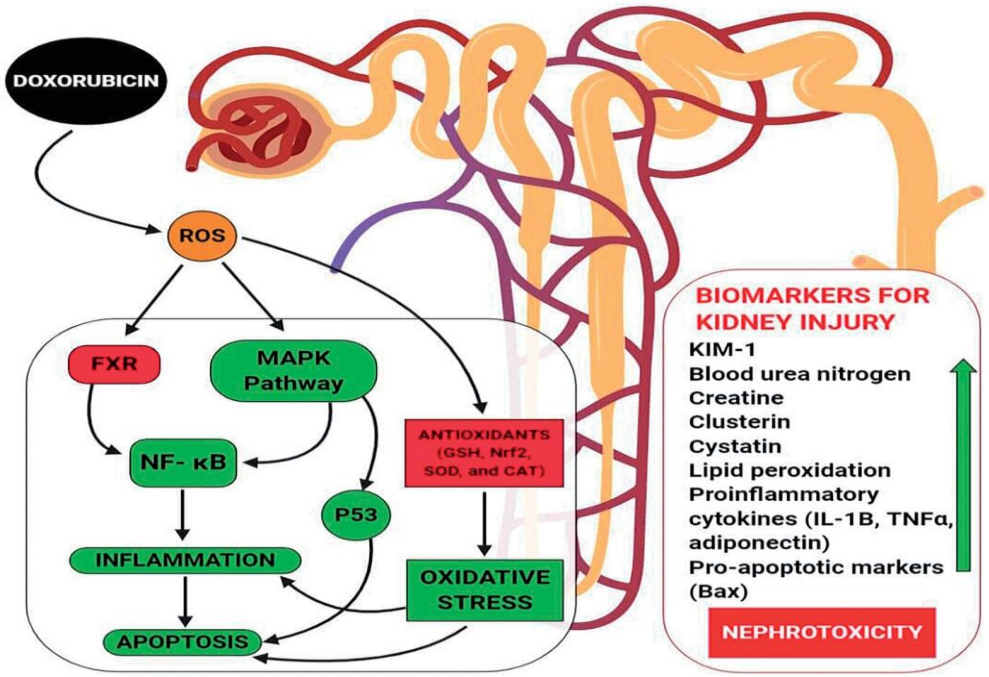

Figure 13: Nephrotoxicity resulting from oxidative stress caused by ROS following doxorubicin administration (Renu *et al*., 2022).

6. Oxidative stress

Oxidative stress, defined by an imbalance favoring the production of free radicals over their removal, is a fundamental factor in the development of chronic diseases and ageing (Jomova *et al*., 2023).

Scientific evidence supports the significant, impact of oxidative stress on the progression of several illnesses (Figure14), encompassing metabolic syndrome, atherosclerosis, cardiovascular disease, cancer, neurodegenerative illnesses, diabetes, infertility, renal diseases, as well as gastrointestinal and hepatic diseases. (Vona *et al*., 2021).

Oxidative stress leads to disease through two primary processes. The initial process entails the generation of reactive species during oxidative stress—specifically •OH, ONOO−, and

HOCl—that directly oxidize macromolecules, including membrane lipids, structural proteins, enzymes, and nucleic acids, resulting in abnormal cellular activity and apoptosis. The second mechanism of oxidative stress is aberrant redox signaling (Box 2). Oxidants, especially H_2O_2 produced by cells under physiological stimulation, may function as second messengers. In oxidative stress, non-physiological generation of H_2O_2 can lead to redox signaling to go awry (Forman, and Zhang, 2021).

Figure 14: Oxidative stress is a fundamental cause of multi-organ damage (Sena *et al*., 2022).

6.1. Free radicals

Free radicals are chemical species that possess at least one unpaired electron in their outer shell, resulting in heightened reactivity. The predominant free radicals and reactive molecules in biological systems originate from oxygen (reactive oxygen species, ROS) and nitrogen (reactive nitrogen species, RNS). (ROS) or (RNS) are generated during electron transfer reactions through the loss or gain of electrons (Jomova *et al*., 2023). ROS and RNS may be radicals or non-radical compounds (Table 5).

Table 05: Main ROS and RNS generated during metabolism (Martemucci *et al*., 2022).

ROS		RNS	
Radicals			
Name	**Symbol**	**Name**	**Symbol**
Superoxide	**$O^{\bullet-}$**	**Nitric oxide**	**NO•**
Hydroxyl	**·OH**	**Nitrogen dioxide**	**NO_2•**
Hydroperoxyl	**HO_2•**	**Nitrate radical**	**NO3•**
Peroxyl	**ROO•-**		
Alkoxyl	**RO•-**		
Organic hydroperoxide	**ROOH**		
Non-radicals			
Hydrogen peroxide	**H_2O_2**	**Nitrous acid**	**HNO_2**
Ozone	**O_3**	**Nitrosonium cation**	**NO+**
Singlet oxygen	**(^{1}O2Dg)**	**Nitroxyl anion**	**NO-**
Hypochlorous acid	**HOCl**	**Peroxynitrite**	**ONOO-**
Peroxynitrite	**ONOO-**	**Dinitrogen trioxide**	**N_2O_3**
		Dinitrogen tetroxide	**N_2O_4**
		Peroxynitrous acid	**ONOOH**
		Nitryl chloride	**NO_2Cl**

Free radicals have an essential role in numerous biological processes. Many of these are necessary for life, including the intracellular elimination of bacteria by phagocytes, particularly granulocytes and macrophages. Researchers believe that free radicals are also involved in some cellular signaling processes, known as redox signaling. At low to- moderate amounts, ROS are beneficial both in regulating processes involving the maintenance of homeostasis as well as a wide variety of cellular functions (Sharifi-Rad *et al*., 2020).

6.2. Production of free radicals in cells

Free radicals are produced from either endogenous or exogenous sources. Exogenous free radicals originate from cigarette smoke, environmental pollutants, pesticides, herbicides, ultraviolet radiation, alcohol, heavy metals, and specific chemotherapeutic agents (e.g., doxorubicin, cyclosporine, tacrolimus), industrial solvents, cooking, and gamma-irradiation (Figure 15). (Santo *et al*., 2016).

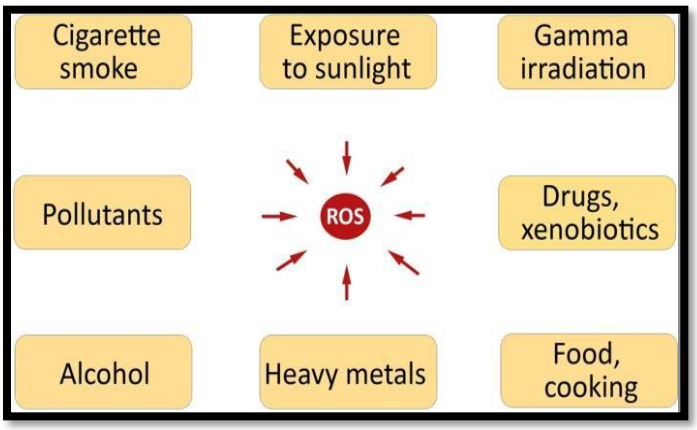

Figure 15: Exogen sources of free radicals (Santo *et al*., 2016).

The primary source of free radicals originates from our own bodies. Free radicals are continuously generated in cells due to both enzymatic and nonenzymatic processes. Enzymatic reactions that generate free radicals encompass those occurring in the mitochondrial respiratory chain, the cytochrome P450 system in the endoplasmic reticulum, oxidative processes in peroxisomes and during phagocytosis, as well as those catalyzed by transition metal ions (Figure 16) (Santo *et al*., 2016).

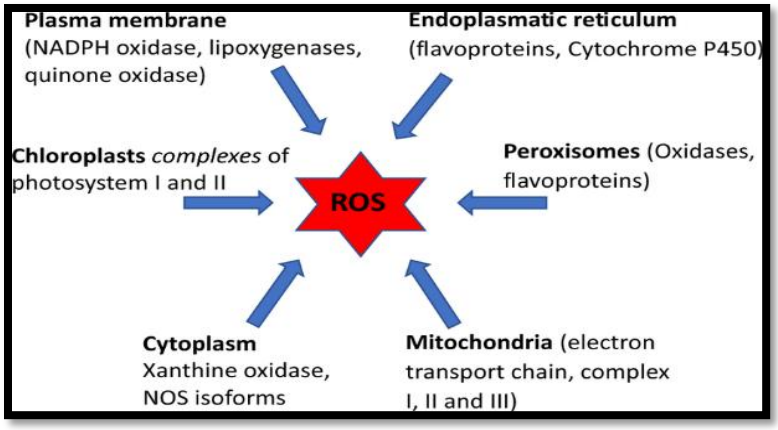

Figure 16: Main cellular sources of ROS formation **(**Jomova *et al*., 2023).

7. Antioxidants

Antioxidants are molecules that suppress or neutralize free radical processes, thereby preventing or mitigating cellular harm. Although antioxidant defenses are different from species to species, their existence is universal. Antioxidants exist both in enzymatic and non-enzymatic forms in the intracellular and extracellular environment (Nimse and Palb, 2015). The mechanism of the antioxidant activity of a phenolic compound could be either through a transfers H-atom (HAT) mechanism or single-electron transfer via proton transfer (SET-PT) or sequential proton loss electron transfer, transition metal chelation (TMC) (Zeb, 2020).

Antioxidants are generally divided into nonenzymatic antioxidants (metabolic antioxidants such as uric acid, reduced glutathione (GSH), bilirubin, transferrin, coenzyme Q10, lipoic acid, and nutrient antioxidants such as vitamins A, C, E, flavonoids, carotenoids, trace metals (manganese, zinc, selenium), omega- 6 and omega-3 fatty acids), and enzymatic antioxidants (such as catalase (CAT), superoxide dismutase (SOD), and glutathione peroxidase (Figure 17) (GPx) (Parcheta *et al*., 2021; Jomova *et al*., 2023).

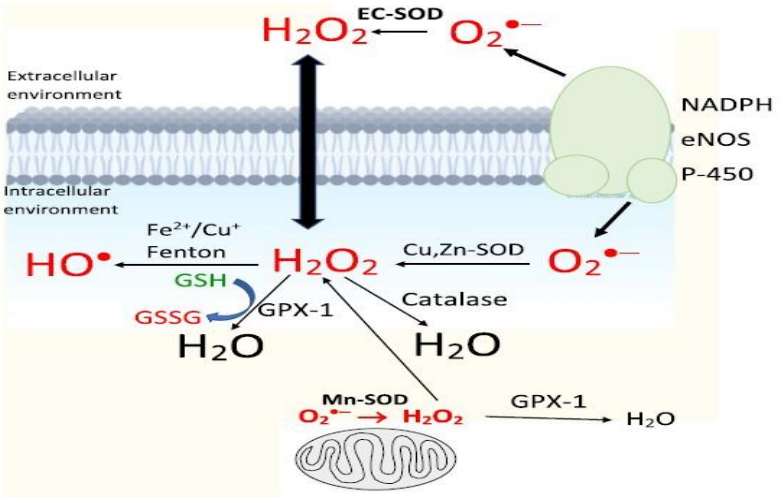

Figure 17: Coordinated activity of Glutathione peroxidase-1, Catalase, and Superoxide dismutase (Jomova *et al*., 2023).

7.1 Phenolic compounds

Phenolic compounds (PC), recognized for their multifunctional bioactivity, are extensively distributed across the plant world. The majority of phenolic compounds are essential components of the human diet and are also ingested as therapeutic formulations (Gulcin, 2020). In terms of chemical features, PC are formed by one or more aromatic rings bonded to one or more hydroxyl

groups; resulting in different chemical structures; these compounds are divided into different groups (Figure18) (Albuquerque *et al*., 2021).

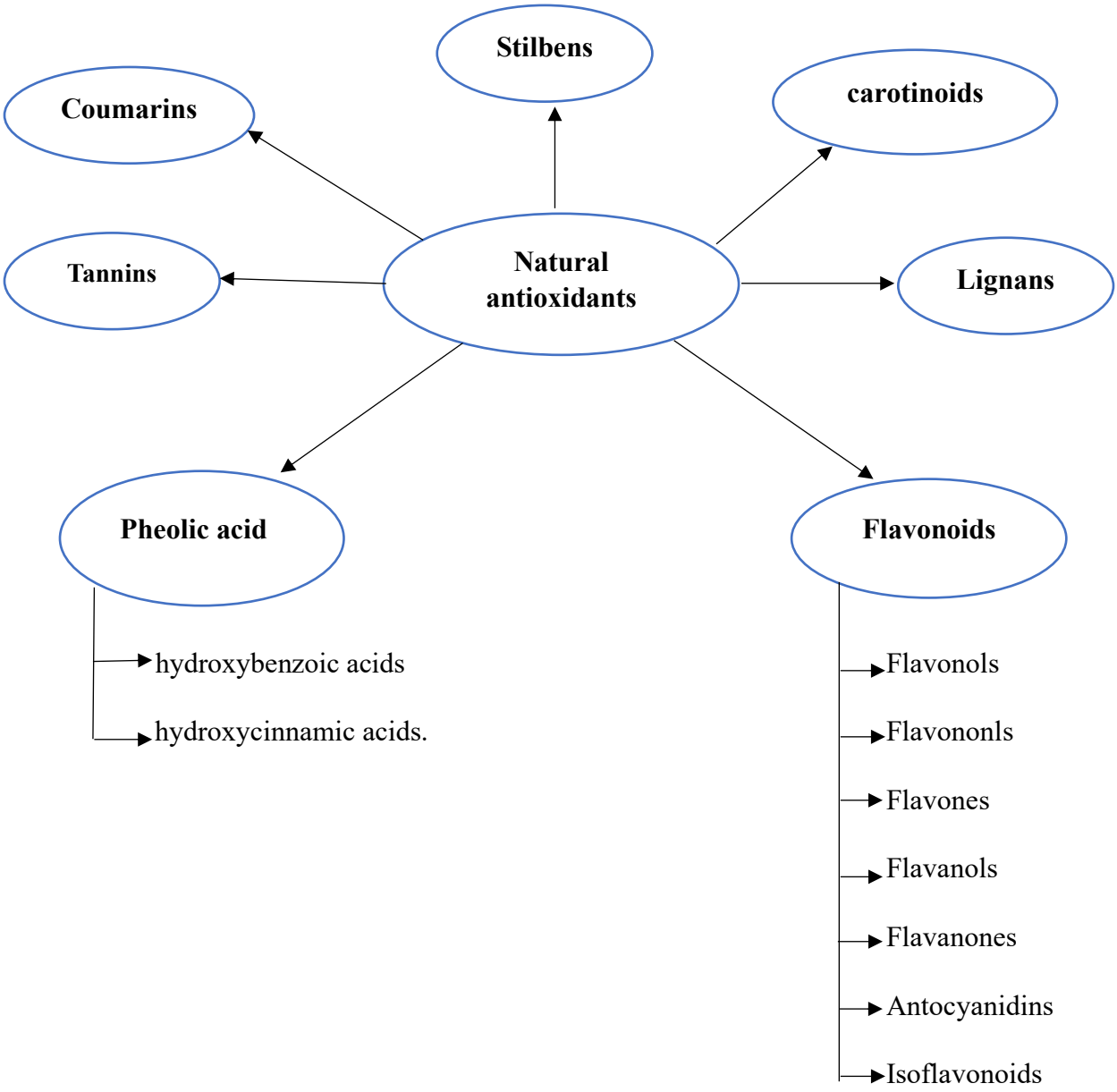

Figure 18: Classification of phenolic antioxidants (Gulcin, 2020).

Phenolic acids generally account for around one-third of total phenolic consumed, whereas flavonoids represent the remaining two-thirds. Phenolic compounds, whether individually or in conjunction with vitamins such as carotenoids, vitamin E, and vitamin C, function as antioxidants, safeguarding diverse tissues in the human body from oxidative stress. Polyphenols are the predominant antioxidants present in diets rich in fruits and vegetables. Gallic, ellagic, protocatechuic, and 4 hydroxybenzoic acids are the most common benzoic acids consumed by humans, whereas caffeic, ferulic, sinapic, and p-coumaric acids are the most common cinnamic acids. Plant-based diets are often rich in polyphenols, offering nutritional benefits and safeguarding against the development of chronic diseases (Rahman *et al*., 2021).

Food processing procedures, such as blanching and thermal treatments, might alter polyphenol levels or facilitate their conversion into secondary metabolites. Enzymatic and nonenzymatic reactions can activate the absorption and metabolism of phenolics, in addition to molecular changes that might occur during food production (Figure 19). Conjugation reactions may also increase or decrease the bioavailability of these molecules (Minatel *et al*., 2017).

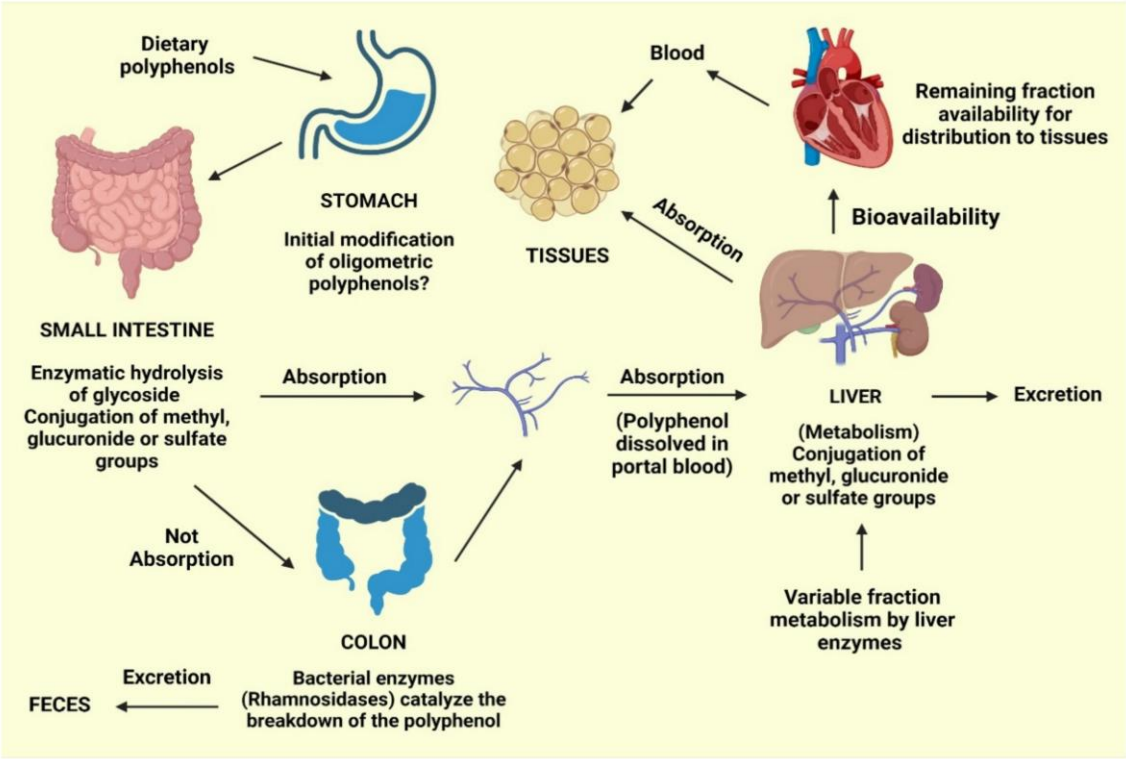

Figure 19: Anticipated pathways for the assimilation of dietary phenolics (Minatel *et al*., 2017).

8. *Allium sphaerocephalon* L.

The genus Allium L. is among the major genera within the Amaryllidaceae family, comprising over 1000 species that are distributed to the Northern Hemisphere. The primary center of variety is situated between Southwest and Central Asia and the Mediterranean areas (Jang *et al*., 2024).

Allium sphaerocephalon L. (round-headed leek) is a herbaceous, perennial plant with large, globe shaped flower heads that inhabits insolated rocky slopes, sandy ground, vineyards and dry shrubby habitats (Figure 20). Numerous literary sources document the ethnobotanical applications of A. *sphaerocephalon*. The entire plant is utilized as a condiment and as a substitute for onion (*A. sativum*) (Lazarević *et al*., 2011). *Allium sphaerocephalon* L. species are found in Algeria and Tunisia, Egypt, Sicily, Malta, Southern Greece, and Albania (Tornadore, 1989).

Allium sphaerocephalon L. species had antioxidant and antimicrobial, Antibiofilm, and Antimutagenic properties (Lazarević *et al*., 2011; Ceylan, 2014).

- Kingdom: Plantae
- Phylum: Trachephyta
- Class: Liliopsida
- Order: Asparagales
- Family: Amaryllidaceae
- Genus: Allium L.
- Species: *Allium sphaerocephalon* L. (Linnaeus, 1797).

Figure 20: *Allium sphaerocephalon* L**.** (Web site).

Chapter 2:

Phenolic profiles and antioxidant activities of *Allium sphareocephalon* L.

1. Materials

1.1. Vegetative matter

A. sphaerocephalon L. naturally growing plant, was obtained in July 2018 at Megress district of Setif. Professor Smain Amira from the Department of Animal Biology and Physiology at Setif 1 University, Algeria, carried out the taxonomic identification of the plant. A voucher number 81 A.S. 02/07/18 set/SA/ was deposed at the laboratory of Phytotherapy Applied to Chronic Diseases, Faculty of Nature and Life Sciences, University of Setif 1, Algeria.

2. Methods

2.1. Methods of extraction

2.1.1. Hydro-ethanolic extract

We macerated 500 grams of flowers powder in 1000 milliliters of 80% ethanol for three days at room temperature while being constantly agitated to produce the hydro-ethanolic extract of flowers (ASHE). The mixture underwent filtering, condensing in a vacuum evaporator, and oven drying at 38°C (Markham,1982).

2.1.2. Aqueous extract

The aqueous extract (AQE) was prepared using the methodology outlined in Kaoudoune *et al*. (2022). Ten grams of powdered flower parts were boiled for twenty minutes with agitating magnetically in 200 milliliters of distilled water. Subsequently, the blend was filtered using Wattman filter paper N°1, then the resulting dried extract (AQE) was next examined for pharmacological characteristics.

1.2. Extraction yield

The weight difference between the extract's and the treated plant's weight is known as the plant extract yield. It is represented as a percentage, and was computed using the following Eq.:

$$\text{Extraction yield } (\%) = \frac{M_1}{M_2} \times 100 \qquad (1)$$

Were, M_1- weight of sample extract, g

M_2- weight of sample, g

2.3. Phenolic compounds

2.3.1. Measurement of total phenolic content

Folin–Ciocalteu reagent (FCR) was utilized to evaluate total phenolic content (TPC) in accordance with the method described by Müller et al. (2010). A well microplate containing 100 µL of diluted FCR (1:10) was filled with a volume of 20 µL of extract or different concentrations of standard. A further addition of 75 µL of 7.5% sodium carbonate was made. Two hours later, in low light conditions and at a stable ambient temperature. A Perkin Elmer 96-well microplate reader (USA) was then used to measure the absorbance at 765 nm. The TPC was represented as µg gallic acid equivalent for every milligram of extract (Figure 21).

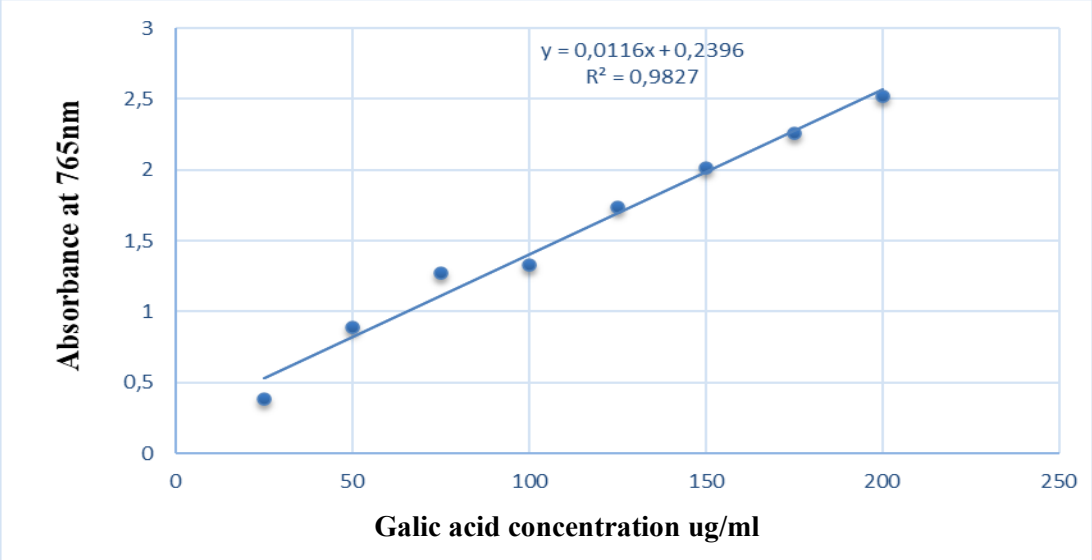

Figure 21: Standard curve of gallic acid for quantifying total polyphenols in AS extracts. Each value represents mean ± SD (n=3).

2.3.2. Determination of the overall amount of total flavonoid

The aluminum nitrate (Al (NO3)3) reagent was used to measure the total flavonoid content (TFC) according to Topçu *et al*. (2007). A 96-well microplate was filled with a volume of 50 µL of every extract, 130 µL of methanol, 10 µL of potassium acetate, and 10 µL of aluminum nitrate. After 40 minutes of incubation, the mixture's absorbance at 415 nm was measured. The TFC was represented as µg QE/mg E, or quercetin equivalent per milligram of extract (Figure22).

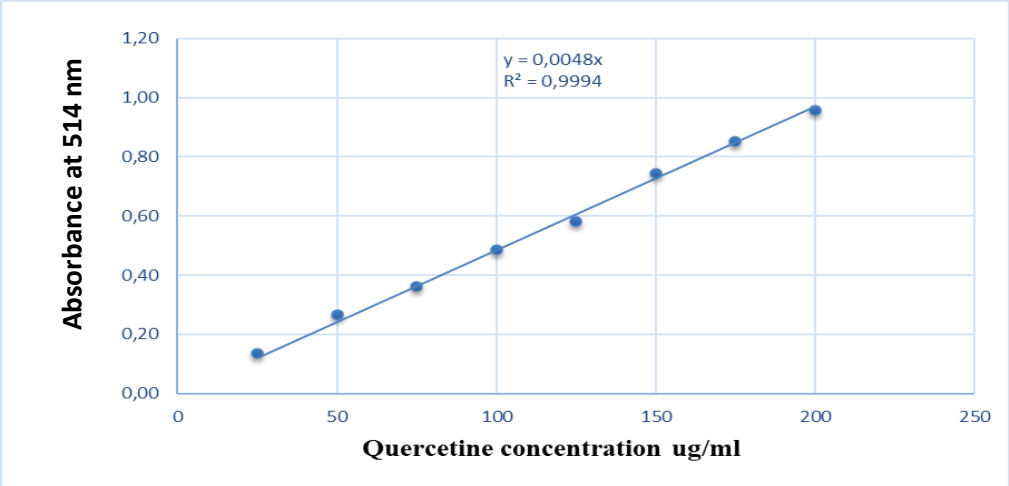

Figure 22: Standard curve of quercetin for the determination of flavonoids in AS. extracts. Each value represents mean ± SD (n=3).

2.3.3. Total Tannins Content

Total tannin content (TTC) was evaluated by Vanillin pursuant to the methodology defined by Hagerman (2002). In the 96-well microplate, a volume of 25 µL of the extract was mixed with 150 µL vanillin (4%, dissolved in methanol) and 75 µL HCl (30%). The mixture was incubated at 30°C for 15 min and then the absorbance was measured at 500 nm using a PerkinElmer 96-well microplate reader (USA). The TTC was expressed as µg catechin equivalent per mg of extract (µg CE/mg E). (Figure23).

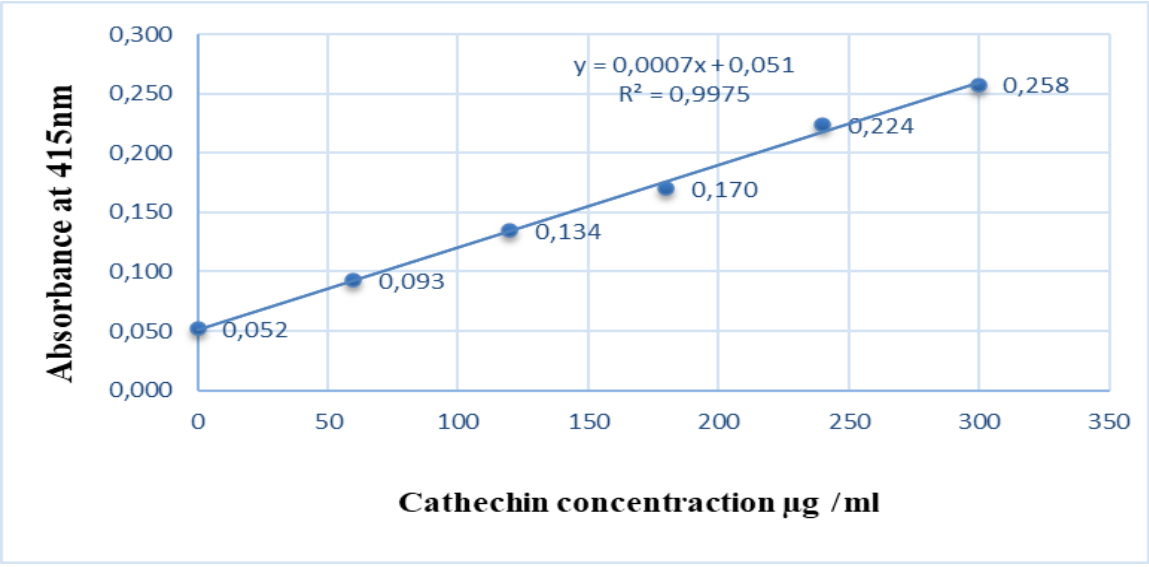

Figure 23: Standard curve of cathechin for quantifying total tannin in AS extracts. Each value represents mean ± SD (n=3).

2.4. Identification and quantitation of phenolic compounds of the ASHE extract

The studies were conducted using a previously established and validated liquid chromatography-mass spectrometer/mass spectrometry (LC-MS/MS) technology (Yilmaz, 2020). A Shimadzu-Nexera model ultrahigh performance liquid chromatograph (UHPLC) coupled with a tandem mass spectrometer was used to accomplish quantitative evaluation of phytochemicals. The reversed-phase UHPLC was equipped with an autosampler (SIL-30AC model), a column oven (CTO-10ASvp model), binary pumps (LC-30AD model), and a degasser (DGU- 20A3R model).

2.5. Assessment of the anti-oxidant capacity

2.5.1. DPPH radical scavenging test

The approach outlined by (Blois,1958), was used to determine this activity. In a 96-well microplate, 160 µL of DPPH reagent (0.006%) was combined with 40 µL of various extract concentrations or the standard solution. Following that, the mixture was allowed to remain at room temperature in the dark for 30 minutes, at which point the absorbance at 517 nm was measured. Eq. (2) was used to compute the percent inhibition.

$$\% \text{ inhibition} = \frac{(\text{A of control-A of sample})}{\text{A of control}} \times 100$$

(IC_{50} refers to the concentrations at which 50% of the DPPH radical was scavenged).

2.5.2. Ferrous ion chelating activity

To summarize, 50 µL of $FeCl_2$ (0.6 mM) and 450 µL of methanol were combined with 250 µL of various extract concentrations or an EDTA solution. After five minutes, 50 µL of ferrozine (5 mM) was added to begin the reaction. Let the mixture sit for 10 minutes at room temperature. The produced Fe^{2+}-ferrozine complex's absorbance was measured at 562 nm, and Eq. (3) was used to report the chelating activity as a percentage of inhibition. (Benchikh *et al*., 2022).

Where, AS and AC represent the absorbance values of the control and test sample, respectively.

$$Fe_2\text{chelating effect}(\%) = \frac{(\text{AS-AC})}{\text{AC}} \times 100 \qquad (3)$$

2.5.3. Method of bleaching β-carotene

The β-carotene bleaching technique as outlined by Mamache *et al*. (2020) was used to calculate how well the molecules of antioxidants in the extract blocked the oxidation of β-carotene. The β-carotene/linoleic acid emulsion stock solution was prepared by first combining 25 µL of linoleic acid, 200 mg of Tween 40, and β-carotene solution (containing 0.5 mg of β-carotene dissolved in 1 mL of chloroform). Following this, chloroform was extracted via vacuum evaporation. The residue was combined with 100 mL of oxygenated distilled water for 30 minutes. After a vigorous shake of the mixture, 2.5 mL of this blend was incorporated and thoroughly mixed with 350 µL of BHT or flowers' extract (2 mg/mL). The absorbance was calculated at 490 nm at zero, one, two, four, six hours, and after 1 day. (Shimadzu1601). This formula (Eq. (4) has been used to calculate the antioxidant activity (AA):

$$AA = 1 - \frac{(AS_0 - AS_t)}{(AC_0 - AC_t)} \times 100 \qquad (4)$$

Where AS_0 and AC_0 are, in the order mentioned, the absorbance levels of the test sample and the control after zero minutes of incubation. The absorbance of the test sample A_{St} and the control A_{Ct} are calculated after incubation for 24 hours.

2.5.4. Reducing power assay

Method (Oyaizu,1986), was used to determine the extract's reducing power. 10 µL of various concentrations of extracts or the standard solution was added to 40 µL of 0.2 M phosphate buffer (pH 6.6) and 50 µL of potassium ferricyanide (1%). After 20 minutes of incubation at 50 °C, the solution was supplemented with 50 µL of trichloro acetic acid (TCA, 10%), combined with 40 µL of distilled water and 10 µL of ferric chloride (0.1%). The absorbance at 700 nm was then measured.

2.5.5. Cupric reducing antioxidant capacity

The extracts' cupric-reducing capacity was determined using the procedure described by Apak *et al.* (2004). 50 µL of Cu2+ solution (10 mM) was combined with 60 µL of ammonium acetate buffer (1 M, pH 7.0) and 50 µL of neocuproine solution (7.5 mM). The mixture was added to 40 µL of the sample solution of each extract at different concentrations. The absorbance at 450 nm was measured using a 96-well microplate reader after 60 minutes in the absence of light, with

a reagent blank as reference. The positive control utilized was BHT. The findings were reported as the EC_{50} value (µg/mL) corresponding to the concentration indicating 50% of absorbance.

2.6. Statistical analysis

The data was shown as means ± standard deviation (SD). In three determinations (n=3), every measurement was performed. Using Graph Pad Prism 8.00, we conducted an analysis of variance using the student's and one-way ANOVA tests. Statistical significance was assumed at the 0.05 level.

3. Results

3.1. Phytochemical analysis

The results of extraction yield, TPC, TFC, and TTC of *A. sphaerocephalon* L. ASHE and AQE were summarized in table 6.

The yield percent from the EOH was higher (18.30%) than the AQE (11.80%). The results show that ASHE had the highest TPC level (12.73 ± 0.91 µg GAE/mg DW) than AQE (9.71 ± 0.53 µg GAE/mg DW). In addition, ASHE had a higher TFC level (7.67 ± 0.53 µg QE/mg) than AQE (5.68 ± 0.90 µg QE/mg). Whereas the TTC for both extracts is close in quantity.

Table 06: Extract yields of total phenolics, flavonoids, and tannins content of ASHE and AQE.

	ASHE	**AQE**
Extract yield (%)	18.30	11.80
TPC (µg GAE/mg DW)	12.73 ± 0.91	9.71 ± 0.53
TFC (µg QE/mg DW)	7.67 ± 0.24	5.68 ± 0.90
TTC (µg CE/mg DW)	17.02 ± 0. 20	16.54 ± 0.41

ASHE: Hydroethanolic extract, AQE: Aqueous extract, DW: Dry weight.

3.2. Identification and quantitation of phenolic compounds in the ASHE extract

The results of the LC-MS/MS analysis presented in table 7 and figure 24 revealed the presence of 16 phytochemical compounds in the hydroethanolic extract of *Allium sphareocephalon* L., of which 75% are flavonoids, with quinoic acid and acetin (13.808 and 12.616 mg/g of dry extract, respectively) being the major compounds.

Table 07: Parameters for the validation of analytical methods pertaining to the LC-MS/MS technique.

No	Analytes	RT[a]	M.I. (m/z)	F.I. (m/z) c	Ion mode	r2d	ASHE
1	Quinic acid	3.0	190.8	93.0	(-)	0.996	13.808
2	Fumaric aid	3.9	115.2	40.9	(-)	0.995	N.I.
3	Aconitic acid	4.0	172.8	129.0	(-)	0.971	N. I
4	Gallic acid	4.4	168.8	79.0	(-)	0.999	N. I
5	Epigallocatechin	6.7	304.8	219.0	(-)	0.998	N. I
6	Protocatechuic acid	6.8	152.8	108.0	(-)	0.957	0.555
7	Catechin	7.4	288.8	203.1	(-)	0.999	N. I
8	Gentisic acid	8.3	152.8	109.0	(-)	0.997	N. I
9	Chlorogenic acid	8.4	353.0	85.0	(-)	0.995	N. I
10	Protocatechuic aldehyde	8.5	137.2	92.0	(-)	0.996	0.021
11	Tannic acid	9.2	182.8	78.0	(-)	0.999	N. I
12	Epigallocatechin gallate	9.4	457.0	305.1	(-)	0.999	N. I
13	1,5-dicaffeoylquinic acid	9.8	515.0	191.0	(-)	0.999	N. I
14	4-OH Benzoic acid	10.5	137,2	65.0	(-)	0.999	N. I
15	Epicatechin	11.6	289.0	203.0	(-)	0.996	N. I
16	Vanilic acid	11.8	166.8	108.0	(-)	0.999	N. I
17	Caffeic acid	12.1	179.0	134.0	(-)	0.999	0.815
18	Syringic acid	12.6	196.8	166.9	(-)	0.998	N. I
19	Vanillin	13.9	153.1	125.0	(+)	0.996	N. I
20	Syringic aldehyde	14.6	181.0	151.1	(-)	0.999	N. I
21	Daidzin	15.2	417.1	199.0	(+)	0.996	N. I
22	Epicatechin gallate	15.5	441.0	289.0	(-)	0.997	N. I
23	Piceid	17.2	391.0	135/106.9	(+)	0.999	N. I
24	*p*-Coumaric acid	17.8	163.0	93.0	(-)	0.999	0.171
25	Ferulic acid-D3-IS[h]	18.8	196.2	152.1	(-)	N.A.	N.A.
26	Ferulic acid	18.8	192.8	149.0	(-)	0.999	N. I
27	Sinapic acid	18.9	222.8	193.0	(-)	0.999	N. I

28	Coumarin	20.9	146.9	103.1	(+)	0.999	N. I
29	Salicylic acid	21.8	137.2	65.0	(-)	0.999	N. I
30	Cynaroside	23.7	447.0	284.0	(-)	0.997	N. I
31	Miquelianin	24.1	477.0	150.9	(-)	0.999	N. I
32	Rutin-D3-IS[h]	25.5	612.2	304.1	(-)	N.A.	N.A.
33	Rutin	25.6	608.9	301.0	(-)	0.999	N. I
34	Isoquercitrin	25.6	463.0	271.0	(-)	0.998	0.157
35	Hesperidin	25.8	611.2	449.0	(+)	0.999	0.051
36	*o*-Coumaric acid	26.1	162.8	93.0	(-)	0.999	N. I
37	Genistin	26.3	431.0	239.0	(-)	0.991	N. I
38	Rosmarinic acid	26.6	359.0	197.0	(-)	0.999	N. I
39	Ellagic acid	27.6	301.0	284.0	(-)	0.999	N. I
40	Cosmosiin	28.2	431.0	269.0	(-)	0.998	0.166
41	Quercitrin	29.8	447.0	301.0	(-)	0.999	N.I.
42	Astragalin	30.4	447.0	255.0	(-)	0.999	0.207
43	Nicotiflorin	30.6	592.9	255.0/284.0	(-)	0.999	N. I
44	Fisetin	30.6	285.0	163.0	(-)	0.999	N. I
45	Daidzein	34.0	253.0	223.0	(-)	0.999	N. I
46	Quercetin-D3-IS[h]	35.6	304.0	275.9	(-)	N.A.	N.A.
47	Quercetin	35.7	301.0	272.9	(-)	0.999	0.078
48	Naringenin	35.9	270.9	119.0	(-)	0.999	0.053
49	Hesperetin	36.7	301.0	136.0/286.0	(-)	0.999	N. I
50	Luteolin	36.7	284.8	151.0/175.0	(-)	0.999	0.473
51	Genistein	36.9	269.0	135.0	(-)	0.999	0.011
52	Kaempferol	37.9	285.0	239.0	(-)	0.999	0.132
53	Apigenin	38.2	268.8	151.0/149.0	(-)	0.998	2.528
54	Amentoflavone	39.7	537.0	417.0	(-)	0.992	N. I
55	Chrysin	40.5	252.8	145.0/119.0	(-)	0.999	N. I
56	Acacetin	40.7	283.0	239.0	(-)	0.997	12.616

aR.T.: Retention time, bMI (m/z): Molecular ions of the standard analytes (m/z ratio), cFI (m/z): Fragment ions dr2: Coefficient of determination, eRSD: Relative standard deviation, fLOD/LOQ (µg/L): Limit of detection/quantification, gU (%): percent relative uncertainty at 95% confidence level (k = 2), hIS: Internal standard, iGr. No: Represents grouping of internal standards, these numbers indicate which IS stands for which phenolic compound.

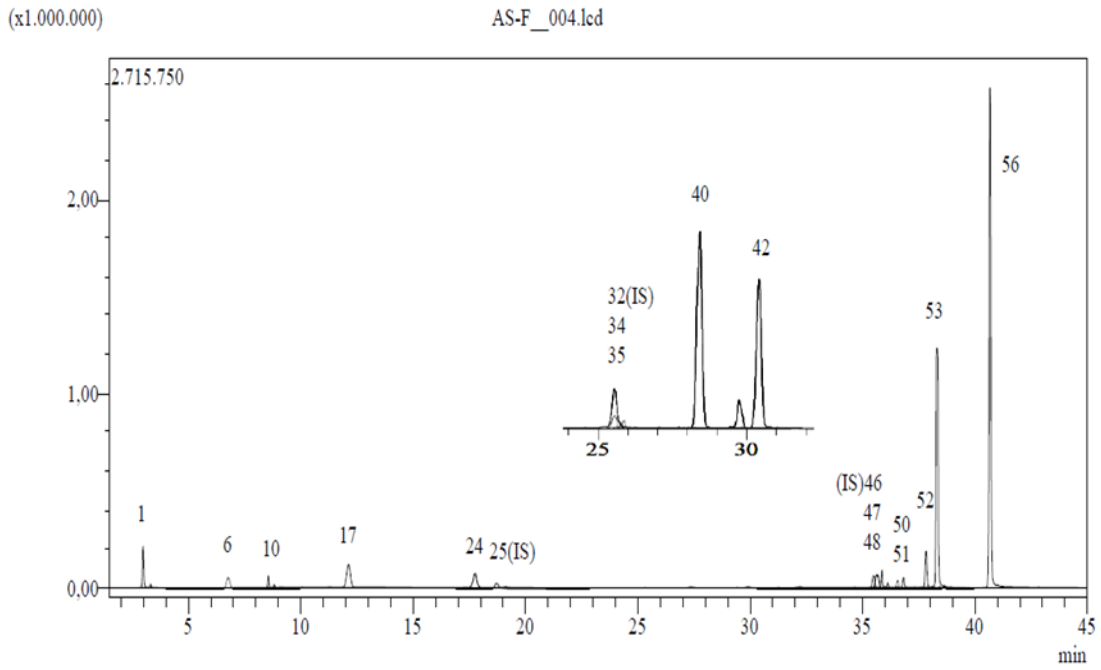

Figure 24: LC-MS/MS chromatogram of ASHE extract.

3.3. Antioxidant activity

3.3.1. Activity of radical DPPH scavenging

As seen in table 2, ASHE. had the strongest radical-scavenging effect ($IC_{50=}$ 0.28±2.02 mg/mL) compared to AQE (IC_{50} >0.8 mg/mL) (Table 08).

3.3.2. Ferrous ion chelating activity

AQE. displayed a chelating activity to Fe^{2+} ions (IC_{50}=0.076±0.006mg/mL), higher than EOH (IC_{50}=0.161±0.012 mg/mL), but it appeared to be weaker than the positive control EDTA (IC_{50}=0.005±0.0002) in this test (Table 08).

3.3.3.β-carotene bleaching method

EOH showed high inhibition percent (67±0.009%) than AQE (60±0.037%). These values still lower than BHT as a positive control (96±0.005%) (Table 8).

Table 08. DPPH scavenging assay metal chelating and β-carotene bleaching of *A. sphaerocephalon* L. flowers' hydroethanolic and aqueous extracts.

	IC_{50} (mg/mL)		Inhibition (%)
	DPPH	**Fe^{2+} ion chelating**	**β-carotene bleaching**
ETOH	0.28±2.02	0.161±0.012	67±0.009
AQE	>0.80	0.076±0.006	60±0.037
BHA	0.0061±0.41	Nt	Nt
BHT	0.012±0.41	Nt	96±0.005
α-Tocopherol	0.01±5.17		Nt
EDTA		0.005±0.0002	Nt

Nt: not tested

3.3.4. Reducing power assay

AQE had higher activity (EC_{50}=0.29±0.00 mg/mL) than EOH (EC_{50}=0.36±6.66 mg/mL). However, their effect was lower than that of α-Tocopherol (EC_{50}=0.03±2.38 mg/mL) and ascorbic acid (EC_{50}=0.0067±1.15 mg/mL) (Table 9).

3.3.5. CUPRAC reducing antioxidant capacity

The ASHE activity (EC_{50}=0.39 ± 6.35 mg/mL) was lower than AQE (EC_{50}=0.35 ± 9.07 mg/mL), but both were lower than the standards BHA (EC_{50}=0.005 ± 0.71 mg/mL) and BHT (EC_{50}=0.008 ± 3.94 mg/mL).

Table 09. Reducing power assay and Cupric reducing antioxidant capacity of ASHE and AQE

	EC_{50}mg/mL	
	Reducing power assay	**Cupric reducing capacity**
ASHE	0.36 ± 6.66	0.39 ± 6.35
AQE	0.29 ± 0.00	0.35 ± 9.07
BHA		0.005 ± 0,71
BHT		0.008 ± 3.94
Ascorbic acid	0.0067 ± 1.15	
α-Tocopherol	0.03 ± 2.38	

4. Discussion

4.1. Phytochemical analysis

In the present study, the percentage yield of hydroethanolic extract was approximately comparable with the flowers of *A. atroviolaceum Bois* (Emir and Emir, 2022) and *paniculatum* subsp. *Villosulum* (Emir and Emir, 2021) with 19.44% and 19.12%, respectively. The present values were higher than the previous findings in the flowers of *A.pallens* (from different localities in Turkey) which were 11.65% and 14.75%, respectively (Emir and Emir, 2020), and *A. paniculatum* subsp *Paniculatum* (15.43%)(Emir and Emir, 2021) and lower than those of *A. ampeloprasum* L. (27.31%) (Emir *et al*.,2022), and *A. stylosum O. Schwarz* (26.25%) (Emir and Emir, 2021). AQE extract was comparable with *A. pallens* (11.65%) (Emir and Emir, 2020) and *Allium stylosum* O. Schwarz (12.36%). In this comparison, there is a difference in allium species, collected regions, and solvent of extraction. According to (Elias *et al.*, 2010; Sultana *et al*., 2009), the nature of the extracting solvent and its polarity, nature and polarity of the extracting solvent as well as variety diversity, growth conditions, ripening degree, and climate, can all have an impact on the extract yields of plant materials.

The phenolic compounds are secondary metabolites with miscellaneous protective roles; their synthesis is carefully controlled through many stress signals and environmental factors. (Laura *et al*., 2010). They are aromatic hydroxylated compounds that have one or more hydroxyl groups on their aromatic rings, Polyphenols possess the ability to function as antioxidants due to their capacity to undergo robust hydrogen or electron donor reactions, stabilize chain-breaking reactions, and terminate Fenton reactions (Khatua *et al*., 2013).

The TPC of hydroethanolic and aqueous extracts of *A. sphaerocephalon* flowers was approximately similar to those of flowers of *A. sphaerocephalon* subsp. *Sphaerocephalon*, *A. sphaerocephalon* subsp. *Trachypus* (Emir Emir *et al.*, 2020). *A. paniculatum* subsp. *Villosulum* and *A. Paniculatum* subsp. *Paniculatum* (Emir and Emir, 2021) with (14.83mg GAE/g, 11.44mg GAE/g, 15.19mg GAE/g, 10.97 mg GAE/g), respectively. However, our results were higher than those of flowers of *A. roseum* var. *odoratissimum* (135 mg GAE/100 g) (Dziri *et al*.,2012), and lower than *A. atrovioleceum* Boiss. (33.72mg GAE /g and 25.81mg GAE /g) (Emir and Emir, 2022). Collected from two different localities in İzmir (Turkey).

TFC value was approximately similar to those of flowers of *A. atrovioleceum* Boiss (8.63mg QE/gand 6.93mg QE/g) (Emir and Emir, 2022), and higher than flowers of *A. sphaerocephalon* subsp. *Sphaerocephalon*, *A. sphaerocephalon* subsp. *Trachypus* (1.56 mg QE/g 2.07mg QE/g, respectively) (Emir and Emir,2020) , *A. ampeloprasum* L (1.78 mg QE/g 1.14 mg QE/g) (Emir *et al*., 2022), and *A. roseum* var. *odoratissimum)* (74.3mg QE/100 g).(Dziri *et al*., 2012).

The CTC of hydroethanolic and aqueous extracts of *A. sphaerocephalon* flowers was higher than *Allium cepa* flower parts (Halder and Khaled, 2021) and (*Allium sativum*) and (*Allium cepa*) (Bouhennı *et al*., 2021).

According to Mohammed *et al*. (2022)'s investigation, the solvent's properties and polarity have a significant impact on phenolic and antioxidant extraction. Transport and storage conditions, along with genetic and environmental factors, exerted a substantial impact on the concentrations of plant metabolites. In addition to growth-influencing elements including light, temperature, humidity, soil type, fertilizer applications, damage brought about by microorganisms and insects, UV radiation stress, heavy metal exposure, as well as pesticide application, alter the metabolite profile of plants (de Mello and Fasolo, 2014).

4.2. Identification and quantitation of phenolic compounds of the ASHE extract

To determine which compound may contribute more to the biological activity of the plant, the quantification of fifty-three selected phenolic compounds in ASHE flower's part was carried out by (LC-MS/MS). Among the identified phenolic chemicals in general, flavonoids were the major compounds and, acetin (12.616 µg/g) and quinoic acid (13.808 µg/g) as a phenolic acid as had the highest values. Our results do not align with the findings of Emir and Emir (2020). Phenolic molecules are believed to have several functions in plants, such as attracting pollinators, exhibiting antioxidant activity, and providing protection against ultraviolet light and pests. Consequently, physiological and environmental factors, including soil structure and temperature, may have resulted in varying phenolic concentrations among the samples.

4.3. Antioxidant activity

The use of antioxidant therapy in the treatment of illness has become increasingly important. Antioxidant compounds interfere with oxidative stress by a variety of mechanisms including interactions with free radicals, chelating, catalytic metals, and by oxygen scavenger

activity (Mathew *et al*., 2012). In the present work, the antioxidant activity of *A. sphaerocephalon* L. flowers were determined using five different assays: DPPH radical scavenging assay, reducing power, cupric reducing antioxidant capacity, ferrous ion chelating, and β-carotene bleaching test.

4.3.1. Activity of radical DPPH scavenging

DPPH is a free radical distinguished by its purple hue; when interacting with an antioxidant, it generates a compound that is persistently yellow in color, the quantity of the reaction is ascertained by the hydrogen-donating capacity of the antioxidant (Muthukumaran *et al*., 2011). The activity of the ETOH extract of this study was higher than flowers' methanolic extract of *A. roseum* var. *odoratissimum* (Dziri *et al*., 2012)· and lower than flowers of methanolic extract of *A. atrovioleceum* Boiss (Emir, Emir, 2022). and *A. nevsehirense*, *A. sivasicum*, *A. dictyoprosum,* and *A. scrodoprosum* subsp. *Rotundum* (Tepe *et al*., 2005).

However, the AQE extract was lower than all species. There is a difference in the capacity of radical scavenging between the species of Allium. Through these comparisons, it was observed that extracts with higher total phenolic content exhibited a stronger DPPH scavenging ability. Beretta et al. (2017) demonstrated a significant correlation between total phenolic content and antioxidant activity. In addition, several publications proved the existence of a relationship between the greater TPC which has stronger radical scavenging activities (Tepe *et al*. ,2005; Beretta *et al*., 2017; Emir and Emir 2021; Emir and Emir, 2022). But the AQE extract was lower than all species mentioned. In this case, it appears that the conflicting results are very likely because regarding discrepancies in approach and experimental circumstances employed.

4.3.2. Ferrous ion chelating activity

Due to its potent reactivity with transition metals, iron is regarded as the most significant lipid pro-oxidant (Gulcin, 2020). Lipid peroxidation is induced via the Fenton and Haber-Weiss reaction, and the lipid hydroxide is decomposed into peroxyl and alkoxyl radicals, which have the potential to sustain the chain reactions (Jaiswal and Rizvi, 2017). The metal chelating capacity is crucial since it reduces the concentration of metals, which in turn has a catalytic impact on lipid peroxidation. Metal-chelating compounds act as secondary antioxidants by reducing the redox potential, which stabilizes oxidized molecules (Gulcin, 2022). These extracts and standard prevented the production of a ferrous-ferrozine combination, indicating that they possessed chelating properties and absorbed iron ions before ferrozine.

The antioxidant capacity of phenolic compounds is also attributed to their ability to chelate metal ions involved in free radical formation (Pereira *et al*., 2009). Specifically, flavonoids have demonstrated the capability to bind and eliminate excess metal ions in the human body (Gulcin, 2022). The antioxidant efficacy of flavonoids is affected by the quantity and positioning of their aromatic hydroxyl groups (Fernandez-Panchon, *et al.,* 2008).

Our investigation revealed that the existence of polyphenols and flavonoids in these extracts is accountable for their capacity to chelate metals. Nevertheless, the efficacy of this action is not contingent upon the amount of these chemicals. In fact, AQE extract had a lower amount of polyphenols and flavonoids but had good metal-chelating activity.

4.3.3.β-carotene bleaching method

The β-carotene bleaching assay measures the capacity of antioxidants to shield target molecules from the effects of free radicals through the prevention of lipids oxidation. When compared with the negative control (methanol or distilled water), the flowers' extracts of *A. sphaerocephalon* L. and standard at 2 mg/demonstrated a substantial inhibition.

Muthukumaran *et al*. (2011) evaluated the antioxidant activity of five *Allium* species from Turkey and demonstrated their inhibitory effect on linoleic acid oxidation. In this study, the ethanol extract showed lower activity compared to *A. atroviolaceum* and *A. dictyoprosum*, with inhibition rates of 71.2±2.20% and 72.3±1.20%, respectively. These values were close to those of *A. nevsehirense* and *A.scrodoprosum* subsp. Rotundum, but higher than those of *A. sivasicum*and *A. tuncelianum* bulbs (51.1±5.5 %) (Yumrutaş *et al*., 2009). The aqueous extract (AQE) demonstrated greater activity than the previously mentioned species and was roughly on par with *A. sivasicum*, but lower than that of the other species. This variation in activity may be attributed to differences in phenolic content or the presence of other compounds, such as sulfur compounds, which could also play a role in antioxidant activity.

4.4.4. Reducing power assay

The reducing power and CUPRAC assays are commonly employed to evaluate the electron transfer capability of antioxidants in the presence of radicals. The reducing capacity method is commonly associated with the presence of reductants, whose antioxidant properties have been established through the disruption of the free radical chain and the donation of a hydrogen atom

(Choi *et al.,* 2008). Within this research, each extract demonstrated a perceived decreasing power capacity.

According to the literature, the aerial parts and bulbs of *A. scabriscapum* (Nabavi *et al*., 2013) and *A. triquetrum* L. (Menacer *et al*., 2017) demonstrated significant activity; however, this activity was not comparable to that of the control, similar to what was observed with our samples.

In addition, the reducing power of the extract increases in a concentration dependent manner (Elias *et al.*, 2010). It was said that the blooms and leaves of *A. roseum* var *odoratissimum* have the highest antioxidant activity, while the bulbs, showed the lowest antioxidant activity, which was linked to the presence of specific phenolic components as well as their structures, in addition to the sugar moieties, also known as glycosylated phenolics, are present and have a rather low antioxidant activity. Antioxidants transform Fe^{3+} ferricyanide complexes into the ferrous (Fe^{2+}) form (Beretta *et al*., 2017). This conversion is facilitated by the reducing capacity of the antioxidants, which is likely due to the presence of a hydroxyl group that may donate electrons (Darshani and Priyantha, 2020).

4.4.5. CUPRAC reducing antioxidant capacity

The methodology of this assay involves the reduction of Cu (II) to Cu(I) through the collective activity of antioxidants (reducing agents) present in a sample containing neocuproine (2,9-dimethyl-1,10-phenanthroline) (Gulcin, 2020). Antioxidants that are both hydrophilic and lipophilic can be quantified using the CUPRAC method. In this study, there is no significative difference between the two extracts, where the ability of reducing Cu (II) to Cu(I) was almost equal, but it was lower than the standards BHA and BHT.

It is hard to compare our results to other results, because of the difference in the expression of results, but according to the following species (*A. ampeloprasum*, *A.atrovioleceum Boiss. A.pallens* L.), it has an activity that is attributed to the presence of phenolic and flavonoid components.

Chapter 03:
Antiulcer Activity of
Allium sphareocephalon L.

1. Materials

1.2. Animals

Male Wistar rats weighing between 150–250 g were employed during the current study. Rats were purchased from the Pasteur Institute, Algiers, Algeria. Initially, the rats were housed in groups in available stainless-steel cages. They were allowed free access to tap water and food ad libitum for a week. In all studies, the animals were starved for 18-20 hours with free access to water until 60 minutes before the start of the experiment. In anti-ulcer activity, during the fasting period, the animals were placed individually in cages with wide-mesh wire bottoms to prevent coprophagy.

2. Methods

2.1. Acute oral toxicity

The acute oral toxicity of ASHE extract was assessed using a limited number of mice in accordance with the OECD guideline 423 (2001) for limit testing. The extract was administered at two single oral doses (2000 and 5000 mg/kg). We observed the animals for signs of death and toxicity within 24 hours and then again after 14 days.

2.2. Gastric ulcer

- **Ethanol-induced gastric ulceration in rats**

The animals were divided into 5 groups, consisting of six rats each. Each rat in each group was subsequently separately placed in a cage. Group 1 rats were treated with CMC (1.5%) as the negative control. Group 2 received 5 mg/kg ranitidine (positive control). Groups 3, 4, and 5 were treated with hydroethanolic extract of *A. sphaerocephalon* L. at doses 25, 50, and 100 mg/kg. 60 minutes after the oral respective treatments, the acute gastric ulceration was induced by a gavage of 70% ethanol (0.5 mL/200 g).

Thirty minutes later, the animals were killed with cervical dislocation, and each stomach was opened along the greater curvature and rinsed with normal saline. Samples of the flattened stomach were photographed and the ulcer area (Cm^2) was measured using ImageJ software (developed by the National Institutes of Health, USA). The inhibition percentage was calculated using the following formula:

$$[(\text{Ulcer area(control)} - \text{Ulcer area (treated)}) / \text{Ulcer area(control)}] \times 100\%.$$

2.3. Histopathological examinations

A small piece of the ulcerated gastric mucosal tissue from each rat was fixed in10% formalin and dehydrated using mixtures of alcohol varying degrees, cleared in xylene making use of a tissue processor and finally embedded in paraffin wax. Tissue sections were cut to a thickness of 5 µm using a standard microtome and stained with hematoxylin and eosin (H&E) for light microscopic examination.

2.4. Evaluation of *in vivo* antioxidant activity

2.4.1. Preparation of homogenate

Part of stomach tissues, was washed with frozen normal saline, dried using bandages, weighed, and homogenized in Tris HCl buffer (50 mM, pH 7.4) on ice using Dounce Homogenizer to get homogenate 10% (w/v) and then were centrifuged at 4000 g at 4°C for 15 min. The supernatants were used to determine the activities of catalase (CAT), and levels of reduced glutathione (GSH) and lipid peroxidation (MDA), and total proteins.

2.4.2. Assessment of the total protein content

We quantified the total protein concentration using the Gornall et al. (1949) method and the Biuret kit total protein reagent, which includes potassium iodide, potassium sodium tartrate, copper sulphate, and sodium hydroxide. Proteins have a blue-violet hue when reacted with copper sulphate in an alkaline environment. To sum up, 1 mL of the Biuret reagent was mixed with 25 µL of the tissue homogenate or standard (bovine serum albumin), and the mixture was left to sit at room temperature for 10 minutes. The absorbance was subsequently measured at 540 nm. The absorbance was subsequently measured at 540 nm. The total protein quantity was determined using the subsequent formula:

Total proteins (mg/ml) = (Abs of sample / Abs of standard) X n

Where n is standard concentration.

2.4.3. Assessment of catalase (CAT) activity

Catalase activity was assessed using the method of Clairborne (1985) with minor modifications.

The CAT catalyzes the reduction of H_2O_2 to water and molecular oxygen, according to the following reaction:

$$2H_2O_2 \xrightarrow{\text{Catalase}} 2H_2O + O_2$$

A complete reaction mixture contained 19 mM H_2O_2 (1.45 mL) in 50 mM phosphate buffer pH 7.4 was placed into a quartz cuvette followed by the addition of 25 µL of tissue homogenate. The degradation rate of H_2O_2 in the presence of catalase (CAT) was measured spectrophotometrically at 240 nm. Measurements were taken over a duration of 30 seconds, recording the absorbance every 15 seconds. The enzymatic activity was expressed as micromoles of H_2O_2 consumed per minute per milligram of protein (µM H_2O_2/min/mg protein).

2.4.4. Evaluation of glutathione levels (GSH)

Reduced glutathione was quantified using Ellman's technique (1959). Spectrophotometric examination of GSH typically relies on the colorimetric interaction between GSH and 5,5'-dithiobis 2-nitrobenzoic acid), DTNB, also known to as Ellman's reagent. In this reaction, DTNB is transformed into 2-nitro-5-mercapto-benzoic acid (TNB), which has an absorbance maximum at 412 nm. The DTNB-based technique offers the significant advantages of speed, cost-effectiveness, precision, and accuracy. For this test, 25 µL of the tissue homogenate was diluted in 5 mL of phosphate buffer (0.1 M, pH 8). 10 µL of DTNB (0.01 M) were added to 1.5 mL of the dilution mixture, and after incubating for 5 minutes, the yellow color developed was read at 412 nm. The concentration of GSH expressed in mmol/g of tissue was extrapolated from a curve of standard concentrations of GSH realized in the same conditions.

2.4.4. Estimation of lipid peroxidation (LPO)

Lipid peroxidation in homogenate tissue was evaluated by quantifying malondialdehyde (MDA) production according to the methodology established by Ohkawa *et al*. (1979). The principle of the method was spectrophotometric measurement of the color created during the

reaction between thiobarbituric acid (TBA) and MDA. For this purpose,125 µL of TCA (20 % w/v) was added to 125 µL of tissue homogenate, then 250 µL of TBA (0.67 % w/v) was added. The mixture was incubated at 100°C for 15 min in a boiling water bath, cooled immediately in ice and mixed with 1mL of n-butanol and centrifuged at 3000 rpm for 15 min. The absorbance of the clear pink supernatant was measured spectrophotometrically at 532 nm against a blank. The concentration of MDA was determined from a standard curve of 1,1,3,3 tetraethoxypropane (serial dilutions of the stock 10 mM). The results were expressed as nmol TBA / g of homogenate tissue

3. Results

3.1. Acute oral toxicity

During an acute toxicity test, at the test dose (2000 mg/kg), no mortality was noted throughout the 2-week observation period, and no behavioral, neurological, or physical changes were seen in any of the animals. But all animals died at the dose (5000 mg/kg). So, the LD_{50} was 2000 mg/kg.

3.2. Effect of ASHE on macroscopic analysis of ulcer lesions

Figure 25 displays the macroscopic results of gross stomach examination acquired through the ethanol-induced gastric ulcer technique. In the negative control group, ethanol exposure showed a deteriorated gastric mucosa with the presence of petechiae, hemorrhage, and oedema. This deterioration was attenuated by pretreatment of ASHE at different doses (25, 50, and 100 mg/kg).

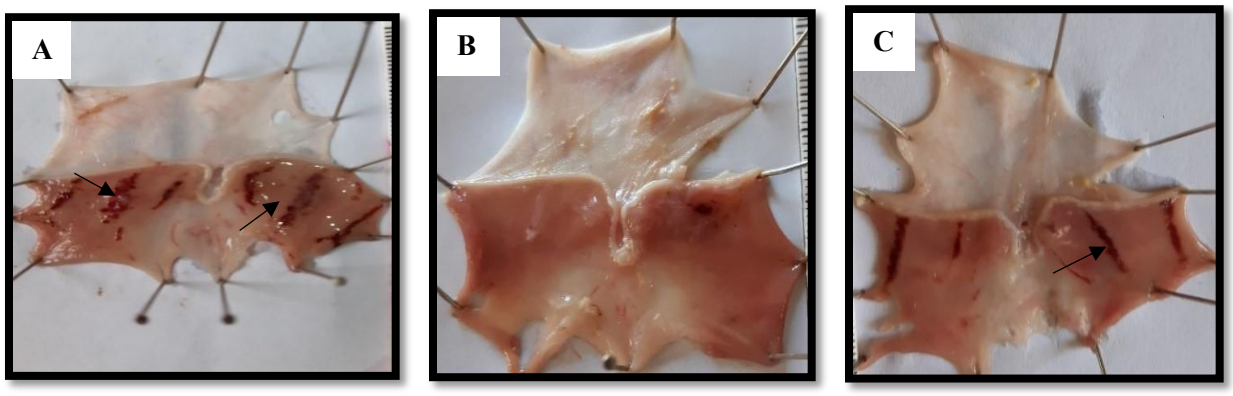

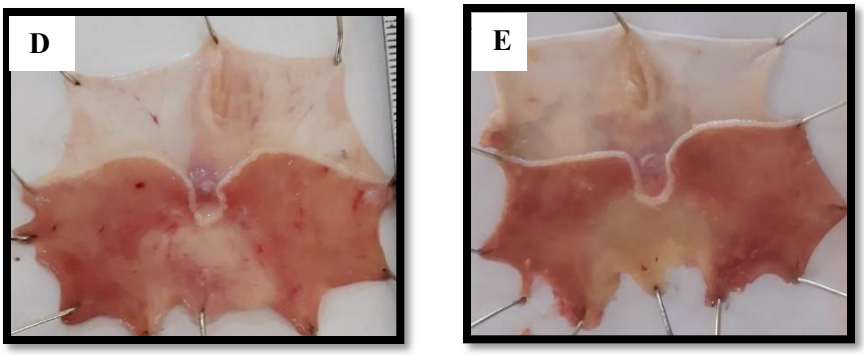

Figure 25: Macroscopic evaluation of the effect of ASHE on ethanol-induced gastric mucosal damage in rats. (A): negative control group. (B) the ranitidine-pretreated group (5 mg/kg). (C, D, E): ASHE (25, 50, and 100 mg/kg, respectively).

Results indicated that rats' gastric ulceration (Figure 26) was significantly higher in the negative control group (8.22 ± 2.56%) compared to the positive control and the tested doses (25 mg/kg, 50 mg/kg, and 100 mg/kg). However, the groups treated with ASHE at 25, 50, and 100 mg/kg and ranitidine at 5 mg/kg demonstrated a significant decrease in gastric ulceration, with protection rates of 65.62%, 87.87%, 99.76%, and 90.70%, respectively.

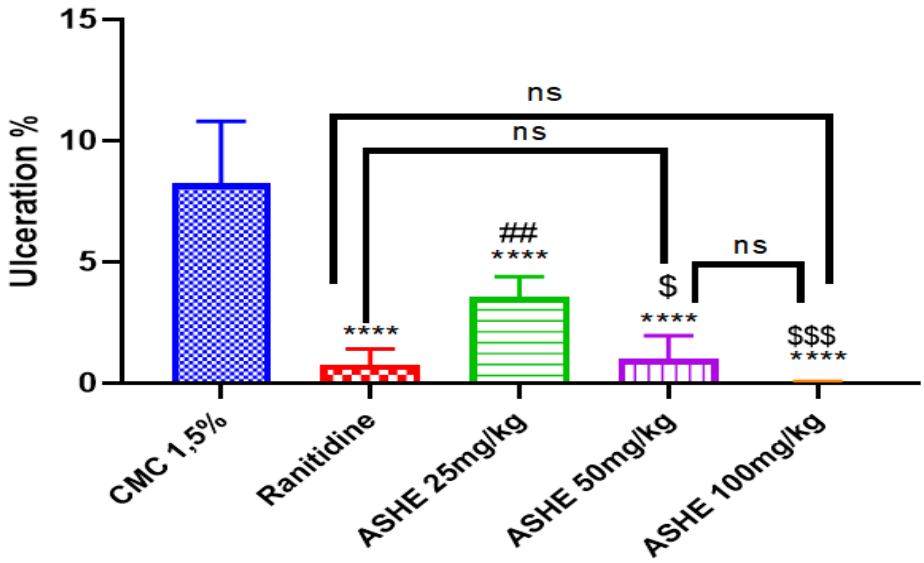

Figure 26: Effect of ASHE extract and ranitidine on gastric ulceration in rats subjected to ethanol treatment**.** Results were expressed as mean ± SEM (n=5) and analyzed by ANOVA followed by Tukey test. (****: P ≤ 0.0001) vs vehicle (CMC 1.5%) group. (##: P ≤ 0.01, ns: not significant) vs positive control group. ($$$:P ≤ 0.001, $: P ≤ 0.05, ns: not significant) between studied doses.

3.3. Histopathological examinations

The histological analysis of the stomach in the negative control (acute exposure to 70% ethanol) group indicated gastric erosions, venous congestion in the submucous, and infiltration of inflammatory cells. The ranitidine (5 mg/kg)-treated positive control showed normal epithelium and congestion of submucosa capillary polynuclear neutrophils, lymphocytes, and eosinophils. As is the case in dose 25 mg/kg, it showed a zone of gastric erosions, inflammation of the submucous plus lymphocytes, and arterial congestion, a slight erosion with acute inflammations and discrete to moderated polynuclear neutrophils noted at the dose of 50 mg/kg, in addition to venous congestion. There are no indicators of ulcers in the group treated with 100 mg/kg of extract. The wall mucus and sub mucus are typical, with no erosion, inflammatory reaction, or congestion. Figure 26.

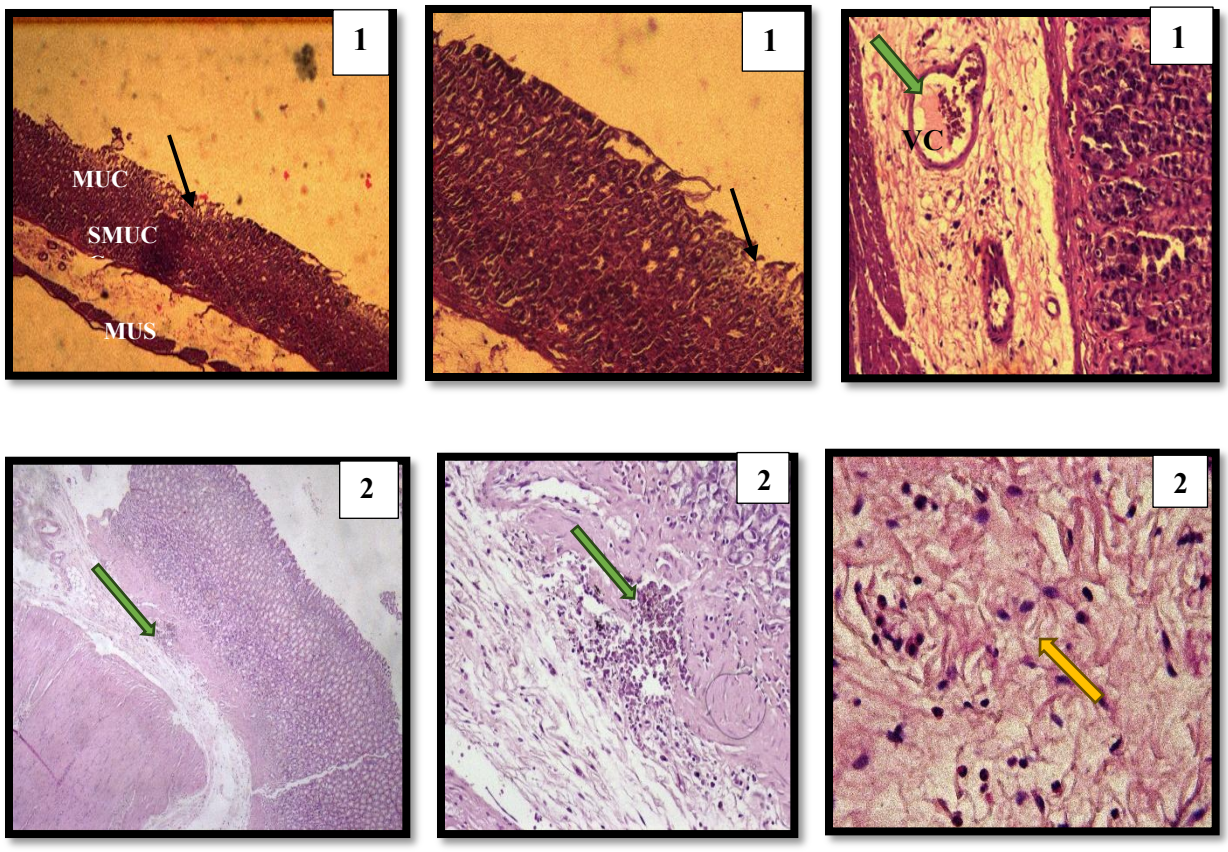

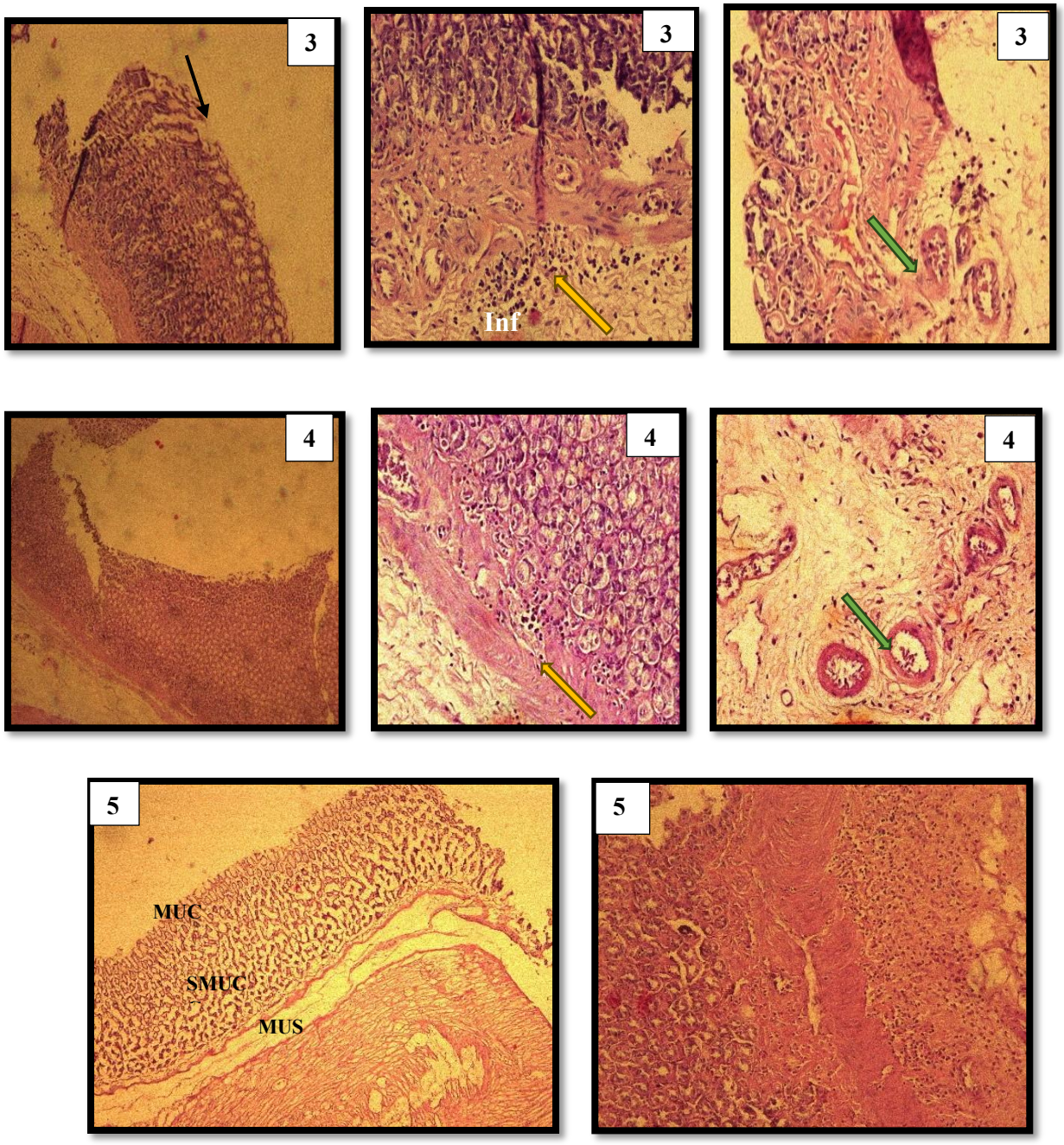

Figure 27: Impact of ASHE on the histological examination of the rat stomach**.** The stomach tissues were subjected to hematoxylin-eosin staining. (X 4,10,20,40). (1): Section of gastric mucosa of rats exposed to 70% ethanol. (2): Section of gastric mucosa of rats pretreated by ranitidine (5 mg/kg). (3, 4, 5): Section of gastric mucosa of rats pretreated by ASHE extract at 25,50, and 100 mg/kg, respectively. Black arrow: surface epithelium damage green arrow: vascular congestion. yellow arrow: infiltration of inflammatory cells.

3.4. Effects of ASHE on the antioxidant activity in the gastric tissue of rats.

3.4.1. Effect of ASHE on catalase activity

Results indicated that rats' catalase activity (Figure 28) was significantly lower ($P \leq 0.0001$) in the negative control group compared to the positive control and the selected doses. The dose (100 mg/kg) has a higher value of catalase activity (9.17 ± 0.96 µmol/min/mg of protein) than the positive control and the other doses (25 mg/kg and 50 mg/kg) (8.49 ± 0.83, 5.33 ± 0.35, 7.90 ± 0.48 µmol/min/mg of protein), respectively.

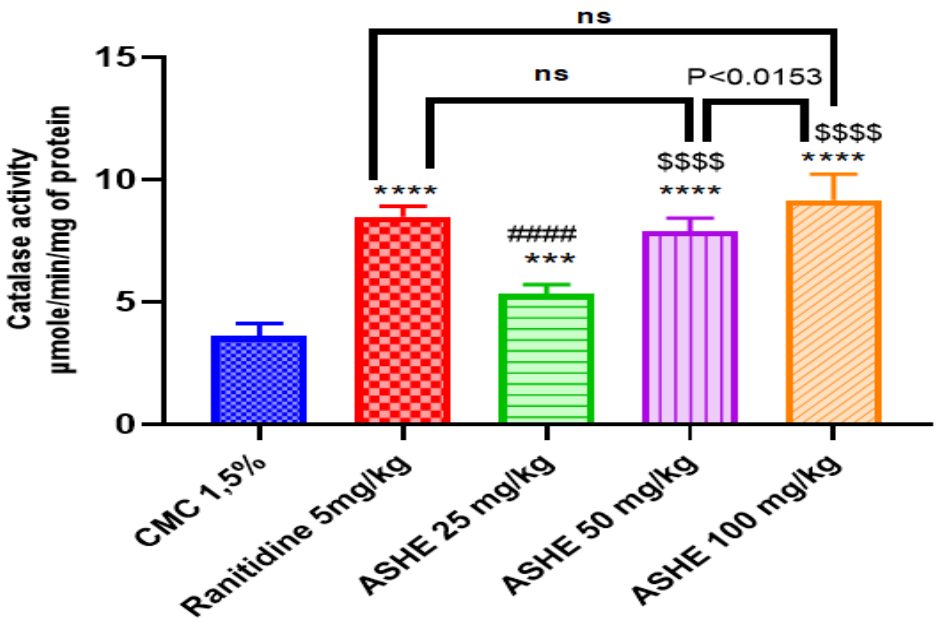

Figure 28: Effect of ASHE and Ranitidine on catalase activity in rats subjected to ethanol treatment. The results were expressed as mean ± SEM (n=5) and analyzed by ANOVA followed by Tukey test. (****: $P \leq 0.0001$, ***:$P \leq 0.001$) vs vehicle (CMC 1.5%). (####: $P \leq 0.0001$, ns: not significant) vs positive control group (Ranitidine 5 mg/kg p.o.). ($$$$: $P \leq 0.0001$) vs AS 25 mg/kg. ($P \leq 0.0153$) between AS 50 mg/kg and AS 100 mg/kg.

3.4.2. Effect of ASHE on GSH levels

The pretreatment with ASHE extract showed a significant increase in GSH level at doses 25, 50, and 100 mg/kg compared to the negative control (1.86 ± 0.03 µmol/g tissues). At these doses, the GSH level was 2.13 ± 0.04, 2.50 ± 0.05, and 2.66 ± 0.14 µmol/g tissues, respectively. The highest dose showed higher values (*$P \leq 0.01$) than ranitidine as a positive control (2.51 ± 0.04 µmol/g tissues) (Figure 29).

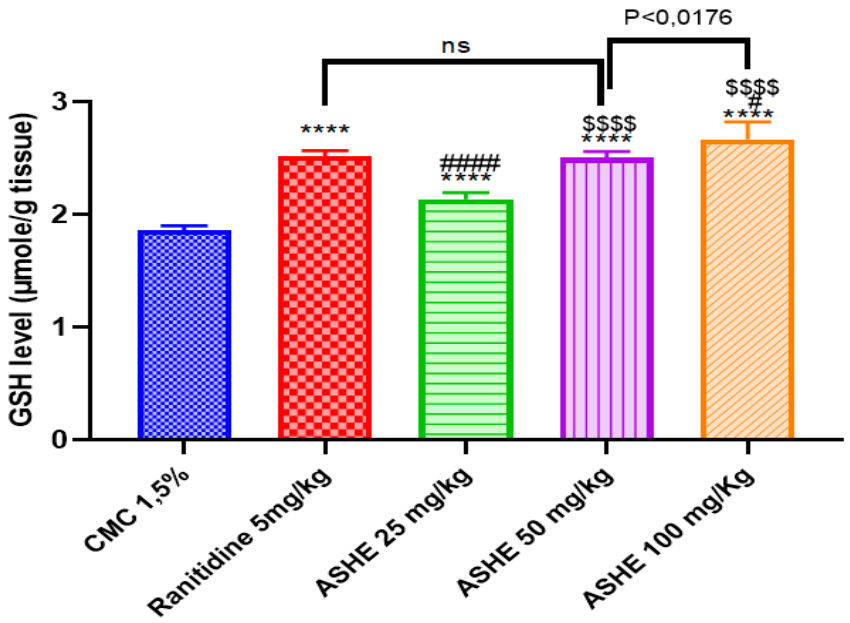

Figure 29: Effect of ASHE and Ranitidine on GSH levels in rats subjected to ethanol treatment**.** The results were expressed as mean ± SEM (n=5) and analyzed by ANOVA followed by Tukey test. (****: $P \leq 0.0001$) vs vehicle (CMC 1.5%). (####: $P \leq 0.0001$, #: $P \leq 0.01$ ns: not significant) vs positive control group (Ranitidine 5 mg/kg p.o.). ($$$$: $P \leq 0.0001$) vs AS 25 mg/kg. ($P \leq 0.0176$) between AS 50 mg/kg and AS 100 mg/kg.

3.4.3. Effect of ASHE on MDA Levels

Results indicated The MDA levels (Figure 30) were significantly higher in the negative control group (42.69 ± 2.8 nmol/g of tissue) than in the positive control (10.29 ± 1.17 nmol/g of tissue) or in the selective doses (25 mg/kg, 50 mg/kg, and 100 mg/kg). At these doses, the MDA levels were 10.29 ± 1.17, 23.25 ± 2.88, 16.83 ± 2.74, and 9.95 ± 0.64 nmol/g of tissue respectively. There was no significant difference between the higher dose and the positive control.

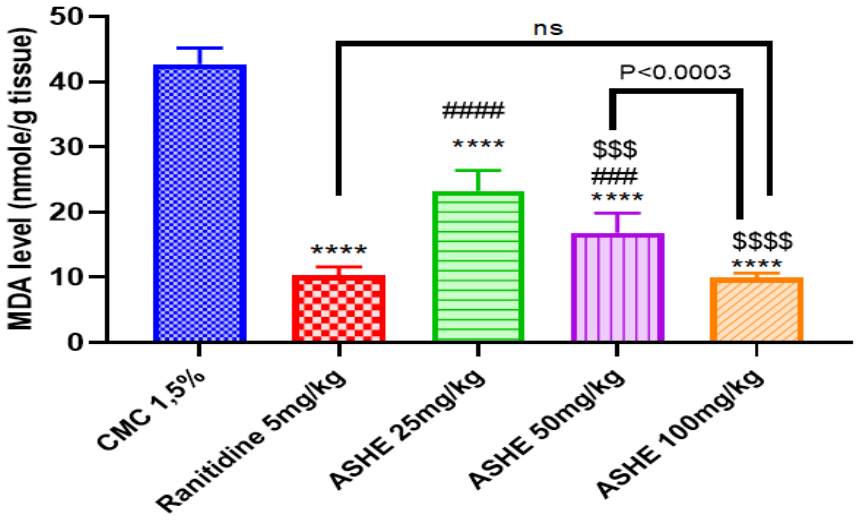

Figure 30: Effect of ASHE and Ranitidine on MDA levels in rats subjected to ethanol treatment. The results were expressed as mean ± SEM (n=5) and analyzed by ANOVA followed by Tukey test. (****: $P \leq 0.0001$) vs vehicle (CMC 1.5%). (####: $P \leq 0.0001$, ###: $P \leq 0.0001$ ns: not significant) vs positive control group (Ranitidine 5 mg/kg p.o.). ($$$$: $P \leq 0.0001$, $$$: $P \leq 0.0001$) vs AS 25 mg/kg. ($P < 0.003$) between AS 50 mg/kg and AS 100 mg/kg.

3.5. The mechanism of ASHE in gastroprotective effect by arginine, L-NNA, and indomethacin.

3.5.1. Effect of ASHE on macroscopic analysis

Figure 31 displays the macroscopic results of the gross stomach examination acquired through the ethanol-induced gastric ulcer technique. Compared to the damage seen in the negative control, arginine, whether used in the presence or absence of ASHE, reduced mucosal damage. In contrast, L-NNA increased ulceration and gastric membrane injury in the absence of ASHE and improved them in the presence of ASHE. These results were proven and supported by histological sections.

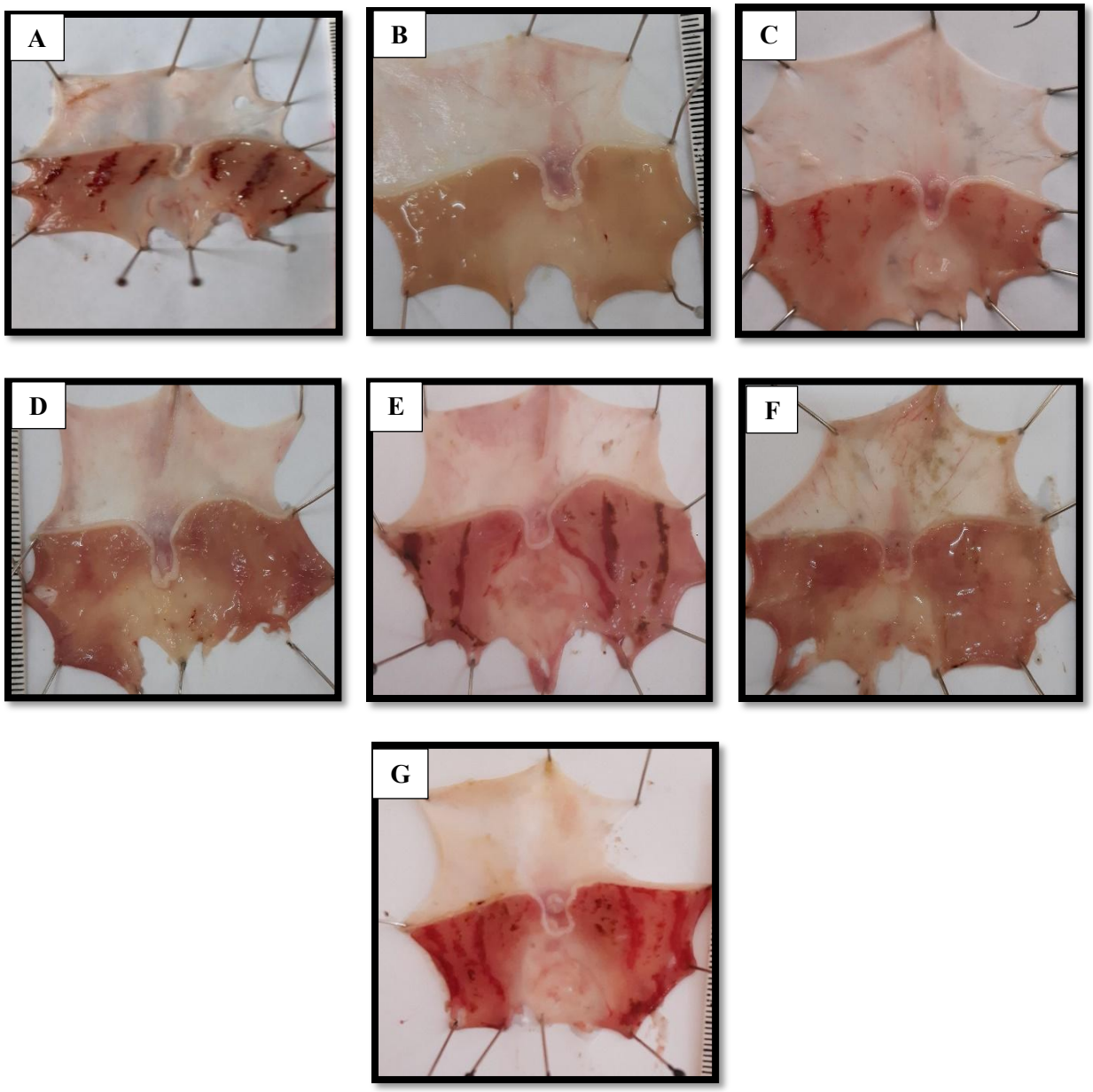

Figure 31: Macroscopic assessment of the preventive effect of ASHE on ethanol-induced stomach mucosal injury in rats, with or without arginine, L-NNA, and indomethacin. (A): negative control group, (B): group treated by arginine and ASHE extract, (C): group treated by arginine alone, (D): group treated by L-NNA and ASHE extract, (E): group treated by L-NNA alone, (F): group treated by indomethacin and ASHE extract, (G): group treated by indomethacin alone.

Results indicated that rats' gastric ulceration (Figure 32) was significantly higher in the negative control group (8.22 ± 2.33%) compared to the groups treated with arginine alone 1.53 ± 1.43%, arginine + ASHE (0.48 ± 0.29%), L-NNA + ASHE (0.25 ± 0.34%), and indomethacin + ASHE (0.39 ± 0.36%). However, there was no significant difference between the negative control and the group treated with L-NNA or indomethacin with gastric ulceration (6.012 ± 2.21% and 7.32 ± 0.43%, respectively).

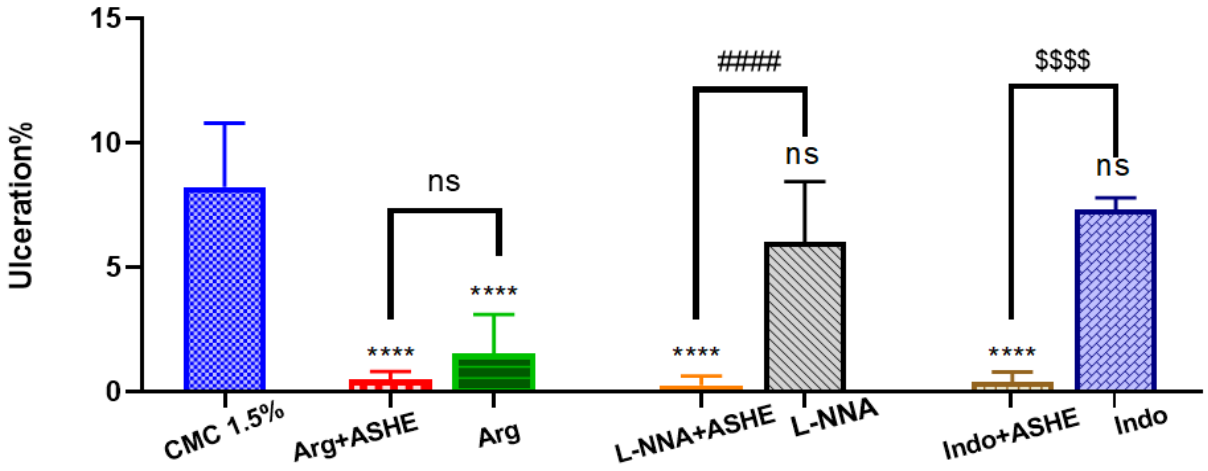

Figure 32: Effect of ASHE with the presence or absence of arginine, L-NNA, or indomethacin on gastric ulceration in rats subjected to ethanol treatment**.** Results were expressed as mean ± SEM (n=5) and analyzed by ANOVA followed by Tukey test. (****: P ≤ 0.0001, ns: ns: not significant) vs vehicle (CMC 1.5%) group, (####: P ≤ 0.0001) between NNA groups, ($$$$: P ≤ 0.0001) between indomethacin groups (ns: ns: not significant) between arginine and indomethacin groups.

3.5.2. Histological examinations

The histological examination showed that the group treated with arginine and ASHE gastric tissue was normal without stomach erosion or signs of ulceration, while the group treated with arginine alone contained small arterial congestion in submucosa. However, the group treated with L-NNA and ASHE showed an intact mucous membrane with a submucosal lymphocyte cluster, but the group treated with L-NNA alone had significant mucosal erosion, oedema, and arterial congestion in submucosa. Additionally, the groups treated with indomethacin and ASHE extract showed a mucosal epithelium intact and an inflammatory infiltration of capillary polynuclear neutrophils and lymphocytes, while the group treated with indomethacin alone showed damage to the mucosal epithelium and submucosal lymphocyte cluster (Figure 33).

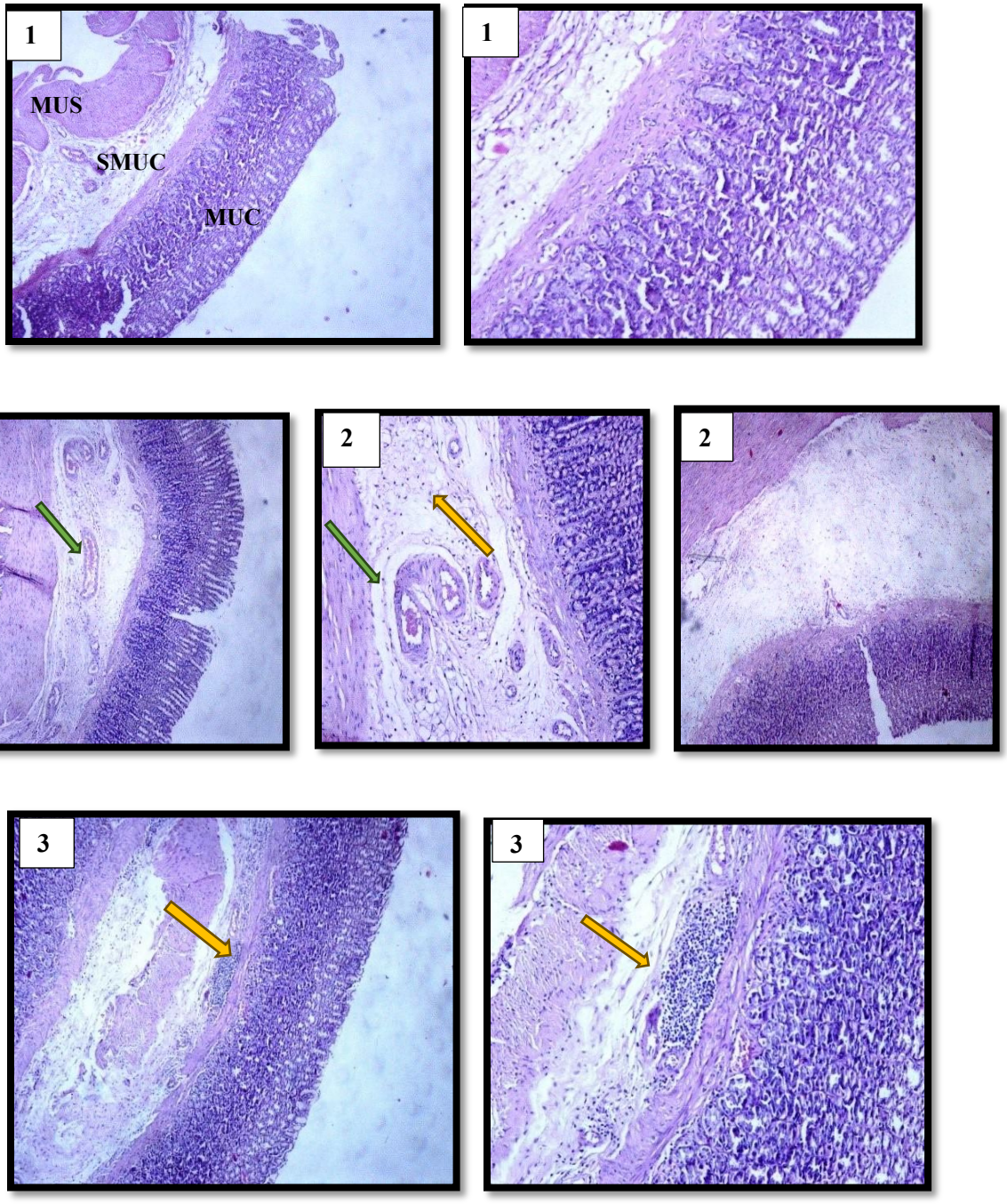
1
MUS
SMUC
MUC
1
2
2
2
3
3

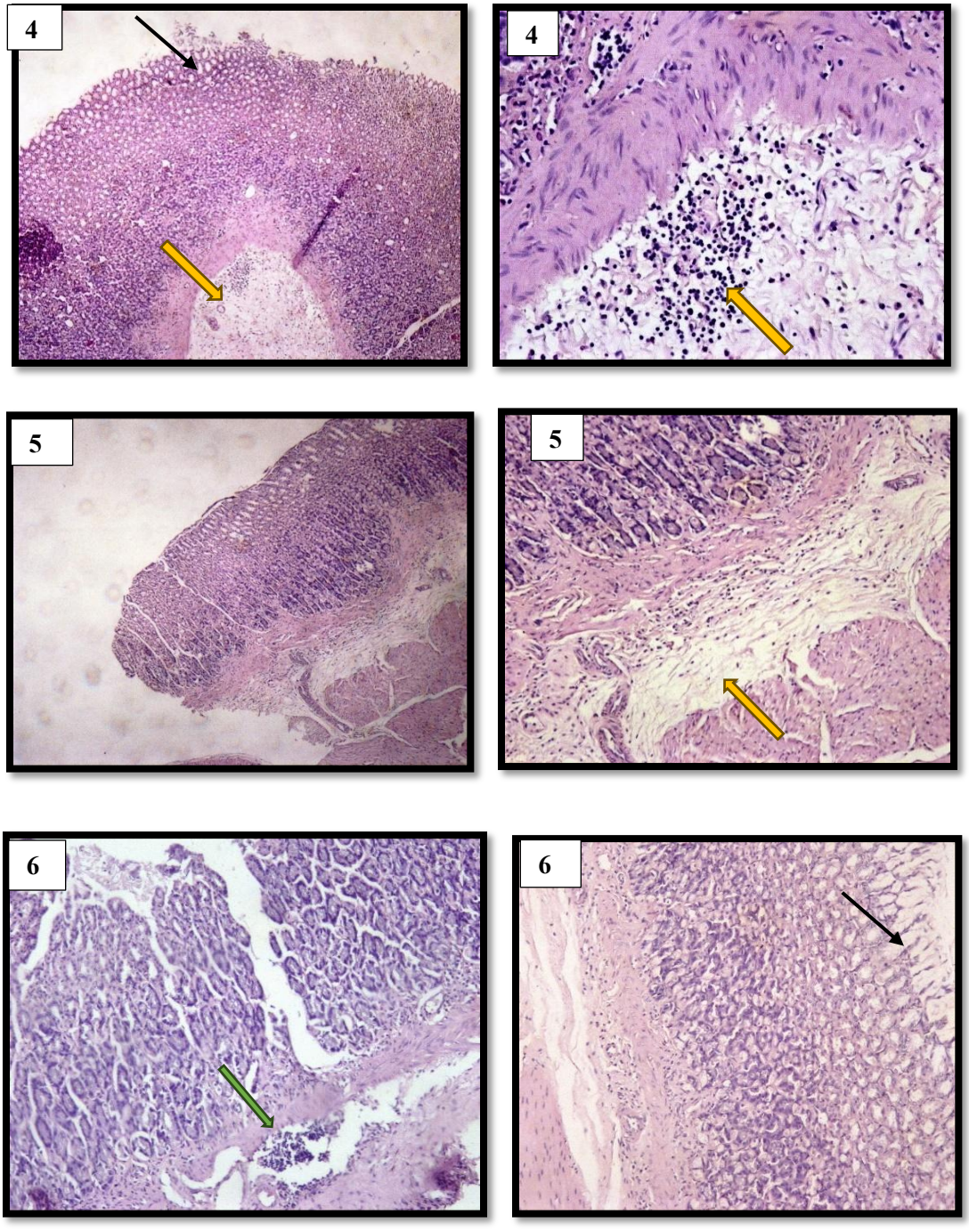

Figure 33: Impact of ASHE on the histological sections of the rat stomach with or without arginine, L-NNA, and indomethacin. The gastric tissues were subjected to staining with hematoxylin and eosin. X4, x10, x20. (1): Section of gastric mucosa of rats treated by arginine and ASHE extract. (2): Section of gastric mucosa of rats treated by Arginine alone. (3): Section of gastric mucosa of rats treated by L-NNA and ASHE extract. (4): Section of gastric mucosa of rats treated by L-NNA alone. (5): Section of gastric mucosa of rats treated by Indomethacin and ASHE extract. (6): Section of gastric mucosa of rats treated by Indomethacin alone. Black arrow: surface epithelium damage green arrow: vascular congestion. Yellow arrow: infiltration of inflammatory cells.

3.5.3 Effects of ASHE on the antioxidant activity in the gastric tissue of rats.

3.5.3.1. Effect of ASHE on GSH, total protein level and catalase activity

The results showed that the negative control group had significantly lower levels of catalase activity (3.49 ± 0.45 µmol/min/mg of protein) compared to the groups that were treated with, arginine (9.08 ± 0.63), ASHE+ arginine (9.11 ± 0.57), L-NNA+ASHE (9.26 ± 0.85), and ASHE + indomethacin (8.37 ± 1.56 µmol/min/mg of protein). However, there was no significant difference between the negative control and the group treated with L-NNA or indomethacin with gastric ulceration (3.99 ± 0.44 and 4.47 ± 1.56 µmol/min/mg of protein, respectively). (Figure 34)

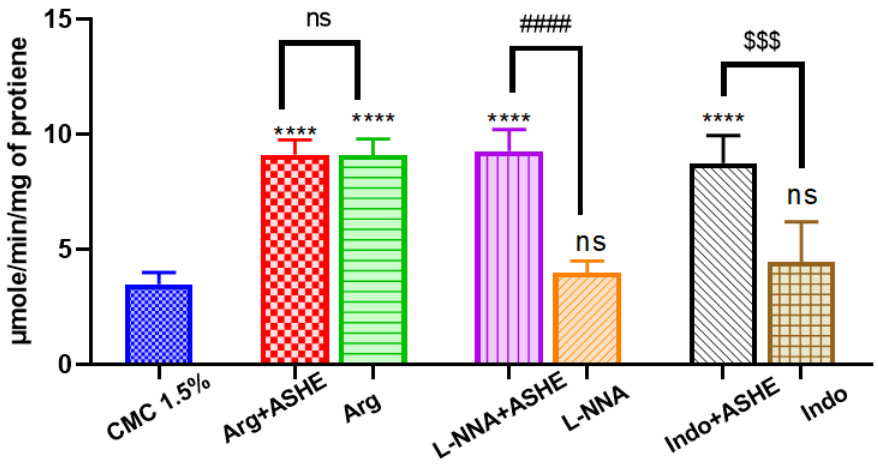

Figure 34: Effect of ASHE with the presence of both arginine, L-NNA, or indomethacin on catalase activity in rats subjected to ethanol treatment. The results were expressed as mean ± SEM (n=6) and analyzed by ANOVA followed by Tukey test. (****: P ≤ 0.0001, ns: not significant) vs vehicle (CMC 1.5%). (####:P ≤ 0.0001, ns: not significant) between within groups of arginine, L-NNA, or indomethacin.

3.5.3.2. Effect of ASHE on GSH level

The results showed that the negative control group had significantly lower levels of GSH 1.86±0.03µmol/g of tissue) compared to the groups that were treated with, arginine (2.49±0.05), ASHE + arginine (2.51±0.05) L-NNA+ASHE (2.53 ± 0.8), and ASHE + indomethacin (2.56±0.07 µmol/g of tissue). However, there was no significant difference between the negative control and the L-NNA group with gastric ulceration (1.95±0.075 µmol/g of tissue), But the indomethacin group showed a significant values (*P ≤ 0.05) (2.00±1.01 µmol/g of tissue). (Figure 35).

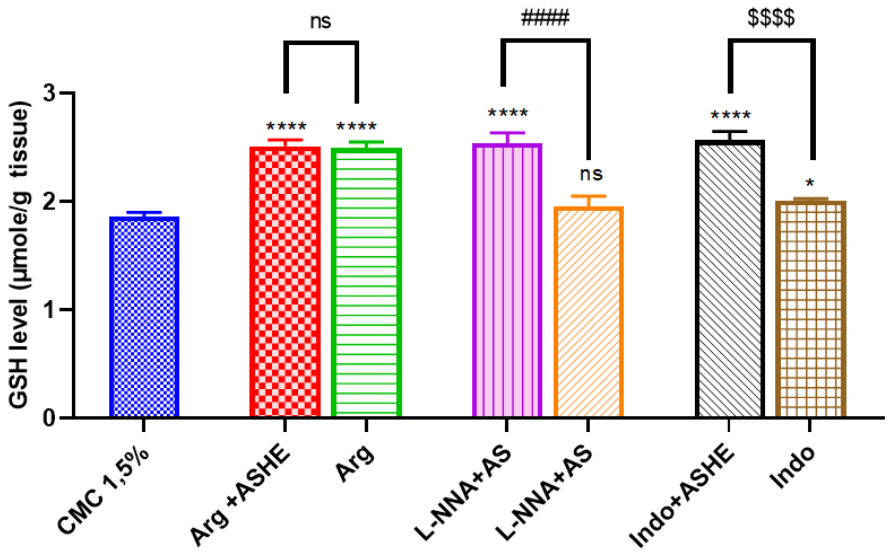

Figure 35: Effect of ASHE with the presence of both arginine, L-NNA, or indomethacin on GSH levels in rats subjected to ethanol treatment**.** The results were expressed as mean ± SEM (n=6) and analyzed by ANOVA followed by Tukey test. (****: P ≤ 0.0001, **: P ≤ 0.001) vs vehicle (CMC 1.5%). (####:P ≤ 0.0001, $: P ≤ 0. 05, ns: not significant) between within groups of arginine, L-NNA, or indomethacin.

3.2. Effect of ASHE on MDA Levels

The results showed that the negative control significantly higher MDA levels (42.69 ± 2.27 nmol/g of tissue) compared to the groups that were treated with arginine 9. 83 ± 2.91, ASHE + arginine (9.56±1.46) L-NNA+ASHE (9.72 ± 0.40), and ASHE + indomethacin (9.79 ± 1.59 nmol/g of tissue) However, there was no significant difference between the negative control and L-NNA or indomethacin groups with gastric ulceration (38.27 ± 0.40 and 37.51 ± 9.36 nmol/g of tissue respectively) (Figure 36).

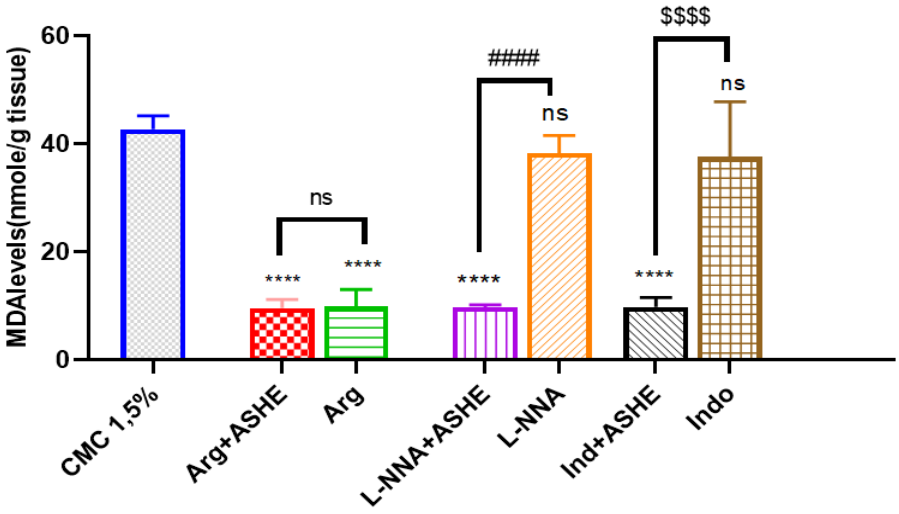

Figure 36: Effect of ASHE with arginine, L-NNA, or indomethacin on MDA levels in rats subjected to ethanol treatment**.** The results were expressed as mean ± SEM (n=6) and analyzed by ANOVA followed by Tukey test. (****: $P \leq 0.0001$, **: $P \leq 0.001$) vs vehicle (CMC 1.5%). (####:$P \leq 0.0001$, ns: not significant) between within groups of arginine, L-NNA, or indomethacin.

4. Discussion

4.1. Effect of ASHE on gastric ulcer

Gastric ulcer is a chronic disease that arises when there is damage to the mucosa lining of the stomach (Ofusori *et al*., 2019). It is characterized by necrosis, infiltration of neutrophils, decreased blood flow, the initiation of oxidative stress, and the release of inflammatory mediators. (Chen et al., 2015). its results from an imbalance between the protective factors (gastric mucin, prostaglandin secretion, blood flow, bicarbonate, nitric oxide, and growth factors) and aggressive factors (gastric acid, pepsin secretion, and *H. pylori*.) at the luminal surface of epithelial cells (Xie *et al*., 2019; Gugliandolo, *et al*., 2121; Jabbar *et al*., 2023). The most frequently employed alcohol to induce gastric ulcers in animal models is ethanol, due to its deleterious impact on the gastric mucosa, it causes significant harm, which is given by the Oral application. Ethanol is often used as a model to evaluate the gastro-defensive effects of different medicinal medications and natural products (Lui *et al*., 2021). It damages the digestive system in many ways, such as by increasing acid production, releasing proinflammatory cytokines, causing oxidative stress, letting activated neutrophils into the system, causing apoptosis, and lowering the levels of protective substances like nitric oxide (NO) and prostaglandin E2 (PGE2) (Katary and Salahuddin, 2017).

Following oral ethanol administration, our findings from the macroscopic observation revealed lesions in the gastric tissue that appeared as unnatural color, petechiae, hemorrhage, and oedema. These lesions are likely caused by elevated acid discharge which leads to decreased mucus and also tissue damage, congestion, and an inflammatory response.

Also, the results of the antiulcer effect have been confirmed by histopathological examination, where the microscopic observation showed damage to stomach tissue exposed to ethanol. The examination indicates erosion at the epithelium surface, congestion, as well infiltration of inflammatory cells. Ethanol has been documented to increase edema and remove epithelium by increasing microvascular and vascular permeability, leading to significant harm to the gastrointestinal mucosa (Beiranvand, 2022).

Pre-treatment with ASHE extract with three different doses (25 mg/kg, 50 mg/kg 100 mg/kg) led to a gradual improvement depending on the dose; by maintaining the integrity of the epithelium and vasculature this effect is reflected as a reduction in the ulcer index and an increased percentage of protection.

Ethanol has been shown to cause oxidative stress, which is characterized by an elevation in malondialdehyde levels and a reduction in the activity of catalase (CAT) and glutathione (Albaayit *et al*., 2016).

Our findings were in line with (Beiranvand *et al*., 2021; Gugliandolo *et al*, 2021), as the oral administration of ethanol caused a significant increase in gastric MDA, while gastric CAT and GSH were significantly decreased.

The enzyme catalase (CAT) facilitates the transformation of hydrogen peroxide (H_2O_2) into water and oxygen. In addition, H_2O_2 can be neutralized by GSH via its role as a cofactor for the glutathione peroxidase (GPx) enzyme 10 (Beiranvand *et al*., 2021).

MDA is the final product of lipid peroxidation and is often used to measure the amounts of peroxidation lipids (Si, *et al*,2020).

The pretreatment of ASHE extract showed a protective effect and reduced oxidative stress in stomach tissue. This extract has a considerable amount of phenolic compounds such as polyphenols, flavonoids, and tannins, which act together to give ASHE extract its antioxidant characteristic, which was represented by good activity in vitro for DPPH, ferrous ion chelating, and b-carotene bleaching assay.

Garlic phenolic compounds demonstrate antioxidant action by donating a hydrogen atom from the hydroxyl group to scavenge free radicals. In addition, garlic extract was discovered to reduce the activity of nicotinamide adenine dinucleotide phosphate-oxidase (NADPH oxidase), resulting in a reduction in lipid peroxidation (El-Ashmawy *et al*., 2016).

4.2. Effect of ASHE on the mechanism of ulcer lesions by arginine, L-NNA, and indomethacin.

The pathogenesis of acute gastric mucosal lesions is caused by several factors, but changes in the blood flow of the gastric mucosa (GMBF) seem to play a significant role in their development (Kalia *et al*., 2000).

L-arginine is a biological precursor for nitric oxide (NO) biosynthesis via nitric oxide synthase (NOS), and it has a role in regulating immunological and inflammatory processes (Heeba *et al*., 2023).

In present study, data showed that the pretreatment of L-arginine led to significant gastroprotective in the presence or absence of the extract. This is shown through macroscopic and microscopic observation, where significantly reduced mucous epithelium damage. Also, levels of catalase and GSH were higher compared to the negative control, while levels of MDA were lower, and this indicates the balance of both antioxidants and free radicals.

The results were consistent with the findings of (Czekaj *et al*., 2018; Kalia *et al*., 2000), where pretreatment of the gastric mucosa of rats with L-arginine alone resulted in a significant reduction in the area of gastric lesions, along with a significant increase in GMBF.

NO plays an important role in the mechanism of gastric mucosal protection and injury induced by pressure, ethanol, stress, and endotoxins, by regulating blood flow in the tissue and significantly contributing to mucus/bicarbonate secretion (Pan *et al*., 2005; Sánchez-Mendoza *et al*., 2020).

The gastroprotective effect of L-arginine (precursor for nitric oxide) is the ability to enhance mucus gel thickness and suppress acid secretion this is through the maintenance of mucosal blood flow (Heeba *et al*., 2023). The mechanism might be linked to an increase in the activity of the calcium-dependent synthase. This would then lead to an increase in cGMP synthesis by activating the GC system (Martin, and Motilva,2001). NO/cGMP plays a central role in inducing relaxation of mouse stomach fundus smooth muscle, and cGMP protects gastric parietal

cells from ethanol-induced cytotoxicity. On the other hand, NO stimulates the release of vasoactive intestinal peptide (VIP) in gastric tissue (Pan *et al*., 2005).

In the present study, the pretreatment with the L-NNA alone exacerbated the ethanol-induced gastric ulcer. This is shown through macroscopic observation, where was there increased ulceration and gastric membrane injury. In addition to histological changes represented by: significant mucosal erosion, oedema, and arterial congestion under the mucosa. Also, levels of catalase and GSH were lower compared to the negative control, while levels of MDA were higher. but the combining of L-NNA and the ASHE extract led to significant improvement and reduced ulcerative indicators.

L-nitro-N-arginine (L-NNA, a nitric oxide synthase inhibitor) is used to inhibit the inhibitory nitrergic pathway, and this effect can be reversed by L-arginine (Chen, *et al*., 2009). There are several studies (Brzozowski *et al*., 1997; Czekaj et al 2018) that have proven that pretreatment with L-NNA increased the injury of stomach ulcers induced by ethanol through the decreased gastric mucosal blood flow, concomitant administration of extract inhibition the effect of L- NNA by improving the damage.

Garlic contains a variety of amino acids, especially arginine (Ashraf *et al*., 2004). whereas previous studies have proven garlic's therapeutic effect by increasing nitric oxide (NO) production (Sooranna *et al*., 1995; Maslin *et al*., 1997). This explains the agonist effect of the extract with L-arginine. and inhibition of L -NNA activity.

Indomethacin is a non-steroidal anti-inflammatory medication (NSAID) derived from indole, exhibiting anti-inflammatory, analgesic, and antipyretic properties. It is utilized in the management of ankylosing spondylitis, osteoarthritis, rheumatoid arthritis, gout arthritis, bursitis, tendonitis, synovitis, and other inflammatory conditions because to its efficacious alleviation of pain, fever, redness, and oedema (Suleyman *et al*., 2010).

The prevailing understanding is that NSAIDs exert their effects by inhibiting both cyclooxygenase-1 (COX-1) and cyclooxygenase-2 (COX-2) isoenzymes within the arachidonic acid cascade. Both COX enzymes generate prostaglandin (PG), although COX-1 is deemed responsible for preserving gastric mucosal integrity. Conversely, COX-2 is stimulated by activities such as inflammation (Kanatani *et al*., 2004). Prostaglandins play a crucial role in maintaining the integrity of the gastric mucosa by stimulating bicarbonate and mucus secretion, preserving

mucosal blood flow, and regulating the regeneration of mucosal cells. PGs have a significant part in the activities of the digestive system (Fulga *et al*., 2020).

Several studies (Pique *et al*., 1988; Kanatani *et al*., 2004) have demonstrated that the administration of indomethacin in low doses with an ulcerating agent promotes the development of gastric mucosal damage, through the reduced gastric mucosal blood flow.

The treatment of ASHE extract led to significant gastroprotective effects, this has been observed through macroscopic and microscopic observation of the stomach, in addition to amendment of the oxidative stress parameters.

Aged garlic extract may augment nitric oxide synthesis by enhancing the activity of constitutive nitric oxide synthase (cNOS), potentially attributable to its capacity to facilitate calcium influx. Prior investigations validated garlic's capacity to preserve endothelial function via the nitric oxide route. Reports indicate that NOS and COX enzymes exhibit favorable mutual interaction, with both NO and PGE2 collaborating in the gastroprotection process (El-Ashmawy *et al*., 2016).

Chapter 4:

Liver between the toxicity of doxorubicin and the protection by *Allium sphaerocephalon* L.

1. Methods

1.1. Treatment of rats

In this experiment, 30 adults' male Wistar rats (weighing 200–250 g) were housed in polypropylene cages under standard conditions of temperature, photoperiod, and free access to food and water. Animals were fed on standard diet containing all essential nutrients.

Animals were divided into 6 equal groups, the control, group 2 (2 mg/kg bw DOX), group 3 (50 mg/kg bw ASHE), group 4 (100 mg/kg bw ASHE), group 5 (50 mg/kg bw ASHE + 2 mg/kg bw DOX), and group 6 (100 mg/kg bw ASHE + 2 mg/kg bw DOX), where DOX was injected on day 1, 7, and 14, whereas AS was administrated by gavage daily, the experiment lasted for three consecutive weeks; the procedure detail is given in table 10.

Table 10: Experimental detail of treating rats with Doxorubicin and ASHE (n= 30) for a period of three weeks**.**

3 weeks		
Groups	**Oral gavage daily**	**Intraperitoneal (*i.p.*) injection on day 1, 7, 14**
Group 1: (CTR)	0.9% NaCl	0.9% NaCl
Group 2: (DOX)	0.9% NaCl	2 mg/kg bw
Group 3 (ASHE)	50 mg/kg bw	0.9% NaCl
Group 4 (ASHE)	100 mg/kg bw	0.9% NaCl
Group 5 (ASHE+DOX)	50 mg/kg bw	2 mg/kg bw
Group 6 (ASHE+DOX)	100 mg/kg bw	2 mg/kg bw

CTR: Control, DOX: Doxorubicin, *AS: Allium sphaerocephalon*, bw: Body weight, Doxorubicin 0.9%, saline solution 0.9% NaCl.

After three weeks, the animals were decapitated, and then blood samples were collected in tubes containing heparin, for biochemical analyses. Immediately, organs (liver, and kidney) were removed, and used for histological and oxidative stress studies. Organs chosen for histology were preserved in 10% Formaldehyde solution, but those selected to study the oxidative stress were frozen at -20°C.

1.2. Biochemical analysis

The enzymatic activity of alanine transaminase, aspartate aminotransferase, and alkaline phosphatase and renal assessment (urea and creatine), is carried out at the laboratory analysis of the anti-cancer center (CAC) El Bez, Setif, by an automated analyzer according to the commercial kite technical

1.2.1. Alanine transaminase (ALT or ALAT)

Principle

Alanine aminotransferase (ALT), also known as glutamate pyruvate transaminase (GPT). ALT present in the sample catalyzes the transfer of the amino group from L-Alanine to 2-oxoglutarate, in the presence of pyridoxal5'-Phosphate, forming pyruvate and L-glutamate. Pyruvate in the presence of NADH and lactate dehydrogenase (LD) is reduced to L-lactate. In this reaction, NADH is oxidized to NAD. The reaction is monitored by measuring the rate of decrease in absorbance at 340 nm due to the oxidation of NADH to NAD.

$$\text{L-Alanine + 2-Oxoglutarate} \xrightarrow{\text{ALT, P-5'-P}} \text{L-Glutamate + Pyruvate}$$

$$\text{Pyruvate + NADH} \xrightarrow{\text{LD}} \text{L-Lactate + NAD}^{+}$$

1.2.2. Aspartate aminotransferase (AST)

Principle

Aspartate aminotransferase (AST) also known as glutamate oxaloacetate transaminase (GOT) AST present in the sample catalyzes the transfer of the amino group from L-aspartate to 2-oxoglutarate, in the presence of pyridoxal-5'- phosphate, forming oxaloacetate and L glutamate. Oxaloacetate in the presence of NADH and malate dehydrogenase (MDH) is reduced to L-malate. In this reaction, the NADH is oxidized to NAD. The reaction is monitored by measuring the rate of decrease in absorbance at 340 nm due to the oxidation of NADH to NAD.

1.2.3. Alkaline phosphatase

Principle

Alkaline phosphatase in the sample catalyzes the hydrolysis of colorless p-nitrophenyl phosphate (p-NPP) to give p-nitrophenol and inorganic phosphate. At the pH of the assay (alkaline), the p-nitrophenol is in the yellow phenoxide form. The rate of absorbance increase at 404 nm is directly proportional to the alkaline phosphatase activity in the sample. Optimized concentrations of zinc and magnesium ions are present to activate the alkaline phosphatase in the sample.

2. Results

2.1. Effect of ASHE on the Serum ALT, AST, and ALP levels in doxorubicin-induced hepatotoxicity in rats

Results indicated that ALAT (Figure 37), ASAT (Figure 38), and ALP (Figure 39) serums of rats were significantly higher in DOX group from 46.15 ± 9.66, 127.61 ± 25.10 U/L and 151 ± 22.44 7 to 248.34 ± 87.39, 270.54 ± 84.46 and 225.13 ± 14.14 U/L compared to the control. However, the pretreatment with both extract doses (50 mg/kg and 100 mg/kg) of ASHE extract significantly reduced AST ALT and ALP levels compared to the DOX group. In addition, there is no significant difference between the two doses.

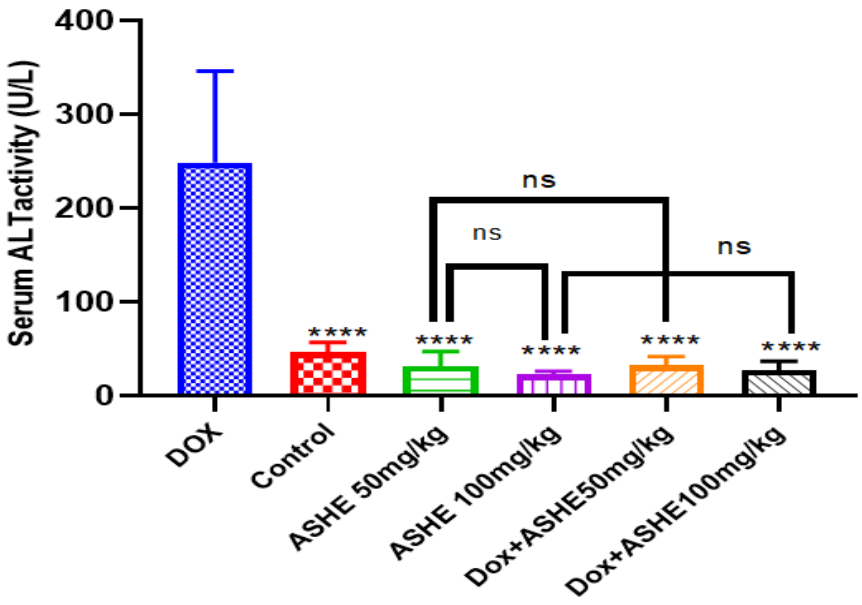

Figure 37. Impact of ASHE on ALAT activity in doxorubicin-induced hepatic injury in rats. The results were expressed as mean ± SEM (n=5) and analyzed by ANOVA followed by Tukey test. (****: $P \leq 0.0001$) vs doxorubicin group. (ns: not significant) between the two doses. (ns: not significant). between each dose and its combined group.

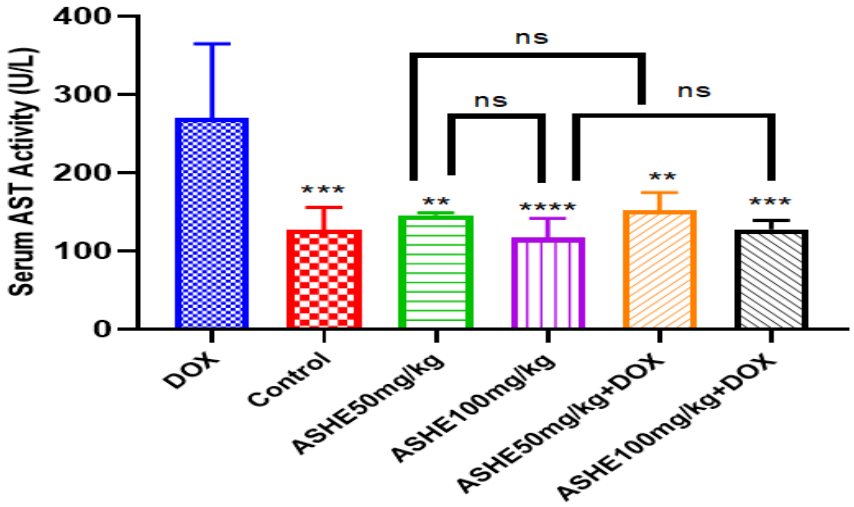

Figure 38: The influence of ASHE on AST Activity in rats treated with Doxorubicin**.** The results were expressed as mean ± SEM (n=5) and analyzed by ANOVA followed by Tukey test. (****: $P \leq 0.0001$, ***: $P \leq 0.001$, **: $P \leq 0.01$) vs doxorubicin group. (ns: not significant) between the two doses (ns: not significant) between each dose and its combined group.

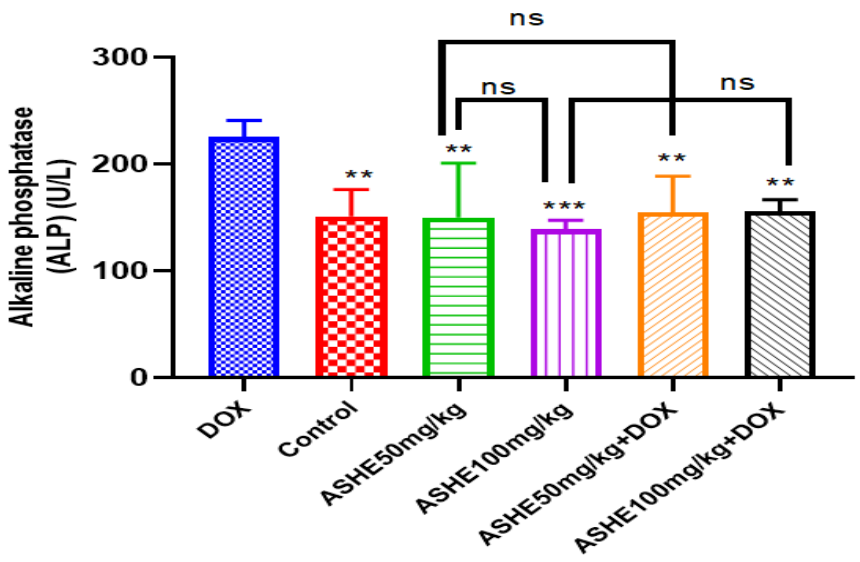

Figure 39: Impact of ASHE on ALP Activity in Doxorubicin-Treated Rats**.** The results were expressed as mean ± SEM (n=5) and analyzed by ANOVA followed by Tukey test. (***: P ≤ 0.001, **: P ≤ 0.01) vs doxorubicin group. (ns: not significant) between the two doses. (ns: not significant) between each dose and its combined group.

2.2. Effects of ASHE extract on the antioxidant activity in the liver tissue of rats.

2.2.1. Effect of ASHE on catalase activity

Treatment of rats with DOX exhibited decreased activity of catalase to 3.02 ± 0.62 µmol/min/mg of protein. This decrease reached a statistically significant difference (P ≤ 0.0001) compared to the control group (10.36 ± 1.03 µmol/min/mg of protein) and at the selective doses (50 and 100 mg/kg). At these doses, the value of catalase activity was 10.57 ± 0.47, 12.97 ± 0.94 µmol/min/mg of protein respectively. no significant difference between these doses. Pretreatment with the different doses of ASHE extract showed a very highly significant improvement in the activity of catalase, while a highly significant (p ≤ 0.0001) improvement was observed in higher doses (Figure 40).

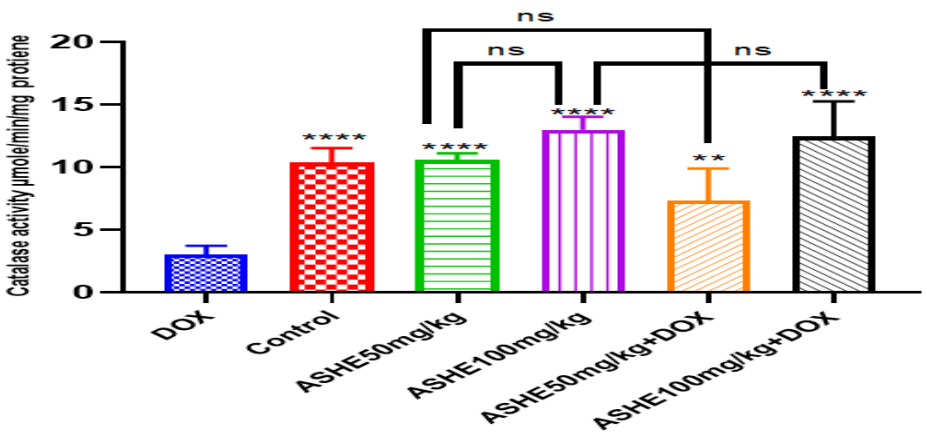

Figure 40: The effect of ASHE on catalase activity in the hepatic tissue of rats exposed to DOX**.** The results were expressed as mean ± SEM (n=5) and analyzed by ANOVA followed by Tukey test. (****: P ≤ 0.0001, **: P ≤ 0.01) vs doxorubicin group. (ns: not significant) between the two doses. (ns: not significant) Compare each dose with the dose given with the doxorubicin.

2.2.2. Effect of ASHE on MDA levels

The results of MDA levels showed that the DOX poisoning in rats induced lipid peroxidation, resulting in a very high-significance increase ($p < 0.001$) of the MDA level in liver (35.69 ± 2.93 nmol/g of tissue) compared to control (23.93 ± 2.71 nmol/g of tissue). In addition, rats pretreated with ASHE extract of 50 and 100 mg/kg orally showed a decrease in cytosolic MDA, where the value was 29.79 ± 2.24 and 27.99 ± 1.85 nmol/g of tissue, respectively (Figure 41).

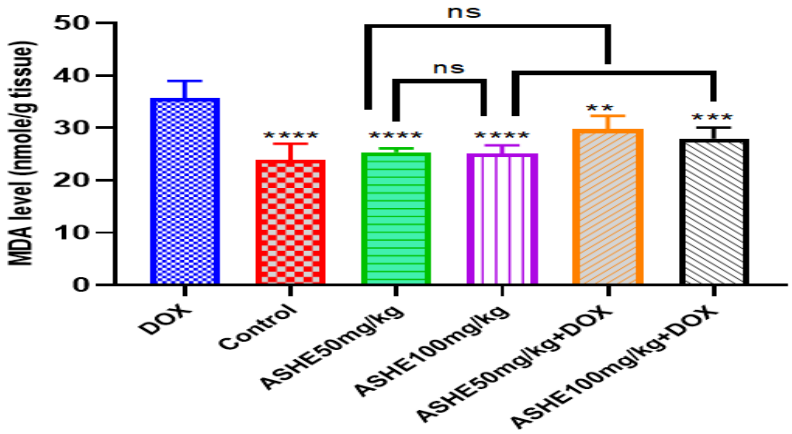

Figure 41: Effect of ASHE on MDA levels in the liver of rats exposed to DOX**.** The results were expressed as mean ± SEM (n=5) and analyzed by ANOVA followed by Tukey test. (****: P ≤ 0.0001, **: P ≤ 0.001) vs doxorubicin group. (ns: not significant) between the two doses. (ns: not significant): Comparing each plant extract dose with the combing groups.

2.2.2. Effect of ASHE on GSH levels

The result showed that the GSH (Figure 42) levels were significantly lower in the DOX group (3.542 ± 0.16 µmol/g of tissue) compared to the control (4.96 ± 0.63 µmol/g of tissue). In addition, rats pretreated with ASHE extract (50 and 100 mg/kg) were restaured the GSH levels to 4.34 ± 0.11and 4.59 ± 0.06 µmol/g of tissue. These values were significantly different between the two doses (P ≤ 0.0 1).

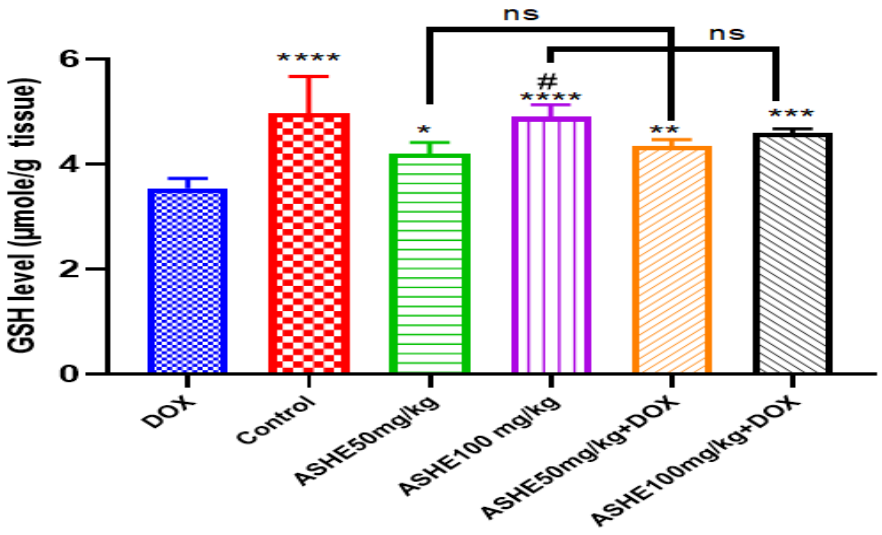

Figure 42: Effect of ASHE on GSH levels in the liver of rats exposed to DOX**.** The results were expressed as mean ± SEM (n=5) and analyzed by ANOVA followed by Tukey test. (****:P ≤ 0.0001, ***:P ≤ 0.0001, **: P ≤ 0.001, *:P ≤ 0.01) *vs* doxorubicin group. (#: P ≤ 0. 1) between the two doses. (ns: not significant) Comparing each plant extract dose with the combing groups.

2.3. Histopathological Analysis

The control group showed typical histological architecture with rounded nuclei and blood sinusoids, a centrilobular vein, and spans of Remak normal. In contrast, liver sections in animals that received Doxorubicin (DOX) at accumulation dose of 6 mg/kg reveal the presence of hepatocyte necrosis, nucleolus disappearing, sinusoids capillaries dilated and congestion in Kiernan space. While the liver section of the group treated with ASHE at doses of 50 mg/kg and 100 mg/kg showed a normal liver structure with congestion in the centrilobular vein in the group treated with 100 mg/kg.

On the other hand, all histopathological changes caused by doxorubicin were prevented by pretreatment of ASHE (50 mg/kg and 100 mg/kg), with the existence of some congestion.

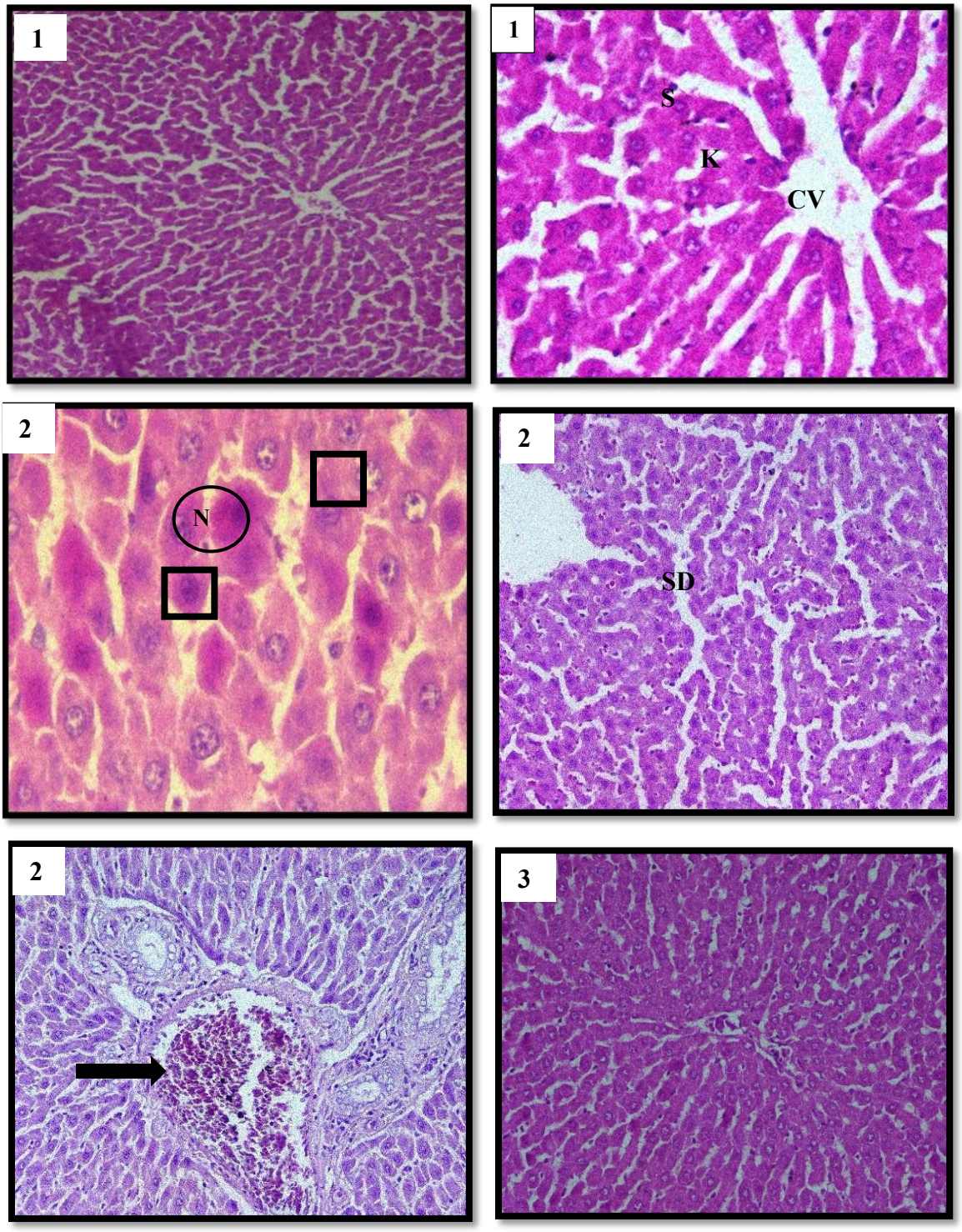
1
1
S
K
CV
2
N
2
SD
2
3

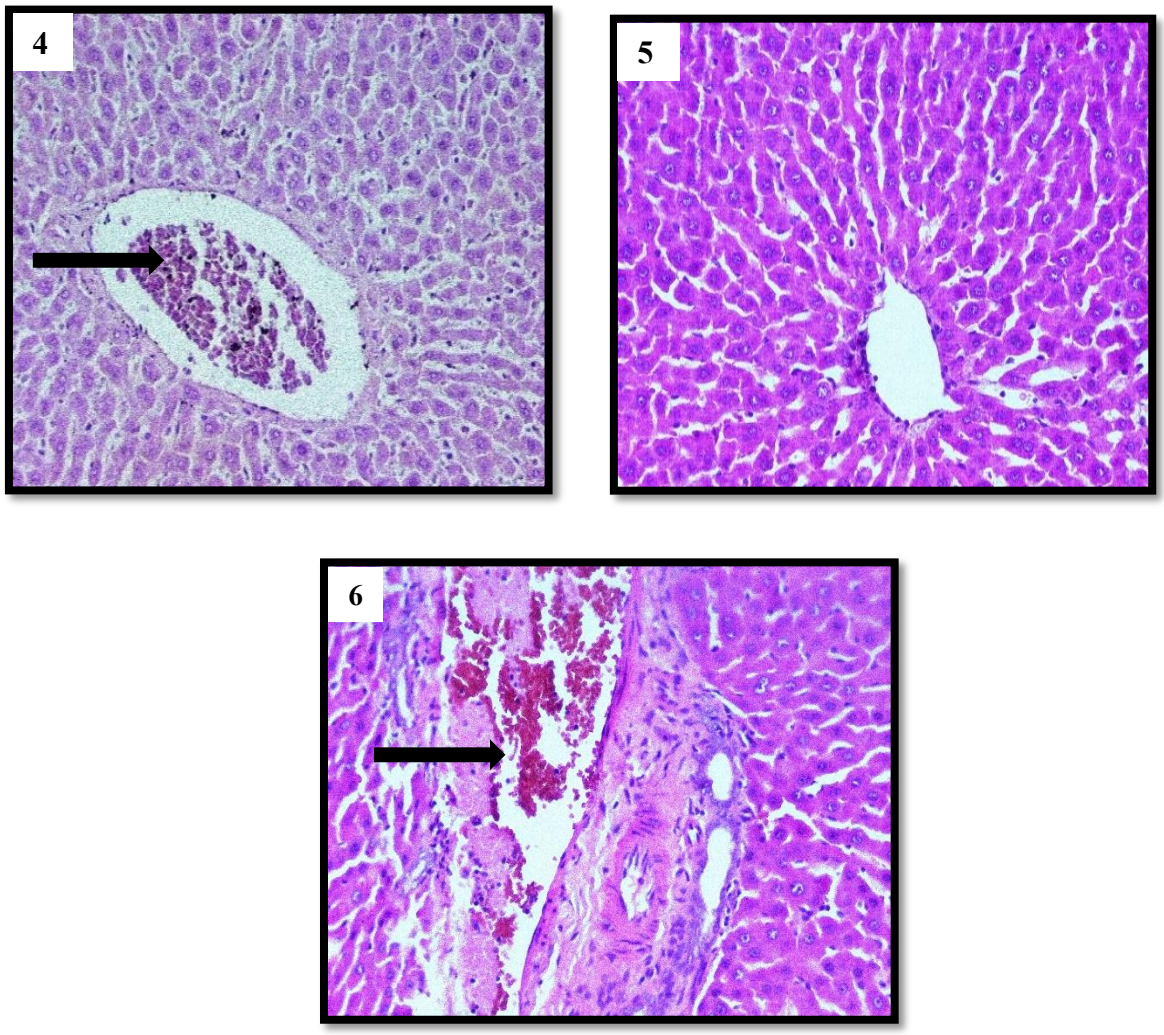

Figure 43: Liver histology of rats exposed to DOX and ASHE extract**.** Hepatic tissues were stained with hematoxylin-eosin .(1) Control groups ,(2) groups treated with DOX , (3): 50 mg/kg of ASHE , (4) 100 mg/kg of ASHE, (5): DOX +ASHE 50 mg/kg, (6): DOX + ASHE 100 mg/kg .
S: blood sinusoids, K: Kupffer cells, CV: centrilobular vein N: necrosis, Arrow: rounded nuclei of hepatocyte, SD: sinusoids capillaries dilated Square: nucleolus disappearing, thick arrow: congestion.

3. Discussion

The liver is an accessory organ in animals, performs several metabolic activities to maintain homeostasis. It synthesizes, stores, and metabolizes many biomolecules, including plasma proteins, enzymes, hormones, vitamins, and cholesterol. It also facilitates the detoxification of xenobiotics via a complicated hepatic enzymatic mechanism (Demir *et al*., 2023; Hossain *et al*., 2023).

Hepatotoxicity is associated with compromised liver function, through exposure to a drug or other factors severely impairing its function (Pieniążek *et al*., 2013).

Hepatotoxicity caused by doxorubicin has been shown in many experimental trials (Yagmurca *et al*., 2007; Injac *et al*., 2009; Petrovic *et al*., 2018). Our study also indicated that intraperitoneal injection of three doses at (2mgkg) of DOX within 3 weeks resulted in hepatic tissue damage, as demonstrated by morphological and biochemical assessments.

In clinical practice, a serum panel of hepatic enzymes, including (GGT), (ALT), (ALP), and (AST), are often evaluated as part of "Liver function tests" (Huang, *et al*., 2023).

In the present investigation has showed that doxorubicin induced a range of adverse effects, including elevation of serum ALT, AST, and alkaline phosphatase (ALP) levels. This data is consistent with (Zhao *et al*., 2012; Omobowale *et al*, 2018).

Cell membrane damage to hepatocytes disrupts membrane permeability, causing hepatocellular enzymes (AST, ALT, ALP) to leak from the cell, increasing serum levels, and is considered an indicator of liver damage. This is because doxorubicin can generate superoxide radicals and peroxynitrite radicals when metabolized in the liver. Consequently, the (ROS) generated triggers the oxidation of lipids, leading to liver damage and the release of hepatic enzymes (Demir *et al*., 2023; Prasanna *et al*., 2020).

The combination of DOX and two different doses of ASHE (50 mg/kg, 100 mg/kg) extracts in this study showed significant decreases in plasma AST, ALT, and ALP levels compared to the DOX group.

There is ample proof that several sulfur compounds included in Allium tissue specimens are accountable for diverse biological effects, including antioxidant and hepatoprotective actions. (Lazarević *et al*., 2011). The hepatoprotective properties of garlic oil may be ascribed to its ability to prevent cellular leakage and preserve the integrity of the liver cell membrane (Azab and Albasha, 2018).

Antioxidant enzymes, including catalase and superoxide dismutase, serve as the primary cellular defense mechanisms against oxidative damage. The equilibrium among these enzymes is essential for mitigating oxidative damage within intracellular organelles (Akinloye *et al*., 2022). The mechanism of DOX toxicity involves oxidative stress, marked by the generation of excessive (ROS) and/or a reduction in antioxidant defenses, resulting in an imbalance in normal oxygen metabolism (Mansouri *et al*., 2017).

The findings of the current investigation indicated that DOX-induced oxidative damage and hepatotoxicity in rats were characterized by an elevation of MDA levels in hepatic tissue as well as a reduction in the levels of the antioxidant enzymes CAT and non-enzyme antioxidant GSH. This data is in accordance with (Yagmurca *et al*., 2007; Mansouri *et al*., 2017).

In the current study, the combination of DOX and two doses of ASHE extracts displayed a reduction in MDA levels. and increases in GSH and CAT levels. This can be explained by improved liver oxidant/antioxidant balance, according to our finding. This extract has a favorable amount of phenolic compounds such as polyphenols, flavonoids, and tannins, which act together to give ASHE extract its antioxidant characteristic, which was represented by good activity in vitro for DPPH, ferrous ion chelating, and bleaching.

Additionally, Emir, and Emir (2020) proved that *Allium sphaerocephalon* L. constitutes a substantial natural reservoir of phenolic chemicals.

According to the study by Mete *et al*. (2015) pretreatment with *Alluim cepa* extract protects rats' livers from damage caused by DOX. This is because this extract has antioxidant properties.

Prior research has identified the following histological alterations after the DOX injection: Hepatic vein congestion, moderate hepatic sinusoidal dilatation, and inflammatory cells. pycnotic nucleus (Demir *et al*., 2023), degeneration hepatocytes, parenchymal necrosis, congestion and thrombosis in the central vein, and inflammation in portal space (Yagmurca *et al*., 2007). edema, sinusoidal dilatation, mononuclear cell infiltration, degeneration in the hepatocytes, focal necrosis, cellular hypertrophy, steatosis, blood vessel congestion, and septa formation (Afsar *et al*., 2019). severe vacuolar degeneration, distributed diffusely within the hepatocytes, along with significant fatty degeneration. Sinusoidal capillaries appear dilated in some areas, together with the presence of a standard central vein (Abdalla *et al*., 2023). oedema, tissue injury, inflammatory cell infiltration, and degeneration in the hepatocytes as well as focal necrosis (Zhao *et al*., 2012).

In the present study, the toxicity of doxorubicin led to Hepatocyte necrosis, nucleolus disappearing, sinusoids capillaries dilated, and congestion. The treatment with the combined ASHE extract + DOX at different doses ameliorated this hepatotoxicity. This can be explained by the presence of natural compounds in this extract that directly remove the toxicity resulting from DOX before it damages liver tissue by scavenging the free radicals responsible for destroying the liver cell due to the antioxidant activity of these natural compounds.

Chapter 5:
Nephroprotective action of *Allium sphareocephalon* L. on doxorubicin-induced toxicity

1. Methods

1.1. Urea Principle

Urease catalyzes urea hemolysis, present in the sample, in ammonia (NH4) and carbon dioxide (CO_2). Ammonium ions react with salicylate and Sodium hypochlorite (NaClO), in the presence Nitroprussiate catalyst, to form a green indophenol.

$$\text{urea} \xrightarrow{\text{Urease}} (NH_4^+)_2 + CO_2$$

$$NH_4 + \text{salicylate} + ClONa \xrightarrow{\text{Nitroprussiate}} \text{indophenol.}$$

1.2. Creatinine

This method is based on a change in the original picrate reaction (Jaffe).
Creatinine in alkaline medium reacts with ions picrate forming a reddish complex. The rate of complex formation measured by the increase in absorbance within a predefined time interval is proportional to the creatinine concentration in the sample.

$$\text{Creatinine} + \text{picric acid} \xrightarrow[37^{\circ}C]{PH > 12} \text{Reddish complex}$$

2. Results

2.1 Effect of ASHE on the Serum Urea and Creatinine levels in doxorubicin-induced nephrotoxicity in rats

Results indicated that Urea (Figure 44) and Creatinine (Figure 45), levels of rats were significantly higher in DOX group from 0.91 ± 0.36 g/L, 09.10 ± 0.28 U/L to 0.36 ± 0.11 g/L, 06.46 ± 0.67 U/L compared to the control. However, the pretreatment with both extract doses (50 mg/kg and 100 mg/kg) of ASHE extract significantly reduced Urea and creatine levels compared to the DOX group. In addition, these parameters were not significantly different between the two doses.

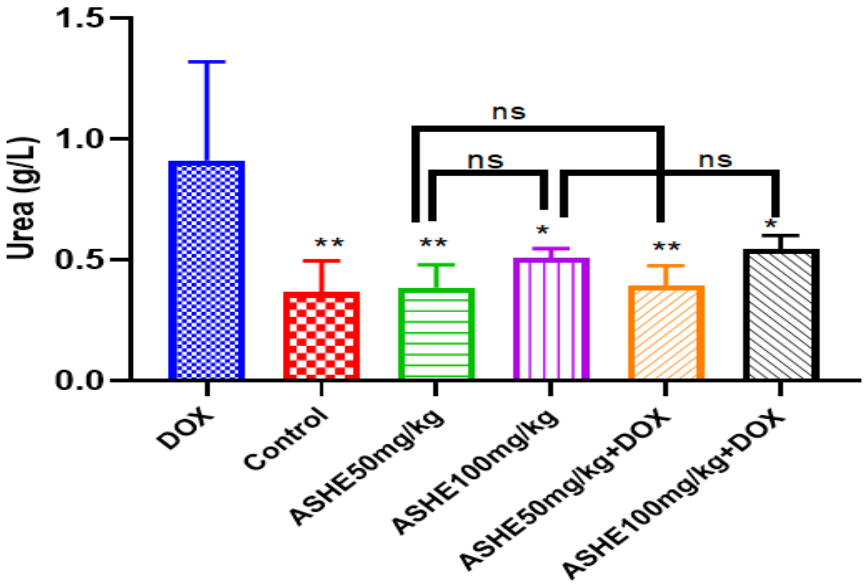

Figure 44. The Influence of ASHE extract on Urea in Rat Treated with Doxorubicin**.** The results were expressed as mean ± SEM (n=5) and analyzed by ANOVA followed by Tukey test. (**: P ≤ 0.001, *: P ≤ 0.05,) vs doxorubicin group. (ns: not significant) between the two doses (ns: not significant) between each dose and its combined group.

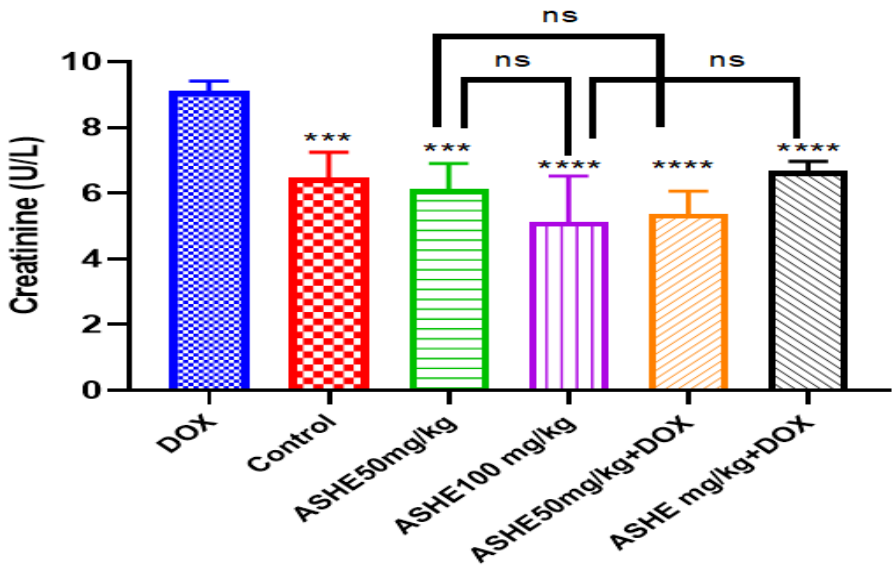

Figure 45: The Influence of ASHE extract on serum Creatinine concentration in rats treated with Doxorubicin. The results were expressed as mean ± SEM (n=5) and analyzed by ANOVA followed by Tukey test. (****: P ≤ 0.0001, ***: P ≤ 0.001,) vs doxorubicin group. (ns: not significant) between the two doses (ns: not significant) between each dose and its combined group.

2.2. Effects of ASHE extract on the antioxidant activity in the Kidney tissue of rats.

2.2.1. Effect of ASHE on catalase activity

Treatment of rats with DOX exhibited decreased activity of catalase to 29.30 ± 3.31 µmol/min/mg of protein. This increase reached a statistically significant difference ($P \leq 0.001$) compared to the control group (43.07 ± 2.01 µmol/min/mg of protein) and at the selective doses (50 and 100 mg/kg). At these doses, the value of catalase activity was (44.20 ± 2.52, 40.97 ± 2.71 µmol/min/mg of protein, respectively). no significant difference between these doses. Pretreatment with the different doses of ASHE extract showed a very highly significant improvement in the activity of catalase, while a highly significant ($p \leq 0.0001$) improvement was observed in higher doses (Figure 46).

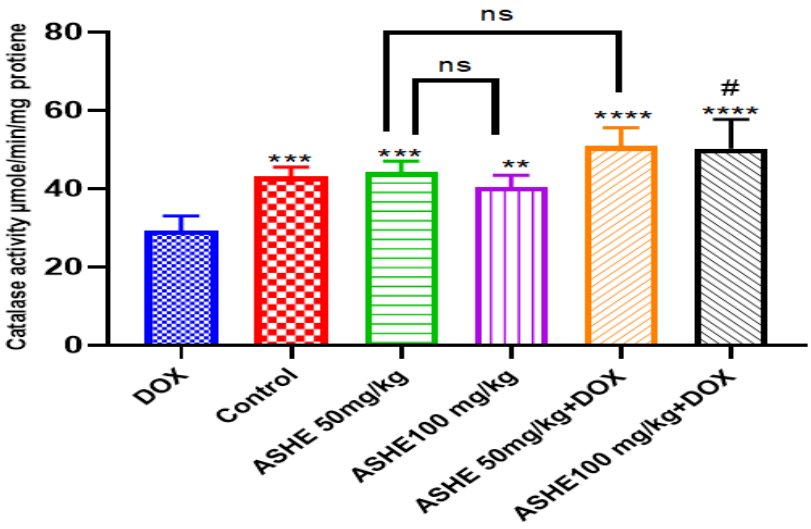

Figure 46: Effect of ASHE extract on catalase activity in the kidney of rats exposed to DOX. The results were expressed as mean ± SEM (n=5) and analyzed by ANOVA followed by Tukey test. (***:$P \leq 0.001$, **: $P \leq 0.01$, *:$P \leq 0.05$) vs doxorubicin group. (ns: not significant) between the two doses. (ns: not significant) Compare each dose with the dose given with the doxorubicin.

2.2.2. Effect of ASHE on MDA levels

The results of MDA levels in kidney are shown in figure 47. DOX poisoning in rats induced lipid peroxidation resulting in a very high significance of the MDA level reached to 138.93 ± 2.42 nmol/g of tissue compared to control 88.31 ± 3.38 nmol/g of tissue. In addition, rats pretreated with ASHE extract (50 and 100 mg/kg) showed a decrease in cytosolic MDA to (100.39±3.40 and 111.92 ±3.18 nmol/g of tissue).

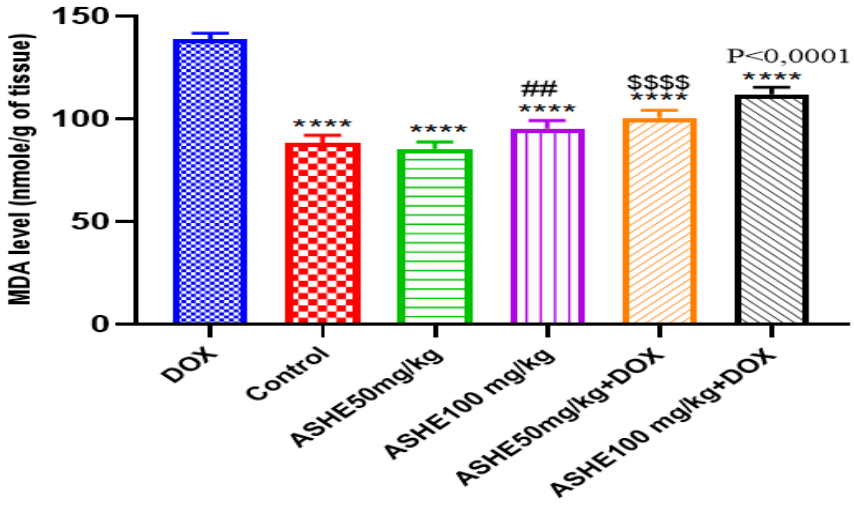

Figure 47: Effect of ASHE extract on MDA levels in the kidney of rats exposed to DOX**.** The results were expressed as mean ± SEM (n=5) and analyzed by ANOVA followed by Tukey test. (****: P ≤ 0.0001) vs doxorubicin group. (##: P ≤0.001) between the two doses. ($$$$: P ≤ 0.0001, P ≤ 0.0001) Compare each dose with the dose given with the doxorubicin.

2.2.2. Effect of ASHE on GSH levels

The result showed that the GSH (Figure 48) levels were significantly lower in the DOX group (2.85 ± 0.01 µmol/g of tissue) compared to the control (3.90 ± 0.11 µmol/g of tissue)). In addition, rats pretreated with ASHE extract (100 mg/kg) showed a significant increase in GSH level of 3.86 ± 0.19 µmol/g of tissue. while being not significantly different in (50 mg/kg) compared to DOX group.

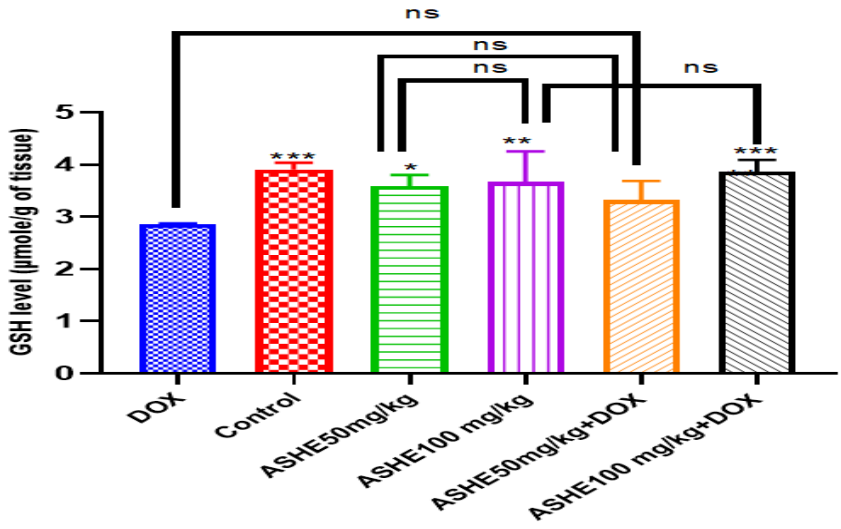

Figure 48: Effect of ASHE extract on GSH levels in the kidney of rats exposed to DOX**.** The results were expressed as mean ± SEM (n=5) and analyzed by ANOVA followed by Tukey test. (***:P ≤ 0.0001, **: P ≤ 0.001, *:P ≤ 0.05) vs doxorubicin group. (ns: not significant) between the two doses. (ns: not significant) Compare each dose with the dose given with the doxorubicin.

2.3. Histopathological analysis

In microscopic observation, normal renal parenchyma was observed in the control group. The parenchyma consists of two layers. The cortex consists of renal corpuscles dense and rounded structures, which are composed of the glomerulus and the surrounding glomerular (Bowman's capsule), enveloping an area full of fluid (Bowman's space). In addition to having proximal and distal convoluted tubes. and medulla with tubules and vessels surrounded by connective tissue. The group treated with doxorubicin showed distortion and atrophy of the glomerulus, vascular congestion, the appearance of intratubular eosinophilic bodies, and lymphoid infiltration.

The kidney histoarchitecture of rats co-treated with ASHE (50 mg/kg and 100 mg/kg) showed a significant improvement with glomerular normal and vascular congestion.

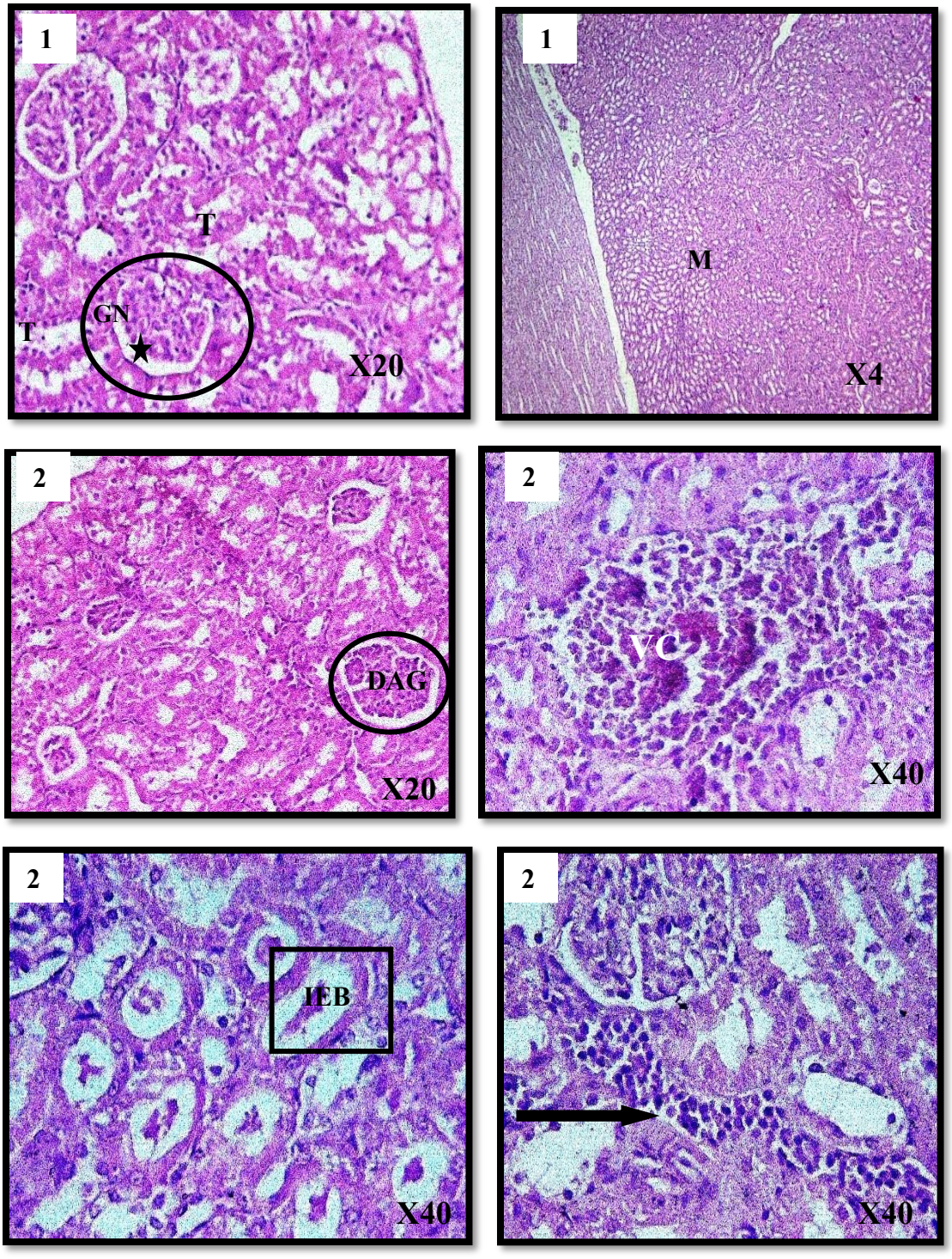
1
T
GN
T
X20
1
M
X4
2
DAG
X20
2
VC
X40
2
IEB
X40
2
X40

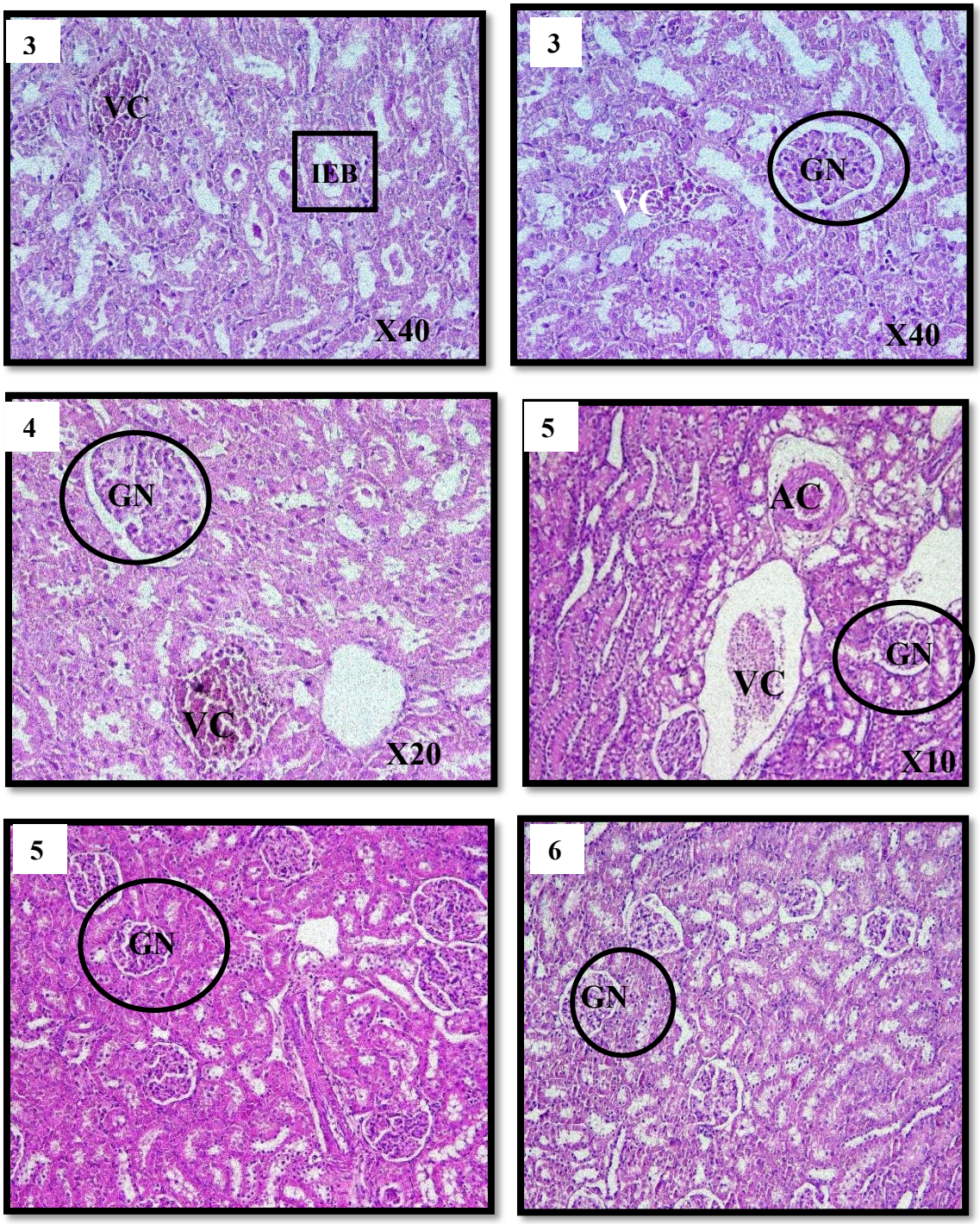

Figure 49: Kidney histology of rats exposed to DOX and ASHE extract**.** Kideny tissues were stained with hematoxylin-eosin.).(1) Control groups ,(2) groups treated with DOX , (3): 50 mg/kg of ASHE , (4) 100 mg/kg of ASHE, (5): DOX +ASHE 50 mg/kg, (6): DOX + ASHE 100 mg/kg .
GN: glomerulus normal, M: Mudella, T: tubules, star: Bowman's capsule, DAG: distortion and atrophy of the glomerulus, VC: vascular congestion, IED: intratubular eosinophilic bodies, Arrow: lymphoid infiltration, AC: Arterial congestion.

3. Discussion

The kidney is a complex and dynamic organ involved in waste disposal, homeostasis maintenance, and acid-base balance regulation. Renal toxicity can compromise kidney function. (Ali *et al*., 2021), Nephrotoxicity is a prevalent side effect of doxorubicin as an anticancer drug. (Su *et al*., 2015). This study examined the preventive effect of ASHE extract against nephrotoxicity.

When DOX was given intraperitoneally at a cumulative dose of 6 mg/kg, blood urea and creatinine levels rose significantly. This was supported by toxic histopathological changes compared to the control group. Serum levels of urea and creatinine are utilized to evaluate renal function and determine drug-induced nephrotoxicity in humans and animals (Molehin *et al*., 2019). The nephrotoxic impact of DOX is marked by a reduction in glomerular filtration rate, resulting in elevated serum urea and creatinine levels (Refaie *et al*., 2016). This aligns with prior research indicating that doxorubicin (DOX) is associated with increased nephrotoxicity markers and glomerular damage, either directly through the accumulation of toxic metabolites in nephrons and reduced glomerular filtration rate, or indirectly via DOX-induced oxidative stress in the kidneys. (Fouad and Ahmed, 2021). Our findings are consistent with prior research (Refaie *et al*., 2016; El-Sayed *et al*., 2017).

The current investigation showed that the injection of DOX, followed by ASHE extract, significantly recovered the serum creatinine and urea levels, which were considerably raised by treatment with DOX alone. It was observed that the kidneys had restored their function. This could be attributed to the cytoprotective effect of this extract. In addition to the ASHE extract's antioxidant properties, according to our previous study (Kaoudoune *et al*., 2024). These data agree with the previous, similar, reports (Anusuya *et al*., 2013; Elbeltagy *et al*., 2022). Conversely, in the doxorubicin-treated group, there was a reduction in the levels of CAT and GSH enzymes, while the concentration of MDA rose. These dates align with the previous investigations (Molehin *et al*., 2019; Nimbal *et al*., 2021).

Numerous papers have documented the rise in oxidative stress due to a reduction in antioxidant enzymes, resulting in a cascade of reactions that ultimately lead to doxorubicin-induced damage to cardiac and renal tissues (Nimbal *et al*., 2021).

DOX, in the form of semiquinone, is proposed to significantly contribute to its nephrotoxic effects. Semiquinones are unstable in aerobic environments, leading to the production of superoxide anion radicals through their reaction with molecular oxygen (Mohan *et al*., 2010).

Doxorubicin induces the generation of free radicals (ROS and RNS) through two mechanisms. The first mechanism is enzymatic, employing cellular oxidoreductases, while the second is non-enzymatic, involving complexation with iron (Fe^{3+}). The "DOX-iron" complex demonstrates a high redox potential, resulting in the production of reactive oxygen species (ROS) and hydrogen peroxide (H_2O_2); the generated H_2O_2 can damage lipid membrane structures and induce lipid peroxidation. DOX-induced H_2O_2 is neutralized by antioxidant enzymes such as catalase (CAT). It was estimated that catalase was severely reduced (Nimbal *et al*., 2021; Fouad and Ahmed, 2021).

In the current investigation, the administration of extract in the combined groups resulted in elevated kidney GSH and CAT activities, and decreased MDA levels, in comparison to the DOX group. The observed ameliorative effect of garlic in this study may be attributed to its phytochemical constituents. Garlic comprises several active constituents, including Sally cysteine (SAC), diallyl disulphide (DAS), diallyl trisulphide (DATS), allium, and its derivatives. These components function as chelating agents due to their abundant and accessible sulfhydryl groups (SH) (Adeniyi *et al*., 2012). The study presented by Lin *et al*. (2019), found that the DAS can prevent Dox-induced nephropathy through enhancing antioxidant activities.

These findings run in parallel with histopathological analysis of DOX-induced kidneys. doxorubicin treated rats showed distortion and atrophy of the glomerulus, vascular congestion, the appearance of intratubular eosinophilic bodies, and lymphoid infiltration, in comparison to the control group, the aforementioned modifications are compared with the previously documented studies: Altinoz *et al*. (2022) showed the dox at a dose of 20 mg/kg caused a hemorrhage and glomerular congestion, infiltration, vacuolization, and loss of microvilli. On the other hand, Hussain *et al*. (2021) showed that the dose (3.5 mg/kg twice weekly for 3 weeks), exhibited distorted stroma, including many vacuoles, congested and dilated blood vessels, several renal corpuscles had oedema with obliterated Bowman's capsules. Some other corpuscles were atrophied. Certain renal tubules exhibited dilation, while others were squeezed and destroyed. These previous studies confirmed our histopathological findings. supposed to the histological changes generated by DOX may be correlated with oxidative stress.

In the present study, the ASHE extract mitigated the histological damage induced by doxorubicin. the phytochemical analysis demonstrated that the ASHE extract contained several flavonoids such as quercetin (data not published). The modest dosage of quercetin may constitute an innovative therapeutic strategy for mitigating DOX-induced nephrotoxicity via its antioxidant, anti-inflammatory, and anti-apoptotic properties (Heeba and Mahmoud, 2016). The findings of Ilic *et al*., (2014) indicated that quercetin had nephroprotective properties and diminishes lipid peroxidation in rats treated with cisplatin.

Conclusion and perspectives

The present study showed that the plant in study contains a moderate number of phenolic compounds. These characteristics have prompted us to study some pharmacological effects and several biological activities.

The hydroethanolic and aqueous extracts of *Allium sphareocephalon* L. flower's part have antioxidant activity for: DPPH radical scavenging assay, reducing power, cupric reducing antioxidant capacity, ferrous ion chelating, and -carotene bleaching test.

Phytochemical analysis of ASHE extract identified sixteen phenolic compounds with quinoic acid and acetin is the major compounds.

The ASHE extract provides excellent protection against ethanol-induced gastric ulcers. This protection effect is due to the extract's effectiveness in scavenging different free radicals that result from ethanol. Furthermore, the NO pathway's activation or the inhibition of cyclooxygenase 2 serve as a gastroprotective mechanism.

On the other hand, hepatotoxicity and nephrotoxicity of drugs are major problems for the pharmaceutical industry and public health. There are still very few studies in the field of new molecules capable of preventing or even improving hepatotoxicity and nephrotoxicity in drugs.

The intraperitoneal administration of doxorubicin dose (2 mg/kg) for three times weekly caused hepatotoxicity and nephrotoxicity, which resulted in a disturbance of biochemical parameters and the antioxidant status as well as the histology of the tissues studied. This is due to the mechanism by which doxorubicin induces toxicity through excessive production of free radicals.

The ASHE extract pretreatment resulted in hepatoprotective and nephroprotective effects. This is due to the presence of phenolic compounds, particularly flavonoids, in the extract, which directly eliminate the toxicity caused by DOX before it damages liver or kidney tissues. This is achieved by scavenging free radicals, a process made possible by the antioxidant activity of these natural compounds.

As a general conclusion, it can be suggested that the extract of *Allium sphareocephalon* L. can be a good source of natural antioxidants, useful to prevent or slow the progression of various diseases related to oxidative stress, which could have pharmaceutical or dietary applications. However, we should enhance the therapeutic impact of this plant by examining its sub chronic and

chronic toxicity to gain a deeper understanding of its safety dose and to ensure a safe and effective pharmacological effect.

This study is considered as a preliminary step to study biological activities and the compounds of natural origin. and represented in:

- Conducting in-depth chemical analysis for isolation of the phenolic compounds and studying their individual effects on biological activities.
- Study of other natural compounds in garlic represented by organosulfur and their therapeutic effect.
- Study the anticancer, antitumor, antibacterial, antifungal activities of this extract.
- Use an *in vitro* method to study the plant's effect on gastric, hepatic, and renal cells.
- Deepen the research by studying the extent to which the plant protects the genetic material (DNA) of the studied organs.

Bibliographic references

Bibliographic references

1) **Abdalla, Z. A**., Abtar, A. N., Kareem, A. A., Ahmed, Z. A., & Aziz, T. A. (2023). Study of the effect of bezafibrate with ginkgo biloba extracts in an animal model of hepatotoxicity induced by doxorubicin. Biochemistry and Biophysics Reports, 36, 101582.

2) **Adams, D. H.** and Eksteen, B. (2006). Aberrant homing of mucosal T cells and extra-intestinal manifestations of inflammatory bowel disease. Nature Reviews Immunology, 6(3), 244-251.

3) **Adeniyi, T. T**., Ajayi, G. O., Sado, M. A., & Olopade, H. J. (2012). Vitamin C and garlic (Allium sativum) ameliorate nephrotoxicity and biochemical alterations induced in lead-exposed rats. The Journal of Medical Sciences, 3(5), 273-280.

4) **Adinortey, M. B.**, Ansah, C., Galyuon, I., & Nyarko, A. (2013). In vivo models used for evaluation of potential antigastroduodenal ulcer agents. Ulcers, 2013(1), 796405.

5) **Afsar, T**., Razak, S., Almajwal, A. (2019). Effect of Acacia hydaspica R. Parker extract on lipid peroxidation, antioxidant status, liver function test and histopathology in doxorubicin treated rats. Lipids in Health and Disease, 18(1), 1-12.

6) **Ahmed, M**. (2019). Peptic ulcer disease. In Digestive System-Recent Advances. Intech Open.

7) **Akilesh S**., (2014) "Normal kidney function and structure," in Pathobiology of Human Disease, pp. 2716–2733.

8) **Akinloye O A**., Sulaimon L A., Adewale A O., Mubaraq T, Salami O, Abiola O, (2022), Allium vineale methanol extract attenuated oxidative stress and inflammation induced by doxorubicin in Sprague Dawley Rats, Scientific African 16 (2022) e01244.

9) **Albaayit S. F. A**., AbbaY, Abdullah R, Abdullah N, (2016) Prophylactic effects of Clausena excavata Burum. f. leaf extract in ethanol-induced gastric ulcers, Drug Design, Development and Therapy,10 1973–1986.

10) **Albuquerque, B. R**., Heleno, S. A., Oliveira, M. B. P., Barros, L., Ferreira, I. C. (2021). Phenolic compounds: Current industrial applications, limitations and future challenges. Food and function, 12(1), 14-29.

11) **Ali, N.,** AlAsmari, A. F., Imam, F., Ahmed, M. Z., Alqahtani, F., Alharbi, M., ... & Alanazi, M. M. (2021). Protective effect of diosmin against doxorubicin-induced nephrotoxicity. Saudi Journal of Biological Sciences, 28(8), 4375-4383.

12) **Altinoz, E**., Oner, Z., Elbe, H., Uremis, N., & Uremis, M. (2022). Linalool exhibits therapeutic and protective effects in a rat model of doxorubicin-induced kidney injury by modulating oxidative stress. Drug and Chemical Toxicology, 45(5), 2024-2030.

13) **Anusuya, N**., Durgadevi, P., Dhinek, A., Mythily, S. (2013). Nephroprotective effect of ethanolic extract of garlic (Allium sativum L.) on cisplatin induced nephrotoxicity in male wistar rats. Asian Journal of Pharmaceutical and Clinical Research, 97-100.

14) **Apak R**, Güçlü K, Özyürek M, Karademir SE. (2004). Novel Total Antioxidant Capacity Index for Dietary Polyphenols and Vitamins C and E, Using Their Cupric Ion Reducing Capability in the Presence of Neocuproine: CUPRAC Method . Journal of Agriculteral Food Chemestry .;52(26):7970-798.

15) **Arab, H. H.,** Salama, S. A., Omar, H. A., Arafa, E. S. A., Maghrabi, I. A. (2015). Diosmin protects against ethanol-induced gastric injury in rats: novel anti-ulcer actions. Plos One, 10(3), e0122417.

16) **Ashfaq M H**., Siddique A., Shahid S. (2021). Antioxidant Activity of Cinnamon zeylanicum: (A Review). Asian Journal of Pharmaceutical Research.; 11(2):106-116.

17) **Ashraf, M. Z**., Hussain, M. E., Fahim, M. (2004). Endothelium mediated vasorelaxant response of garlic in isolated rat aorta: role of nitric oxide. Journal of ethnopharmacology, 90(1), 5-9.

18) **Azab, A. E**., and Albasha, M. O. (2018). Hepatoprotective effect of some medicinal plants and herbs against hepatic disorders induced by hepatotoxic agents. Journal of Biotechnology and Bioengineering; 2(1), 8-23.

19) **Ban, S.** (2013). The Normal Stomach: Anatomy, Specimen Dissection and Histology Relevant to Pathological Practice. Morson and Dawson's Gastrointestinal Pathology, 87-103.

20) **Bastaki, S. M**., Ojha, S., Kalasz, H., & Adeghate, E. (2021). Chemical constituents and medicinal properties of Allium species. Molecular and cellular biochemistry, 476(12), 4301-4321.

21) **Beiranvand M, A.** (2022), review of the most common in *vivo* models of stomach ulcers and natural and synthetic anti-ulcer compounds: A comparative systematic study, Phytomedicine Plus, 2(2), 100264.

22) **Beiranvand M**., Bahramikia S & Dezfoulian O., (2021), Evaluation of antioxidant and anti-ulcerogenic effects of Eremurus persicus (Jaub & Spach) Boiss leaf hydroalcoholic extract on ethanol-induced gastric ulcer in rats, Inflammopharmacology 29:1503–1518.

23) **Benchikh F**. Benabdallah H, Amira H. Amira I, Mamache W, Amira S. (2022),Free Radical Scavenging, Metal chelating and Antiperoxidative Activities of *M. communis Berries* Methanol extract and its Fractions. Turkish Journal of Agriculture - Food Science and Technology ,; 10(6),1089-1094.

24) **Bengaied, D**., Ribeiro, A., Amri, M., Scherman, D., & Arnaud, P. (2017). Reduction of hepatotoxicity induced by doxorubicin. Journal of Integrative Oncology; 6(03), 1-13.

25) **Beretta H.V**., Bannoud F, Insani M, Berli F, Hirschegger P, Galmarini, CR, Cavagnaro PF. Relationships between bioactive compound content and the antiplatelet and antioxidant activities of six *allium vegetable* species. Food Technology and Biotechnology. 2017; 55(2):266 275.

26) **Bertleff, M. J**., & Lange, J. F. (2010). Perforated peptic ulcer disease: a review of history and treatment. Digestive surgery; 27(3), 161-169.

27) **Birben E**. Sahiner UM. Sackesen C. Erzurum S. Kalayci O. (2012). Oxidative stress and antioxidant defense. World Allergy Organ Journal; 5(1):9-19.

28) **Blois M.S**. (1958). Antioxidant determinations by the use of a stable free radical. Nature; 4617 (181): 1119-1200.

29) **Borys J**. and Kurtz J., (2023). The SAGES Manual of Physiologic Evaluation of Foregut Diseases, eBook, chapter .13-22,

30) **Bouaziz-Benzid A** , Hammoudi R , Hadj Amahammed M , Tlili A, Bouaziz s , Bekka C , Mesrouk H.,(2020), Optimization of Extraction conditions of the Polyphenols, Flavonoids and the Antioxidant activity of the plant *Ammosperma cinereum* (Brassicaceae) through the Response Surface Methodology (RSM). Asian Journal of Research in Chemistry; 13(1): 01-06.

31) **Bouhennı, H**., Doukanı, K., Hanganu, D., Olah, N. K., Şekeroğlu, N., & Gezici, S. (2021). Analysis of bioactive compounds and antioxidant activities of cultivated garlic (*Allium sativum* L.) and red onion (*Allium cepa* L.) in Algeria. International Journal of Agriculture Environment and Food Sciences; 5(4): 550-560.

32) **Brzozowska, I**., Konturek, P. C., Brzozowski, T., Konturek, S. J., Kwiecien, S., Pajdo, R., ... & Hahn, E. G. (2002). Role of prostaglandins, nitric oxide, sensory nerves and gastrin in acceleration of ulcer healing by melatonin and its precursor, L-tryptophan. Journal of pineal research, 32(3), 149-162.

33) **Brzozowski, T**., Konturek, S. J., Sliwowski, Z., Drozdowicz, D., Zaczek, M., & Kedra, D. (1997). Role of L-arginine, a substrate for nitric oxide-synthase, in gastroprotection and ulcer healing. Journal of gastroenterology, 32, 442-452.

34) **Carvalho, C**., Santos, R. X., Cardoso, S., Correia, S., Oliveira, P. J., Santos, M. S., & Moreira, P. I. (2009). Doxorubicin: the good, the bad and the ugly effect. Current medicinal chemistry; 16(25): 3267-3285.

35) **Ceylan, O.** (2014). Antibiofilm, mutagenic and antimutagenic activiy of *Allium sphaerocephalon* L. Journal of Pure and Applied Microbiology; 8: 2879-2885.

36) **Chandan, V. S**. (2019). Normal histology of gastrointestinal tract. Surgical Pathology of Non-neoplastic Gastrointestinal Diseases, 3-18.

37) **Chaudhry**, S.R., Liman, M. N. P., Omole, A. E., & Peterson, D. C. (2024). Anatomy, abdomen and pelvis: stomach. Stat Pearls*]*. Stat pearls publishing.

38) **Chen H**., Liaoc H, Liua Y, Zhenga Y, Wu X, Sua Z, Zhang X, Lai Z, Lai X, Lin Z, Sua Z. (2015) Protective effects of pogostone from Pogostemonis Herba against ethanol-induced gastric ulcer in rats. Fitoterapia; 100: 110–117.

39) **Chen, J**., Xing, J., Chen, J. D. (2009). Effects of muscarinic receptor stimulation and nitric oxide synthase inhibition on gastric tone and gastric myoelectrical activity in canines. Journal of gastroenterology and hepatology; 24(6): 1130-1135.

40) **Chen, P. Y**., Wu, M. S., Chen, C. Y., Bair, M. J., Chou, C. K., Lin, J. T., & Liou, J. M. (2016). Taiwan Gastrointestinal Disease and Helicobacter Consortium. Systematic review with meta-analysis: The efficacy of levofloxacin triple therapy as the first-or second-line treatments of Helicobacter pylori infection. Aliment Pharmacology andTherapeutics; 44(5): 427-437.

41) **Choi, S.I**., Hong, E.Y., Lee, J.H., Lee, Y.S. & Kim G.H., (2008). Antioxidant and antimicrobial activities of the ethanol extract of *Allium victoriallis* L. var. platyphyllum. Food Science and Biotechnology;17(2): 313-318.

42) **Cotoi, C. G**., and Quaglia, A. (2016). Normal liver anatomy and introduction to liver histology. Textbook of Pediatric Gastroenterology, Hepatology and Nutrition: A Comprehensive Guide to Practice: 609-612.

43) **Czekaj, R**., Majka, J., Magierowska, K., Sliwowski, Z., Magierowski, M., Pajdo, R., ... & Brzozowski, T. (2018). Mechanisms of curcumin-induced gastroprotection against ethanol-induced gastric mucosal lesions. Journal of Gastroenterology; 53: 618-630.

44) **Darshani K.A.U**.and Priyantha K.D.(2020). Pantioxidant properties of selected culinary flowers. Annals. Food Science and Biotechnology; 21(4):783-791.

45) **David I**, Soybel, M.D., (2005). Anatomy and Physiology of the Stomach, Surgical Clinics of North America; 85: 875–894.

46) **de Mello Andrade J.M**. , Fasolo D.(2014). Polyphenol antioxidants from natural sources and contribution to health promotion. In: Polyphenols in human health and disease. Academic Press, 253-265 p.

47) **Dean, D**. F. and Molitoris, B. A. (2019). The physiology of the glomerulus. In Critical care nephrology (pp. 35-42). Elsevier.

48) **Demir, M**., Altinoz, E. Koca, O., Elbe, H., Onal M.O, Bicer Y. & Karayakali M. (2023). Antioxidant and anti-inflammatory potential of crocin on the doxorubicin mediated hepatotoxicity in Wistar rats, Tissue and Cell 84102182.

49) **Derouiche, S**. Cheradid, T. Guessoum, M. (2020), Heavy metals, Oxidative stress and Inflammation in Pathophysiology of Chronic Kidney disease - A Review. Asian Journal of Pharmacy and Technology: 10(3): 202-206.

50) **Dunlap, J. J.** and Patterson, S. (2019). Peptic ulcer disease. Gastroenterology Nursing; 42(5): 451-454.

51) **Dziri, S.**, Hassen, I., Fatnassi, S., Mrabet, Y., Casabianca, H., Hanchi, B. & Hosni, K. (2012). Phenolic constituents, antioxidant and antimicrobial activities of rosy garlic (*Allium roseum* var. odoratissimum). Journal of Functional Foods; 4(2): 423-432.

52) **El-Ashmawy, N. E**., Khedr, E. G., El-Bahrawy, H. A. & Selim H. M. (2016). Gastroprotective effect of garlic in indomethacin induced gastric ulcer in rats. Nutrition; 32: 849–854.

53) **Elbeltagy, A**., Mohamed, G., Akeel, M., Abdelaziz, K., Elbakry, K., & Elsayed, A. (2022). Modulatory role of garlic (*Allium sativum*) extract against cisplatin-induced nephrotoxicity in female albino rats and their offspring. F1000 Research: 11.

54) **Elias, J.**, Rajesh, M.G., Anish, N.P., Sunny, S. & Jayan, N. (2010). Free Radical Scavenging Activity and Phytochemical Profiling of *Acalypha indica* Linn. Research Journal of Pharmacy and Technology; 3 (4): 1231-1234.

55) **El-Sayed, E. S. M.,** Mansour, A. M., & El-Sawy, W. S. (2017). Protective effect of proanthocyanidins against doxorubicin-induced nephrotoxicity in rats. Journal of Biochemical and Molecular Toxicology; 31(11): e21965.

56) **Emir, A**. and Emir, C. (2020). Chemical profiles and biological properties of methanol extracts of *Allium pallens* L. from different localities in Turkey. Archives of Biological Sciences; 72(2): 193-201.

57) **Emir, A**. and Emir, C. (2022). Chemical composition and inhibitory potentials of key-enzymes linked to neurodegenerative diseases of wild garlic: *Allium atrovioleceum* Boiss. Indian Journal of Traditional Knowledge; 21(2): 332-340.

58) **Emir, A**. and Emir, C.A.(2020). Comparative study of phenolic profiles and biological activities of *Allium sphaerocephalon* L. subsp. sphaerocephalon L. and *Allium sphaerocephalon* L. subsp. trachypus (Boiss. Et Spruner) K. Richter. Journal of Research in Pharmacy; 24(6): 893-900.

59) **Emir, A**., Emir, C. & Yıldırım, H. (2021). Chemical and biological comparison of different parts of two Allium species: *Allium paniculatum* L. subsp. villosulum (Hal.) Stearn and *Allium paniculatum* L. subsp. paniculatum L. Chemical Papers; 75(1): 411-419.

60) **Emir, C**. , Coban, G. & Emir, A.(2022). Metabolomics profiling, biological activities, and molecular docking studies of elephant garlic (*Allium ampeloprasum* L.). Process Biochemistry; 116: 49-59.

61) **Emir, C**. and Emir, A. (2021). Phytochemical analyses with LC-MS/MS and *in vitro* enzyme inhibitory activities of an endemic species "*Allium stylosum* O. Schwarz" (Amaryllidaceae). South African Journal of Botany;136: 70-75.

62) **Fernandez-Panchon, M.S.**, Villano, D., Troncoso, A.M. & Garcia-Parrilla, M.C. (2008). Antioxidant Activity of Phenolic Compounds: From *In Vitro* Results to *In Vivo* Evidence. Critical Reviews in Food Science and Nutrition; 48: 649-671.

63) **Forman, H. J**., and Zhang, H. (2021). Targeting oxidative stress in disease: promise and limitations of antioxidant therapy. Nature Reviews Drug Discovery; 20(9): 689-709.

64) **Fouad, G.I**. and Ahmed, K. A. (2021). The protective impact of berberine against doxorubicin-induced nephrotoxicity in rats. Tissue and Cell; 73: 101-612.

65) **Fraga, C.G**., Croft, K.D., Kennedye, D.O. & -Barberán T. (2019). The effects of polyphenols and other bioactives on human health. Food and Function; 10(2): 514-528.

66) **Fredric C**. (2017). Glomerular Filtration, University of Chicago.

67) **Fulga, S**., Pelin, A. M., Ghiciuc, C. M., & Lupușoru, E. C. (2019). Particularities of experimental models used to induce gastric ulcer. ARS Medica Tomitana; 25(4): 179-184.

68) **Gelberg, H. B**. (2014). Comparative Anatomy, Physiology, and Mechanisms of Disease Production of the Esophagus, Stomach, and Small Intestine. Toxicologic Pathology; 42: 54-66.

69) **Gugliandolo, E.**, Cordaro, M., Fusco, R., Peritore, A. F., Siracusa, R., Genovese, T., ... & Crupi, R. (2021). Protective effect of snail secretion filtrate against ethanol-induced gastric ulcer in mice. Scientific Reports; 11(1): 3638.

70) **Gulcin, İ**. (2020). Antioxidants and antioxidant methods: An updated overview. Archives of Toxicology; 94(3): 651-715.

71) **Gulcin, İ.** and Alwasel, S.H. (2022). Metal ions, metal chelators, and metal chelating assay as antioxidant method. Processes;10(1): 132-132.

72) **Gupta, M**., Kapoor, B., Gupta, R., & Singh, N. (2021). Plants and phytochemicals for treatment of peptic ulcer: An overview. South African Journal of Botany; 138: 105-114.

73) **Halder, S**., and Khaled, K. L. (2021). Anti-nutritional profiling from the edible flowers of Allium cepa, Cucurbita maxima and Carica papaya and its comparison

with other commonly consumed flowers. International Journal of Herbal Medicine; 9(5): 55-61.

74) **Heeba, G. H**. and Mahmoud, M. E. (2016). Dual effects of quercetin in doxorubicin-induced nephrotoxicity in rats and its modulation of the cytotoxic activity of doxorubicin on human carcinoma cells. Environmental Toxicology; 31(5): 624-636.

75) **Heeba, G. H**., Morsy, M. A., Mahmoud, M. E., & Abdel-latif, R. (2023). Gastro-protective effect of L-arginine against nitric oxide deficiency-related mucosal injury induced by indomethacin: Does age matter? Journal of Biochemical and Molecular Toxicology; 37(11): e23479.

76) **Hossain, M**., Suchi, T. T., Samiha, F., Islam, M. M., Tully, F. A., Hasan, J., ... & Reza, H. M. (2023). Coenzyme Q10 ameliorates carbofuran induced hepatotoxicity and nephrotoxicity in wister rats. Heliyon; 9(2).

77) **Huang, W**., Xie, C., Albrechtsen, N. J. W., Sang, M., Sun, Z., Jones, K. L., ... & Wu, T. (2023). Serum alanine transaminase is predictive of fasting and postprandial insulin and glucagon concentrations in type 2 diabetes. Peptides; 169 : 171092.

78) **Hussain, M. A.,** Abogresha, N. M., AbdelKader, G., Hassan, R., Abdelaziz, E. Z., & Greish, S. M. (2021). Antioxidant and anti-inflammatory effects of crocin ameliorate doxorubicin-induced nephrotoxicity in rats. Oxidative Medicine and Cellular Longevity, 2021(1), 8841726**.**

79) **Ilić, S**., Stojiljković, N., Veljković, M., Veljković, S., & Stojanović, G. (2014). Protective effect of quercetin on cisplatin-induced nephrotoxicity in rats. Facta Universitatis, Series: Medicine and Biology; 16(2): 71-75.

80) **Injac, R**., Perse, M., Cerne, M., Potocnik, N., Radic, N., Govedarica, B., ... & Strukelj, B. (2009). Protective effects of fullerenol C60 (OH) 24 against doxorubicin-induced cardiotoxicity and hepatotoxicity in rats with colorectal cancer. Biomaterials; 30(6): 1184-1196.

81) **Jabbar A. A.J**, Mothana R A., Abdulla M A, Abdullah F O, Ahmed K A, Hussen R R, Hawwal M F, Fantoukh O I, Hasson S. (2023). Mechanisms of anti-ulcer actions

of Prangos pabularia (L.) in ethanol-induced gastric ulcer in rats. Saudi Pharmaceutical Journal; 31: 101-850.

82) **Jaiswal N.** and Rizvi S.I. (2017). Amylase inhibitory and metal chelating effects of different layers of onion (*Allium cepa* L.) at two different stages of maturation *in vitro*. Annals of Phytomedicine; 6(1): 45-50.

83) **Jang, J. E**., Baasanmunkh, S., Nyamgerel, N., Oh, S. Y., Song, J. H., Yusupov, Z., ... & Choi, H. J. (2024). Flower morphology of Allium (Amaryllidaceae) and its systematic significance. Plant Diversity; 46(1): 3-27.

84) **Jomova, K**., Raptova, R., Alomar, SY., Alwasel, SH., Nepovimova, E, Kuca, K., Valko, M. (2023). Reactive oxygen species, toxicity, oxidative stress, and antioxidants: chronic diseases and aging, Archives of Toxicology ;97: 2499–2574.

85) **Juza, R. M**. and Pauli, E. M. (2014). Clinical and surgical anatomy of the liver: a review for clinicians. Clinical Anatomy; 27(5): 764-769.

86) **Kalia, N.**, Bardhan, K. D., Reed, M. W., Jacob, S., & Brown, N. J. (2000). L-arginine protects and exacerbates ethanol-induced rat gastric mucosal injury. Journal of Gastroenterology and Hepatology; 15(8): 915-924.

87) **Kanatani, K**., Ebata, M., Murakami, M., Okabe, S. (2004). Effects of indomethacin and rofecoxib on gastric, Journal of Physiology and Pharmacology; 55(1): 207-222.

88) **Kaoudoune, C**., Benchikh, F., Abdennour, C., Benabdallah, H., Mamache, W., Amira, S. (2022). Free Radical Scavenging and Antinociceptive Activities of the Aqueous Extract from *Matricaria chamomilla* L. Flowers. Turkish Journal of Agriculture - Food Science and Technology-;10(10): 2076-2080.

89) **Kaoudoune, C**.., Benchikh, F., Abdennour, C., Benabdallah, H., Souici, C. B., Derafa, I., ... & Amira, S. (2024). Phenolic Content and Antioxidant Activity of Hydroethanolic and Aqueous Extracts of the Inflorescences of *Allium sphaerocephalon* L. Research Journal of Pharmacy and Technology; 17(2): 903-909.

90) **Kasmi, H**., Doukani, K., Ali, A., Tabak, S., & Bouhenni, H. (2020). Epidemiological profile of Helicobacter pylori infection in patients with digestive symptoms in Algeria. Journal of Epidemiology and Global Health; 10(4): 293-297.

91) **Katary, M. A**. and Salahuddin, A. (2017). Gastroprotective Effect of Punicalagin against Ethanol-Induced Gastric Ulcer:The Possible Underlying Mechanisms. Biomarkers Journal; 3:1.

92) **Keshav, S.** (2009). The gastrointestinal system at a glance. John Wiley & Sons.

93) **Khatua, S**., Paul, S. & Acharya, K. (2013). Mushroom as the Potential Source of New Generation of Antioxidant: A Review. Research Journal of Pharmacy and Technology; 6(5): 496-505.

94) **Konturek, S. J**., Konturek, P. C., & Brzozowski, T. (2005). Prostaglandins and ulcer healing. Journal of Physiology and Pharmacology; 56: 5.

95) **Kuna, L**., Jakab, J., Smolic, R., Raguz-Lucic, N., Vcev, A., & Smolic, M. (2019). Peptic ulcer disease: a brief review of conventional therapy and herbal treatment options. Journal of Clinical Medicine; 8(2): 179.

96) **Laura, A**., Moreno-Escamilla, J.O., Rodrigo-García, J. & Alvarez-Parrilla, E. (2019), Phenolic compounds. In Postharvest physiology and biochemistry of fruits and vegetables. Woodhead Publishing; 253-271 p.

97) **Lazarevic, J.S.**, Dor, devic AS, Zlatkovic, BK, Radulovic, NS & Palic, RM. (2011). Chemical composition and antioxidant and antimicrobial activities of essential oil of *Allium sphaerocephalon* L. subsp. sphaerocephalon (Liliaceae) inflorescences. Journal of the Science of Food and Agriculture;91: 322-329.

98) **Lin, S. C**., Chagnaadorj, A., Bayarsengee, U., Leung, T. K., & Cheng, C. W. (2019). The compound, diallyl disulfide, enriched in garlic, prevents the progression of doxorubicin-induced nephropathy. Food Science and Technology; 39: 1040-1046.

99) **Linnaeus, C**. (1797). Species plantarum, exhibentes plantas rite cognitas ad genera relatas, cum differentiis specificis, nominibus trivialibus, synonymis selectis, locis natalibus, secundum systema sexuale digestas (Vol. 2). Impensis GC Nauk.

100) **Liu, Y**., Sui, D., Fu, W, Sun, L., Li, Y, Yu, P., Yu, X, Zhoub, Y., & Xu, H. (2021). Protective effects of polysaccharides from Panax ginseng on acute gastric ulcers induced by ethanol in rats. Food & Function; 12: 2741–2749.

101) **Macallister, C. G**. (1999). A review of medical treatment for peptic ulcer disease. Equine Veterinary Journal; 31(S29): 45-49.

102) **Maes, M.L**. and Fixen, D.R. (2017). Linnebur, S.A. Adverse effects of proton-pump inhibitor use in older adults:A review of the evidence. Therapeutic Advances in Drug Safety; 8: 273–297.

103) **Mahadevan, V**. (2020). Anatomy of the liver. Surgery (Oxford); 38(8): 427-431.

104) **Malfertheiner, P**., Chan, F. K., & McColl, K. E. (2009). Peptic ulcer disease. The lancet; 374(9699): 1449-1461.

105) **Mamache W**., Amira S., Ben Souici C., Laouer H., Benchikh F.(2020). In vitro antioxidant, anticholinesterases, anti-α-amylase, and anti-α-glucosidase effects of Algerian *Salvia aegyptiaca* and *Salvia verbenaca*. Journal of Food Biochemistry; 00: e13472.

106) **Mansouri, E**., Jangaran, A., & Ashtari, A. (2017). Protective effect of pravastatin on doxorubicin-induced hepatotoxicity. Bratislavske Lekarske Listy; 118(5): 273-277.

107) **Markham, K.R**., (1982), Techniques of flavonoid identification (Chap.1 and 2). London Academic: 1-113 p.

108) **Marks, I. N.** (1991). Sucralfate—safety and side effects. Scandinavian Journal of Gastroenterology, 26(sup185), 36-42.

109) **Martemucci, G**., Costagliola, C., Mariano, M., D'andrea, L., Napolitano, P., & D'Alessandro, A. G. (2022), Free radical properties, source and targets, antioxidant consumption and health. Oxygen; 2(2): 48-78.

110) **Martin, M. J**., and Motilva, V. (2001). New issues about nitric oxide and its effects on the gastrointestinal tract. Current Pharmaceutical Design; 7(10): 881-908.

111) **Maslin, D.J**., Brown, C.A., Das, I., Xia-Hua, Z. (1997). Nitric oxide a mediator of garlic action? Biochemical Society Transactions; 25: 408.

112) **Mathew, J**., Arora, KM, Mazumdar, A, Kumar, G, Karthik, L, Bhaskara, Rao, K V. (2012). Evaluation of phytochemical composition and antioxidant activity of aqueous extract of Barleria mysorensis and Furcraea foetida leaves, Research Journal of Pharmacy and Technology; 5(12): 1503-1508.

113) **McQuilken, S. A.** (2021). The mouth, stomach and intestines. Anaesthesia & Intensive Care Medicine; 22(5): 330-335.

114) **Menacer, A**., Boukhatem, M.N., Benhelal, A., Saïdi, F. (2017). In vitro antioxidant activity of different extracts of Algerian allium pdf plant (*Allium triquetrum* L.). Revue des Bio Ressources; 7(1): 12-12.

115) **Mete, R**., Oran, M., Topcu, B., Oznur, M., Seber, E. S., Gedikbasi, A., & Yetisyigit, T. (2015). Protective effects of onion (*Allium cepa*) extract against doxorubicin-induced hepatotoxicity in rats. Toxicology and industrial health; 32(3): 551-557.

116) **Micallef, I**., and Baron, B. (2020). Doxorubicin: An overview of the anti-cancer and chemoresistance mechanisms.

117) **Minatel, I. O**., Borges, C. V., Ferreira, M. I., Gomez, H. A. G., Chen, C. Y. O., & Lima, G. P. P. (2017). Phenolic compounds: Functional properties, impact of processing and bioavailability. Phenolic Compounds - Biological Activity; 8: 1-24.

118) **Miranda-Bautista, J**., Bañares, R. & Vaquero, J., (2017). The Gastrointestinal System: Anatomy and sources of oxidative stress. Gastrointestinal Tissue; 3-20.

119) **Mizokami, Y**., Oda, K., Funao, N., Nishimura, A., Soen, S., Kawai, T., Ashida, K. & Sugano, K. (2018). Vonoprazan prevents ulcer recurrence during long-term NSAID therapy: Randomised, lansoprazole-controlled non-inferiority and single-blind extension study. Gastroduodenal; 67: 1042–1051.

120) **Mohammed, E.A.** , Abdalla, I.G., Alfawaz, M.A., Mohammed, M.A., Al Maiman S.A., Osman, M.A., Yagoub, A.E.A. (2022). Hassan AB. Effects of Extraction

Solvents on the Total Phenolic Content, Total Flavonoid Content, and Antioxidant Activity in the Aerial Part of Root Vegetables. Agriculture;12: 1820.

121) **Mohan, M**., Kamble, S., Gadhi, P., Kasture. (2010). Protective effect of *Solanum torvum* on doxorubicin-induced nephrotoxicity in rats. Food and Chemical Toxicology; 48: 436–440.

122) **Moinuddin, Z**., and Dhanda, R. (2015). Anatomy of the kidney and ureter. Anaesthesia and Intensive Care Medicine; 16(6): 247-252.

123) **Molehin, O. R.,** Adeyanju, A. A., Adefegha, S. A., Oyeyemi, A. O. & Idowu, K. A. (2019). Protective mechanisms of protocatechuic acid against doxorubicin-induced nephrotoxicity in rat model. Journal of Basic and Clinical Physiology and Pharmacology; 30(4): 20180191.

124) **Monnet, E**. (2020). Anatomy and Physiology of the Stomach. Gastrointestinal Surgical Techniques in Small Animals; 129-134.

125) **Moorthy, A. V**. and Blichfeldt, T. C. (2009). Anatomy and Physiology of the Kidney. In Pathophysiology of kidney disease and hypertension (pp. 1-15). WB Saunders.

126) **Mössner**, J. (2016). The indications, applications, and risks of proton pump inhibitors. Deutsches Arzteblatt International; 113: 477–483.

127) **Müller L**. (2010). Gnoyke S, Popken AMV, Böhm V. Antioxidant capacity and related parameters of different fruit formulations, LWT - Food Science and Technology; 43(6): 992–999.

128) **Muthukumaran, P**., Shanmuganathan, P. & Malathi, C. (2011). In Vitro Antioxidant Evaluation of Mimosa pudica. Asian Journal of Pharmaceutical Research; 1(2): 44-46**.**

129) **Nabavi, S.F**., Nabavi, S.M., Ebrahimzadeh, M.A., Eslami, B., Jafari N. (2013). In *vitro* antioxidant and antihemolytic activities of hydroalcoholic extracts of *Allium scabriscapum* Boiss. & Ky. aerial parts and bulbs. International Journal of Food Properties; 16(4): 713-722.

130) **Nimbal, S. K**., Gadad, P. C., & Koti, B. C. (2021). Effect of ethanolic extract of Rosa centifolia against doxorubicin induced nephrotoxicity in albino rats. Journal of Ayurveda and Integrative Medicine; 12(4): 657-662.

131) **Nimse, S.B.** and Palb, D. (2015). Free radicals, natural antioxidants, and their reaction mechanisms. The Royal Society of Chemistry; 5: 27986–28006.

132) **Ofusori, A.E**., Moodley, R. & Jonnalagadda, S. B. (2019). Antiulcerogenic effects of *Celosia trigyna* plant extracts on ethanol induced gastric ulcer in adult Wistar rats. Journal of Traditional and Complementary Medicine; 11.004.

133) **Omobowale, T. O**., Oyagbemi, A. A., Ajufo, U. E., Adejumobi, O. A., Ola-Davies, O. E., Adedapo, A. A., & Yakubu, M. A., (2018), Ameliorative effect of gallic acid in doxorubicin-induced hepatotoxicity in Wistar rats through antioxidant defense system. Journal of Dietary Supplements; 15(2): 183-196.

134) **Oyaizu M**., (1986). Studies on products of browning reactions: antioxidative activities of browning reaction prepared from glucosamine. Japan Journal of Nutrition; 44(6): 307-315.

135) **Pan, L. R**., Tang, Q., Fu, Q., Hu, B. R., Xiang, J. Z., & Qian, J. Q. (2005). Roles of nitric oxide in protective effect of berberine in ethanol-induced gastric ulcer mice. Acta Pharmacologica Sinica; 26(11):1334-1338.

136) **Parcheta, M.**, Swisłocka, R., Orzechowska, S., Akimowicz, M., Nska, R.C. & Lewandowski, W. (2021). Recent Developments in Effective Antioxidants: The Structure and Antioxidant Properties. Materials; 14: 1984.

137) **Patel, V. R.** (Ed.). (2012). Robotic urologic surgery. Springer London.

138) **Pension, J**. And Wormsley, K.G. (1986). Adverse reactions and interactions with H2-receptor antagonists. Medical Toxicology; 1: 192–216.

139) **Pereira, D.M**., Valentão, P., Pereira, J.A. & Andrade, P.B. (2009). Phenolics: From Chemistry to Biology. Molecules; 14: 2202-2211.

140) **Petrovic, D.,** Seke, M., Borovic, M. L., Jovic, D., Borisev, I., Srdjenovic, B., ... & Djordjevic, A. (2018). Hepatoprotective effect of fullerenol/doxorubicin nanocomposite in acute treatment of healthy rats. Experimental and Molecular Pathology; 104(3): 199-211.

141) **Pieniążek, A**., Czepas, J., Piasecka-Zelga, J., Gwoździński, K., & Koceva-Chyła, A. (2013). Oxidative stress induced in rat liver by anticancer drugs doxorubicin, paclitaxel and docetaxel. Advances in medical sciences; 58(1): 104-111.

142) **Pique, J. M**., Yonei, Y., Whittle, B. J., Leung, F. W., & Guth, P. H. (1988). Indomethacin potentiates endotoxin-induced blood flow reduction and histological injury in rat gastric mucosa. British Journal of Pharmacology; 93(4): 925.

143) **Prajapati, P. K**., Singh, S. B. & Jaiswal, S. (2014). Overview on antiulcer activity of Basella alba: a therapeutic herb. International Archive Applied Science Technology; 5: 49-61.

144) **Prasanna, P. L**., Renu, K., Gopalakrishnan, A. V. (2020). New molecular and biochemical insights of doxorubicin-induced hepatotoxicity. Life Sciences; 250: 117-599.

145) **Proboningrat, A**., Jayanti, S., Fadholly, A., Ansori, A. N., Putri, N., Kusala, M. K., ... & Achmad, A. B. (2021). The cytotoxicity of ethanolic extract of *Allium cepa* L. on hela cell lines. Research Journal of Pharmacy and Technology; 14(9): 4969-4972.,

146) **Rahman, M.**, Rahaman, S., Islam, R., Rahman, F., Mithi, F.M., Alqahtani T., Almikhlafi, M.A., Alghamdi, S.Q., Alruwaili, AS., Hossain, S., Ahmed, M., Das, R., Emran, TB., Uddin, S.. (2021). Role of Phenolic Compounds in Human Disease: Current Knowledge and Future Prospects. Molecules; 27(1): 233.

147) **Rathe,r G. A**., Nanda, A., Raj, E.,. Mathivanan, N., Thiruvengadam, K., Sofi1, M. A. & Nayak, B. K. (2023). Determination of Phytochemicals, in vitro Antioxidant and Antibacterial activity of Lavandula angustifolia Mill. Research Journal of Pharmacy and Technology; 16(3):1161-1166.

148) **Refaie, M. M**., Amin, E. F., El-Tahawy, N. F., & Abdelrahman, A. M. (2016). Possible protective effect of diacerein on doxorubicin-induced nephrotoxicity in rats. Journal of Toxicology 2016(1), 9507563.

149) **Renu, K**., Pureti, L. P., Vellingiri, B., & Valsala Gopalakrishnan, A. (2022). Toxic effects and molecular mechanism of doxorubicin on different organs–an update. Toxin Reviews; 41(2): 650-674.

150) **Rice-Evans, C**., Miller, N.J. & Paganga, G. (1997). Antioxidant properties of phenolic compounas. Trends in Plant Science; 2(4):152-159.

151) **Rivankar, S**. (2014). An overview of doxorubicin formulations in cancer therapy. Journal of cancer research and therapeutics; 10(4): 853-858.

152) **Sánchez-Mendoza, M. E**., López-Lorenzo, Y., Cruz-Antonio, L., Cruz-Oseguera, A., García-Machorro, J., & Arrieta, J. (2020). Gastroprotective effect of juanislamin on ethanol-induced gastric lesions in rats: Role of prostaglandins, nitric oxide and sulfhydryl groups in the mechanism of action. Molecules; 25(9): 2246.

153) **Santo, A**., Zhu, H., Li, Y. R. (2016). Free radicals: From health to disease. Reactive Oxygen Species; 2: 245-263.

154) **Scărlătescu, V**., Vasile, D & Voiculescu, I. (2017). The herbarium – a data source for allium genus species. Research Journal of Agricultural Science; 50 (1): 186-193.

155) **Sena, C. M**., Seiça, R., & Perry, G. (2022). Oxidative Stress Revisited—Major Role in Vascular Diseases, Volume II. Frontiers in Physiology;12: 826129.

156) **Sharifi-Rad, M.**, Anil Kumar, N. V., Zucca, P., Varoni, E. M., Dini, L., Panzarini, E., ... & Sharifi-Rad, J. (2020). Lifestyle, oxidative stress, and antioxidants: back and forth in the pathophysiology of chronic diseases. Frontiers in Physiology; 11: 694.

157) **Shell, E. J**., (2021). Pathophysiology of peptic ulcer disease. Physician Assistant Clinics; 6(4): 603-611.

158) **Sherwood, L.** (2015). Physiologie humaine. De Boeck Supérieur.

159) **Si, W. Z**., Hu, X. X., Shen, C., Luo, M. X., Xuan, Y. H., Fu, H. J., ... & Liu, Z. (2020). Protective Effect of Schisandra chinensis extract against ethanol-induced gastric ulcers in mice by promoting anti-inflammatory and mucosal defense mechanisms. Revista Brasileira de Farmacognosia; 30: 780-788.

160) **Sibulesky, L**. (2013). Normal liver anatomy. Clinical liver disease; 2: S1-S3.

161) **Silva, M. I. G**., and de Sousa, F. F. (2011). Gastric ulcer etiology. Peptic Ulcer Disease, 1.

162) **Sooranna, S.R**., Hirani, J. & Das, I. (1995). Garlic induces both GTP cyclohydrase and nitric oxide synthase activity in choriocarcinoma cells. Biochemical Society Transactions; 23: 543S.

163) **Sritharan, S**. and Sivalingam, N. (2021). A comprehensive review on time-tested anticancer drug doxorubicin. Life sciences; 278: 119527.

164) **Su, Z**., Ye, J., Qin, Z., & Ding, X. (2015). Protective effects of madecassoside against Doxorubicin induced nephrotoxicity in vivo and in vitro. Scientific Reports; 5(1): 18314.

165) **Suleyman, H**., Albayrak, A., Bilici, M., Cadirci, E., & Halici, Z. (2010). Different mechanisms in formation and prevention of indomethacin-induced gastric ulcers. Inflammation; 33: 224-234.

166) **Sultana, B**., Anwar, F. & Ashraf, M. (2009). Effect of extraction solvent/technique on the antioxidant activity of selected medicinal plant extracts. Molecules; 14(6): 2167-80.

167) **Survarachakan, S**., Prasad, P. J. R., Naseem, R., de Frutos, J. P., Kumar, R. P., Langø, T., ... & Lindseth, F. (2022). Deep learning for image-based liver analysis—A comprehensive review focusing on malignant lesions. Artificial Intelligence in Medicine; 130: 102331.

168) **Tepe, B.**, Sokmen, M., Akpulat, H.A. & Sokmen, A. (2005). In vitro antioxidant activities of the methanol extracts of five Allium species from Turkey. Food Chemistry; 92(1): 89-92.

169) **Thorn, C. F**., Oshiro, C., Marsh, S., Hernandez-Boussard, T., McLeod, H., Klein, T. E., & Altman, R. B. (2011). Doxorubicin pathways: pharmacodynamics and adverse effects. Pharmacogenetics and Genomics; 21(7): 440-446.

170) **Topçu, G.**, Ay, A., Bilici, A., Sarıkürkcü, C., Öztürk, M., & Ulubelen A. (2007). A new flavone from antioxidant extracts of Pistacia terebinthus. Food Chemistry; 103: 816–822.

171) **Tornadore, N**. (1989). Population variability in *Allium sphaerocephalon* L. Atti Soc. Tosc. Sc. Nat. Mem. ser B, 96, 53-62.

172) **Tsuchiya, I**., Kato, Y., Tanida, E., Masui, Y., Kato, S., Nakajima, A., & Izumi, M. (2017). Effect of vonoprazan on the treatment of artificial gastric ulcers after endoscopic submucosal dissection: prospective randomized controlled trial. Digestive Endoscopy, 29(5), 576-583.

173) **Vona, R**., Pallotta, L., Cappelletti, M., Severi, C., & Matarrese, P. (2021). The impact of oxidative stress in human pathology: Focus on gastrointestinal disorders. Antioxidants; 10(2): 201.

174) **Vora, Z**., Goyal, A., Sharma, R. (2021). Radiological anatomy of stomach and duodenum with clinical significance. Journal of Gastrointestinal and Abdominal Radiology; 4(02): 085-093.

175) **Wilson, R.** L. and Stevenson, C. E. (2019). Anatomy and physiology of the stomach. In Shackelford's Surgery of the Alimentary Tract, 2 Volume Set (pp. 634-646). Elsevier.

176) **Wilson**, R. L., and Stevenson, C. E. (2019). Anatomy and Physiology of the Stomach. In Shackelford's Surgery of the Alimentary Tract, 2 Volume Set (pp. 634-646). Elsevier.

177) **Xie, Y**., Kang, R., Tang, D. (2019). The Flavone Baicalein and Its Use in Gastrointestinal Disease, Herbs and Plants for Treating Liver Disease. Chapter 12,145-155.

178) **Yagmurca, M**., Bas, O., Mollaoglu, H., Sahin, O., Nacar, A., Karaman, O., & Songur, A. (2007). Protective effects of erdosteine on doxorubicin-induced hepatotoxicity in rats. Archives of medical research; 38(4): 380-385.

179) **Yumrutaş, Ö.**, Saygideğer, S.D. & Doğan, M. (2009). The in vitro antioxidant activity of *Allium tuncelianum*: An Endemic. Journal of Applied Biological Sciences; 33: 61-64.

180) **Zarkovic, N**. (2020). Roles and Functions of ROS and RNS in Cellular Physiology and Pathology. Cells; 9(3): 767.

181) **Zatorski, H.** (2017). Pathophysiology and risk factors in peptic ulcer disease. Introduction to Gastrointestinal Diseases Vol. 2, 7-20.

182) **Zeb A**. (2020). Concept, mechanism, and applications of phenolic antioxidants in foods, Journal of Food Biochemistry; 00: e13394.

183) **Zhang, L**., Shao, H., & Alkan, S. (Eds.). (2020). Diagnostic Pathology of Hematopoietic Disorders of Spleen and Liver. Springer Nature.

184) **Zhao, M.**, Ding, X. F., Shen, J. Y., Zhang, X. P., Ding, X. W., & Xu, B. (2017). Use of liposomal doxorubicin for adjuvant chemotherapy of breast cancer in clinical practice. Journal of Zhejiang University-Science B (Biomedicine & Biotechnology); 18(1):15.

185) **Zhao, X**., Jin, Y., Li, L., Xu, L., Tang, Z., Qi, Y., ... & Peng, J. (2019). MicroRNA-128-3p aggravates doxorubicin-induced liver injury by promoting oxidative stress via targeting Sirtuin-1. Pharmacological Research; 146: 104276.

186) **Zhao, X**., Zhang, J., Tong, N., Chen, Y., & Luo, Y. (2012). Protective effects of berberine on doxorubicin-induced hepatotoxicity in mice. Biological and Pharmaceutical Bulletin; 35(5): 796-800.